RUTGERS
THE STATE UNIVERSITY OF NEW JERSEY

Volcanic Aerosols as an Analog for Geoengineering

Alan Robock
Department of Environmental Sciences
Rutgers University, New Brunswick, New Jersey

robock@envsci.rutgers.edu

http://envsci.rutgers.edu/~robock

Solar Radiation Management

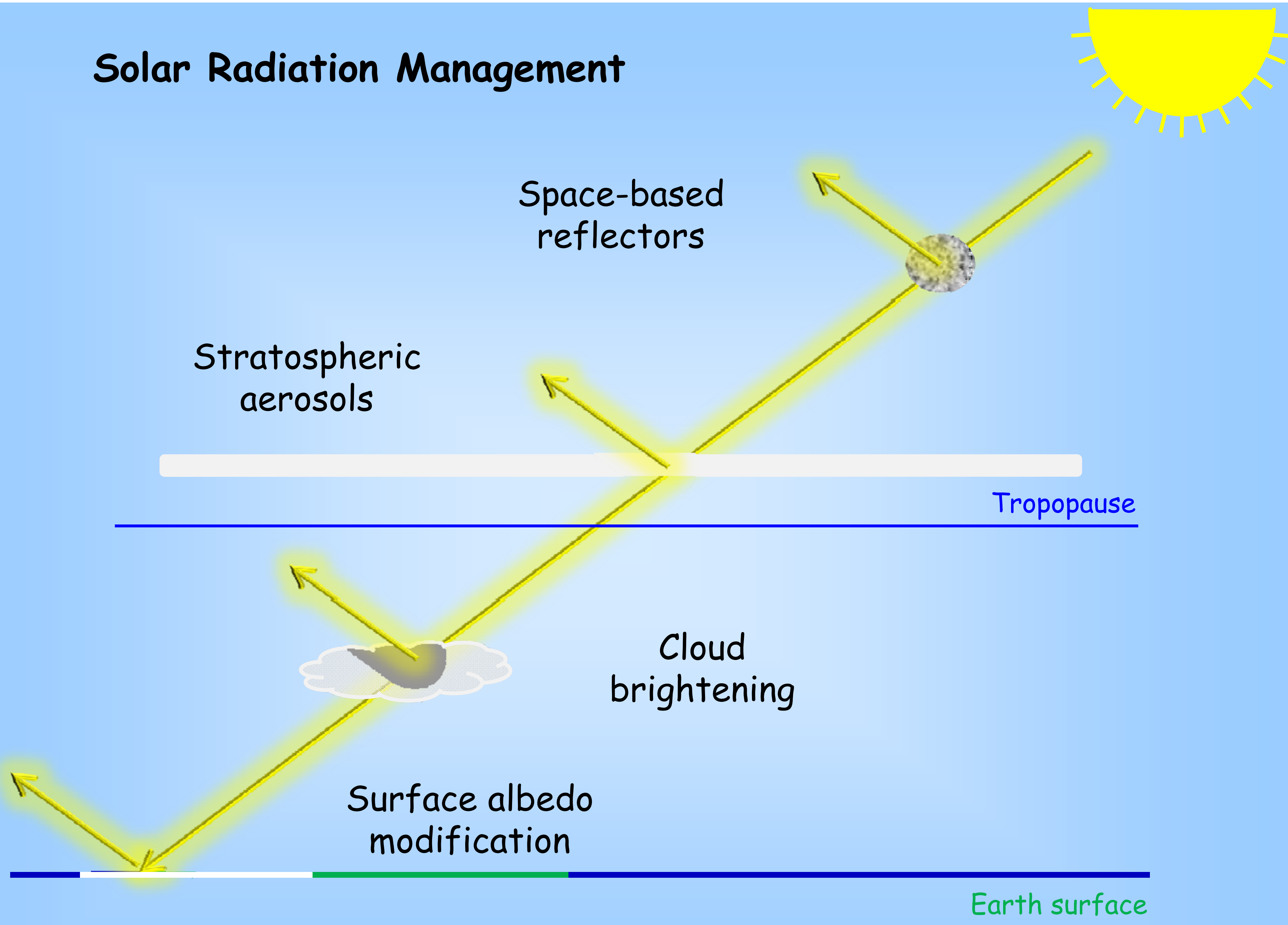

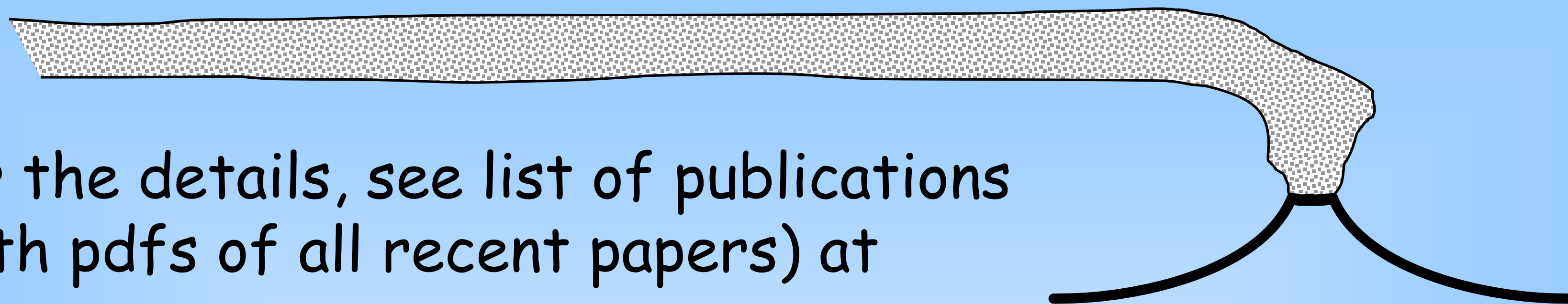

For the details, see list of publications (with pdfs of all recent papers) at

http://climate.envsci.rutgers.edu/robock/robock_volpapers.html

Review article:

Robock, Alan, 2000: Volcanic eruptions and climate. *Rev. Geophys.*, **38**, 191-219.

Latest papers:

Robock, Alan, Caspar M. Ammann, Luke Oman, Drew Shindell, Samuel Levis, and Georgiy Stenchikov, 2009: Did the Toba volcanic eruption of ~74 ka B.P. produce widespread glaciation? *J. Geophys. Res.*, **114**, D10107, doi:10.1029/2008JD011652.

Kravitz, Ben, Alan Robock, and Adam Bourassa, 2010: Negligible climatic effects from the 2008 Okmok and Kasatochi volcanic eruptions. *J. Geophys. Res.*, **115**, D00L05, doi:10.1029/2009JD013525.

Kravitz, Ben, and Alan Robock, 2011: The climate effects of high latitude volcanic eruptions: The role of the time of year. *J. Geophys. Res.*, **116**, D01105, doi:10.1029/ 2010JD014448.

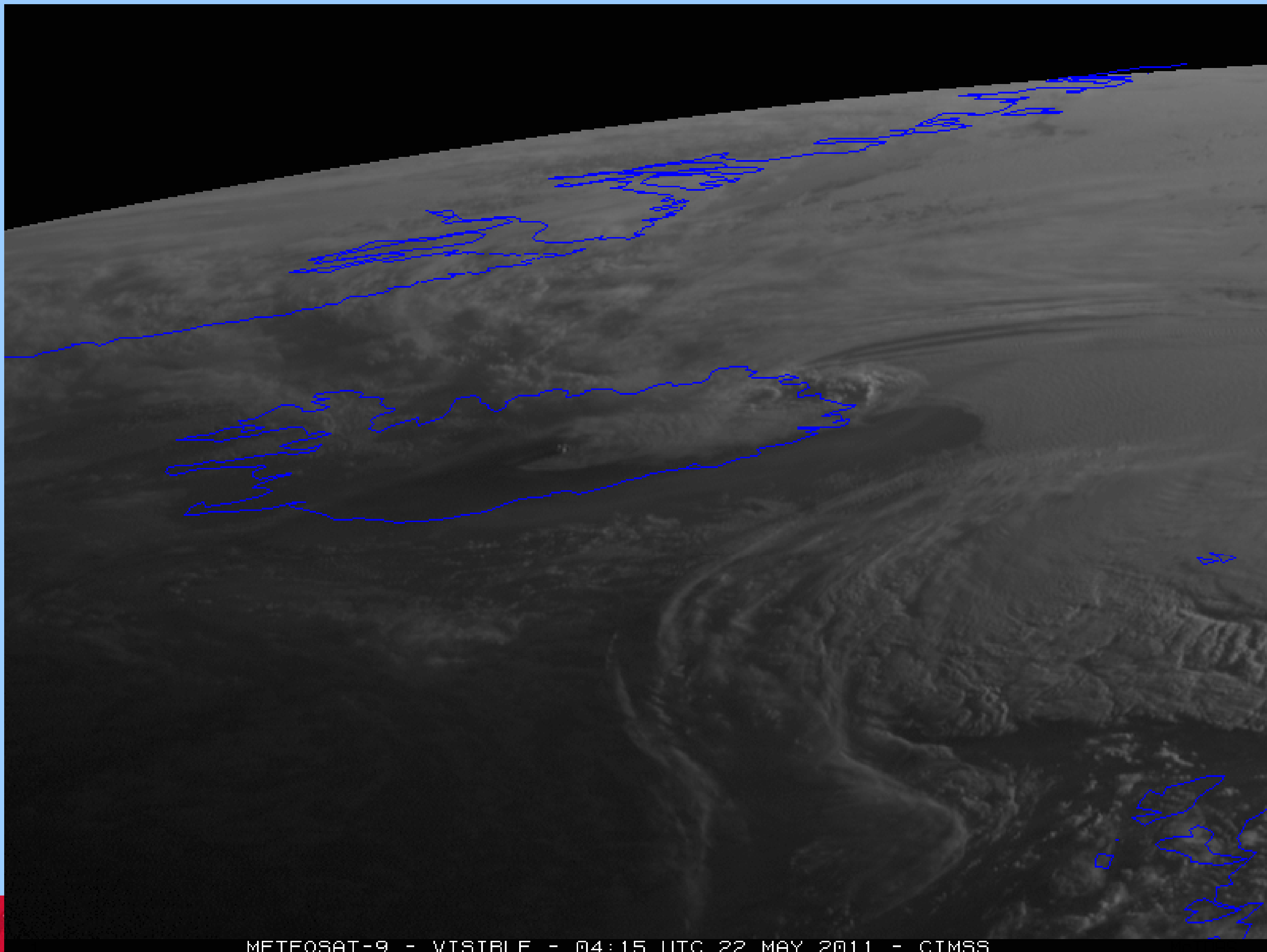
METEOSAT-9 - VISIBLE - 04:15 UTC 22 MAY 2011 - CIMSS


Mt. Erebus, Sept. 22, 2004


Mt. Erebus, Oct. 3, 2004

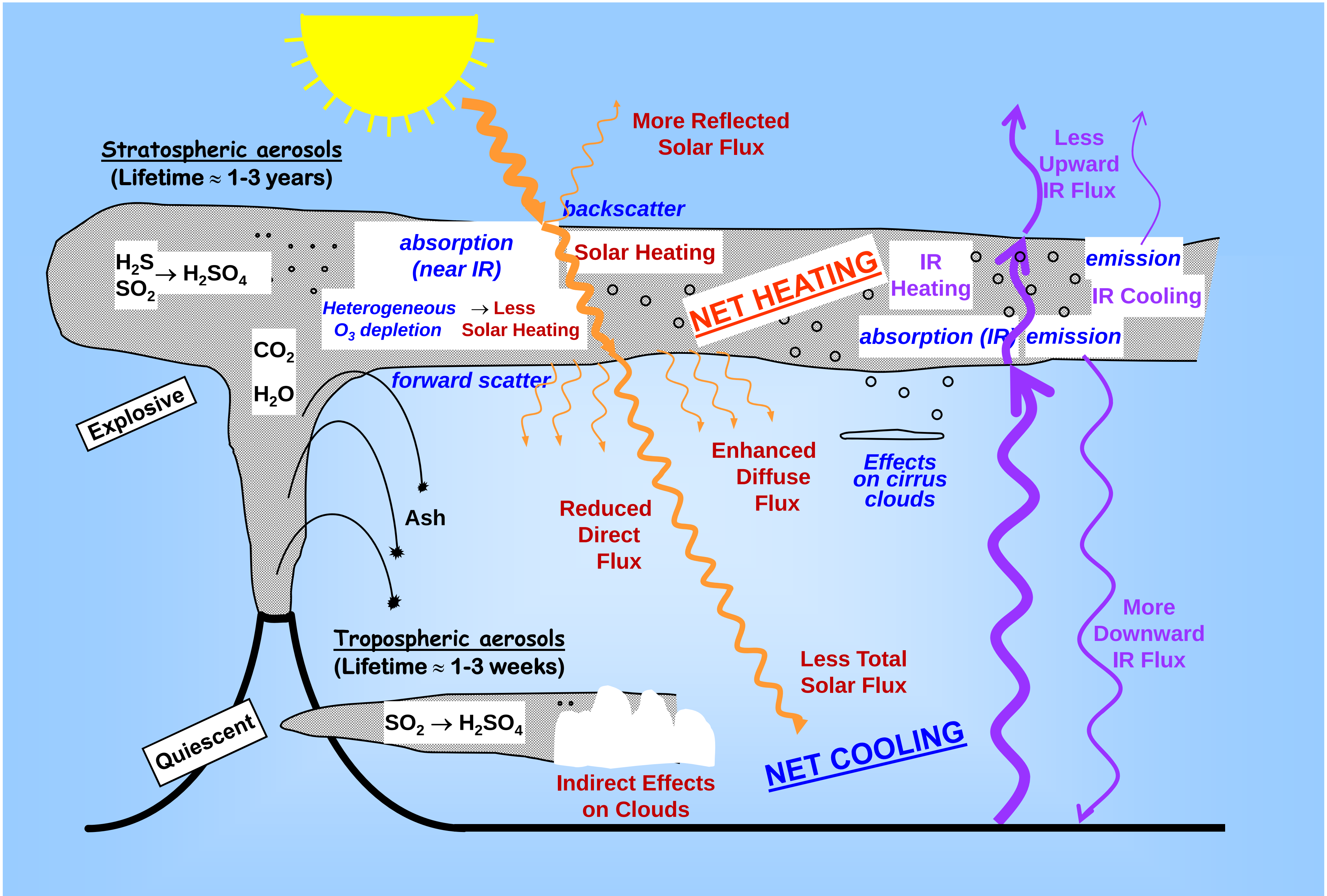

Alan Robock
Department of Environmental Sciences

Aerosol properties

We define the dry aerosol effective radius as 0.25 μm compared to 0.35 μm for our Pinatubo simulations. This creates hydrated sulfate aerosols approx 0.30-0.35 μm for our geoengineering runs and 0.47-0.52 μm for our Pinatubo simulations.

It is difficult to say the size at which the aerosols will end up without a microphysical model that has coagulation but by injecting daily vs. one eruption per year, coagulation would be reduced since concentrations are lower and more globally distributed. On the other hand, particles might grow larger than those typical of a volcanic eruption if existing particles grow rather than having new particles form.

The smaller size aerosols have a slightly longer lifetime so this would reduce the rate of injection needed to maintain a specific loading.

Aerosol properties

By using a smaller aerosol size (about 30% less than Pinatubo), there is about half the heating of the lower tropical stratosphere as compared to the equivalent loading using a Pinatubo size aerosol.

We injected it at about the same altitude as Pinatubo but if the sulfate was closer to the tropopause and larger in size it would warm the tropopause cold point and let a lot more water vapor into the stratosphere, and this could cause additional problems that would have to be considered.

Alan Robock
Department of Environmental Sciences

Heckendorn et al. (2009) showed particles would grow, requiring much larger injections for the same forcing.

Environ. Res. Lett. **4** (2009) 045108 P Heckendorn *et al*

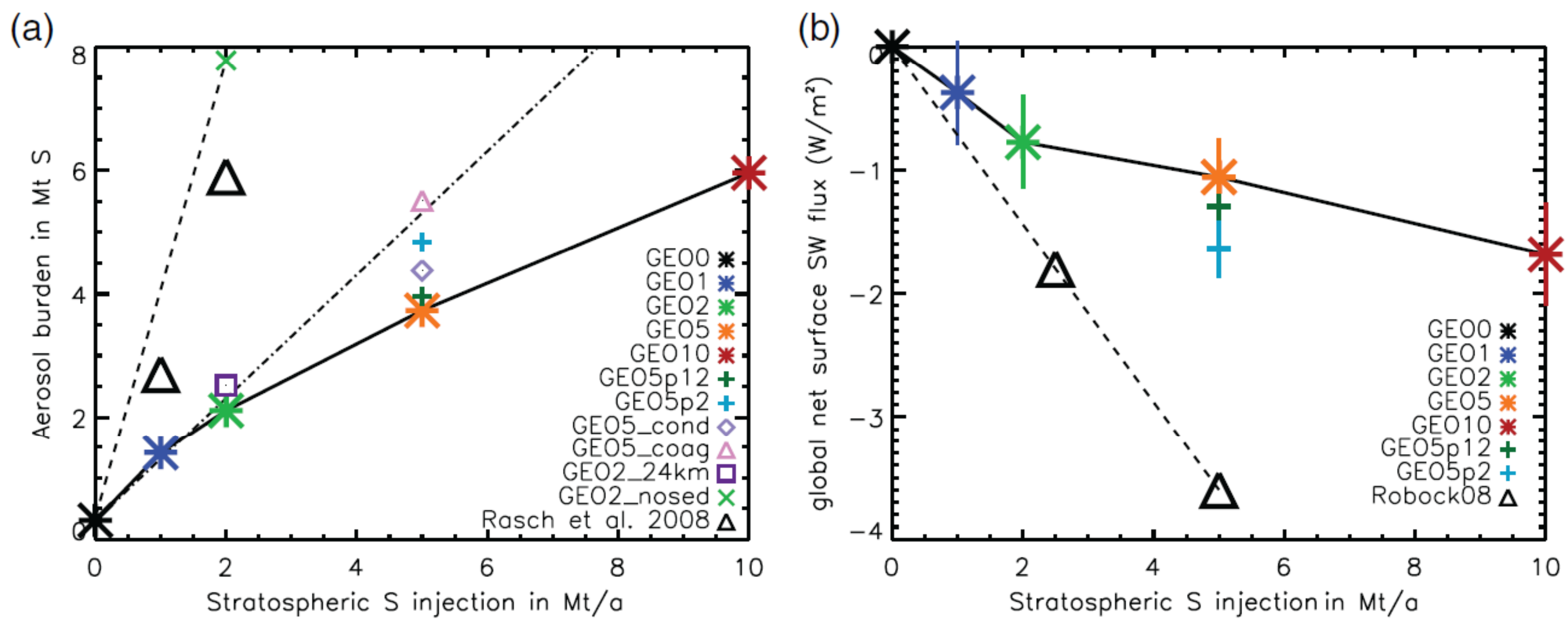

Figure 4. (a) Total aerosol burden as function of sulfur injected annually into the stratosphere (0, 1, 2, 5 and 10 Mt/a S) calculated by the AER model. Dash–dotted line: aerosol burden, if the aerosol residence time were 1 year irrespective of injection strength. Dashed line: aerosol burden when aerosol sedimentation is suppressed in the stratosphere. All results for injections at 20 km, except black square for 24 km emissions. (b) Change in global annual mean net SW flux change at the surface due to geoengineering in comparison with GEO0 calculated by SOCOL for all-sky conditions. Vertical bars: standard deviation of monthly values. Triangles: SW downward flux changes due to geoengineering as proposed by Robock *et al* (2008). All lines in both panels are meant to guide the eye.

Pierce et al. (GRL, 2010) claim emitting sulfuric acid directly will produce larger particles, helping solve the problem of aerosol growth.

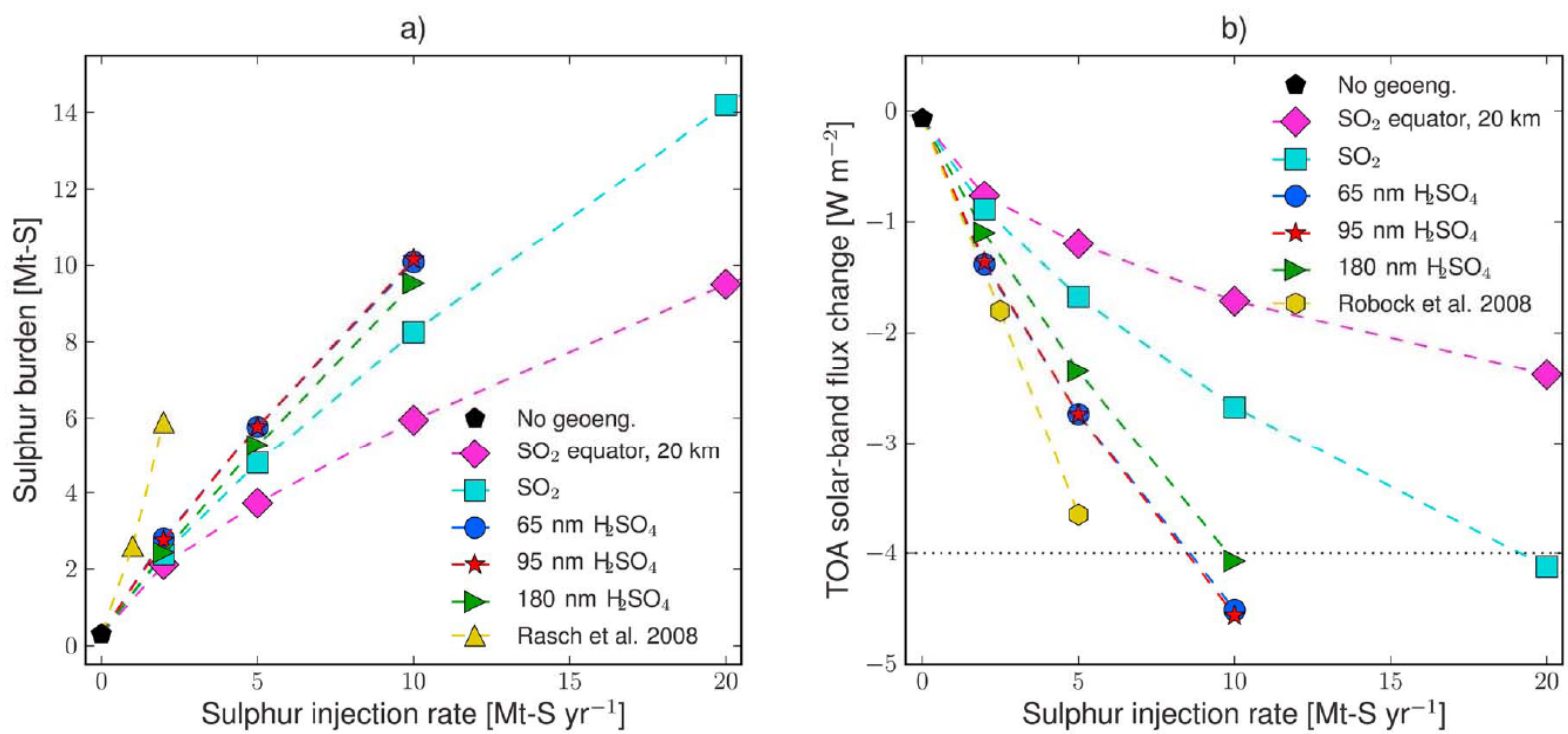

Figure 4. Steady-state (a) stratospheric sulfur burden and (b) top-of-atmospheric solar-band (shortwave) radiative flux change from the stratospheric aerosols as a function of sulfur injection rate. All simulations have emissions evenly distributed between 30°S–30°N and 20–25 km, except results for SO_2 emitted only above the equator (5°S–5°N) at 20 km (19.5–20.5 km). Also included for comparison are the stratospheric sulfur burdens computed by *Rasch et al.* [2008a] (with fixed effective radius of 0.43 μm) and the solar flux changes by *Robock et al.* [2008], both without aerosol microphysics. Black horizontal dotted line in Figure 4b represents the approximate cooling necessary to offset a doubling of CO_2 in the global-mean energy budget.

Brewer-Dobson Circulation (Plumb, 2007)

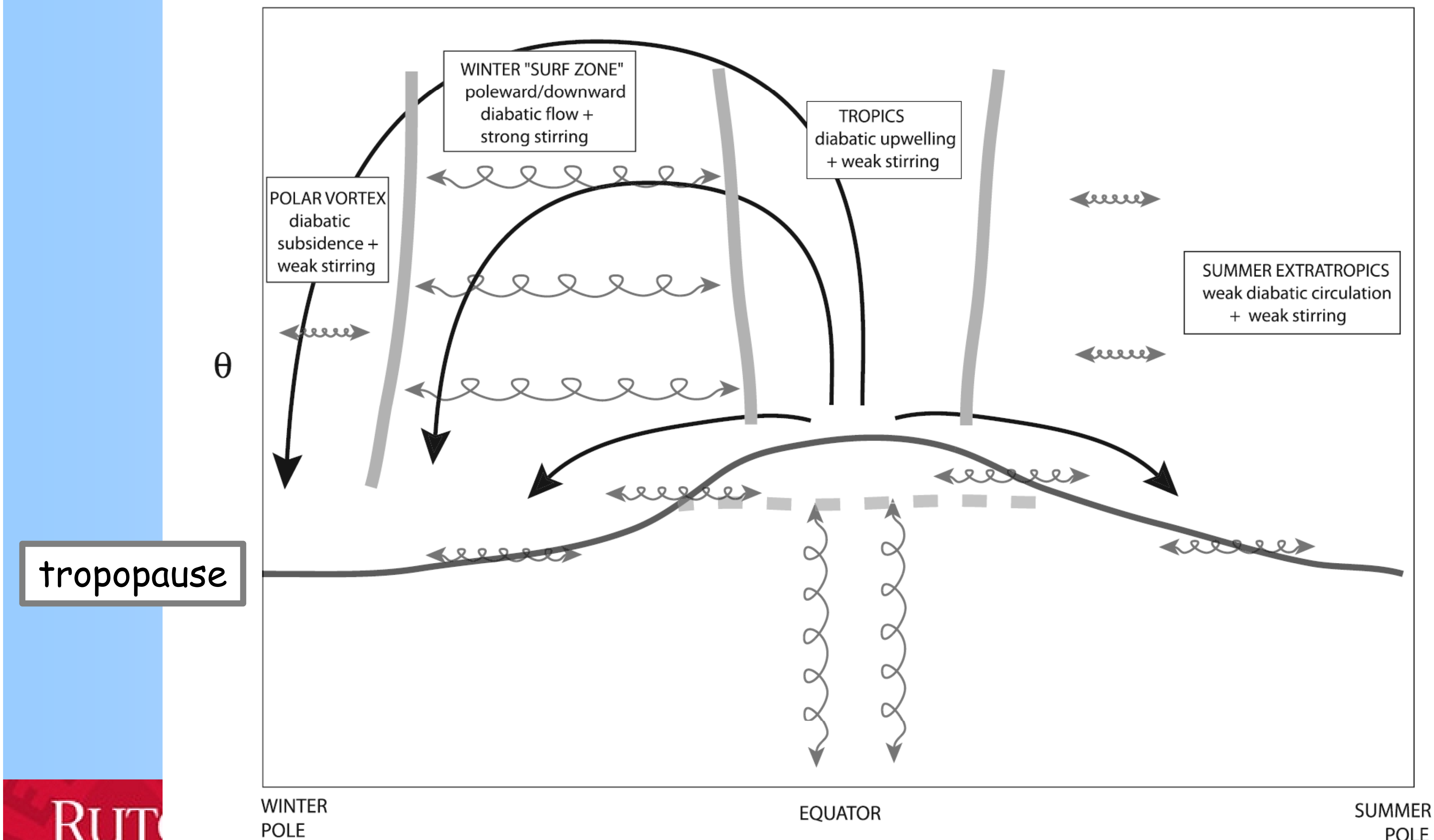

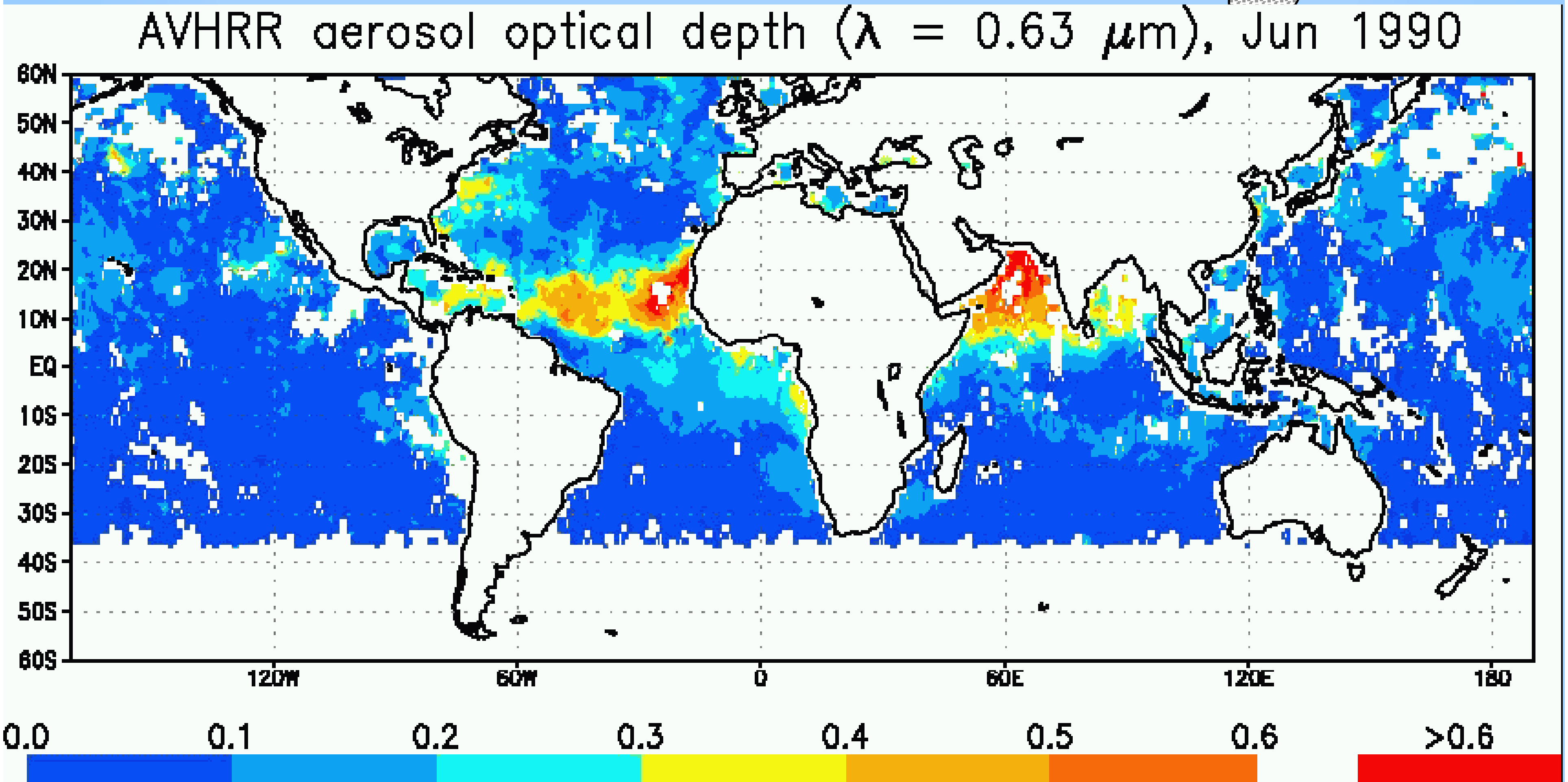

Show with QuickTime

RUTGERS

Stowe *et al.* (1997)

Alan Robock
Department of Environmental Sciences

Change in downward solar radiation at Earth's surface

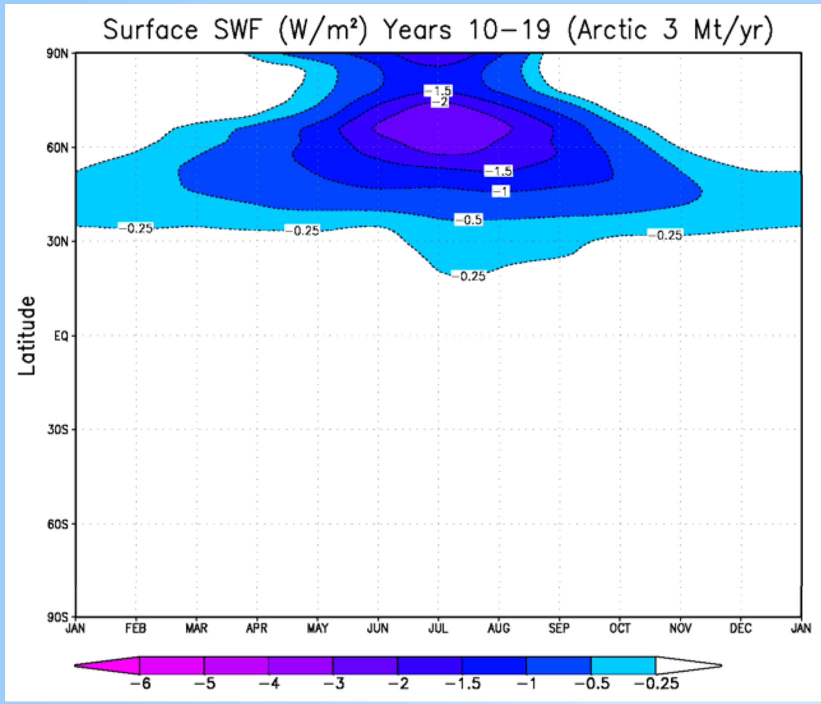

Arctic emission at 68°N leaks into the subtropics

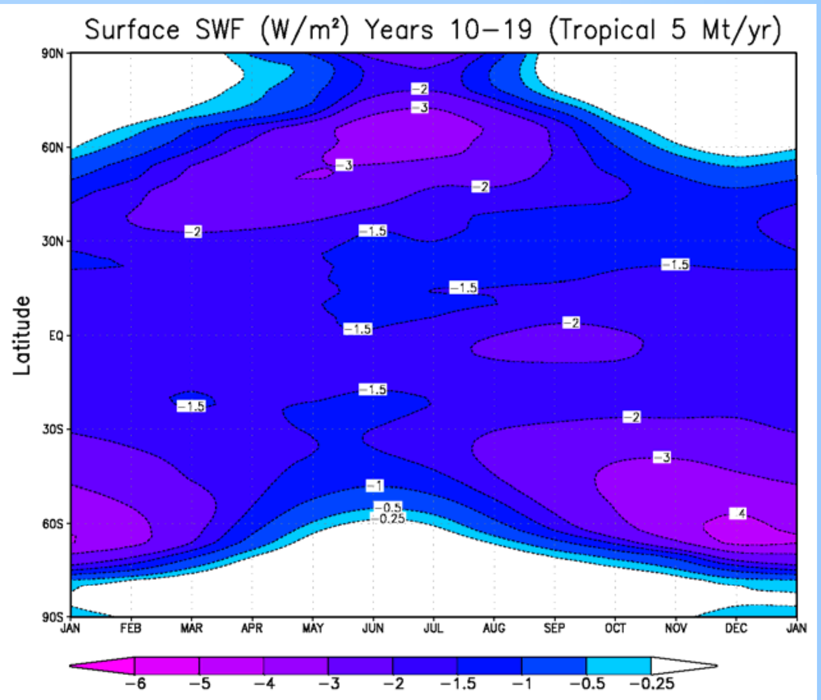

Tropical emission spreads to cover the planet

RUTGERS
Alan Robock
Department of Environmental Sciences

EFFECTS OF LARGE EXPLOSIVE TROPICAL VOLCANOES ON WEATHER AND CLIMATE

EFFECT/MECHANISM	BEGINS	DURATION
1. Enhance or reduce El Niño? Tropospheric absorption of shortwave and longwave radiation, dynamics	1-2 weeks	1-2 months
2. Reduction of diurnal cycle Blockage of shortwave and emission of longwave radiation	Immediately	1-4 days
3. Summer cooling of NH tropics, subtropics Blockage of shortwave radiation	Immediately	1-2 years
4. Reduced tropical precipitation Blockage of shortwave radiation, reduced evaporation	Immediately	~1 year
5. Reduced Sahel precipitation Blockage of shortwave radiation, reduced land temp., reduced evaporation Weaker African monsoon	1-3 months	1-2 years

RUTGERS
Alan Robock
Department of Environmental Sciences

EFFECTS OF LARGE EXPLOSIVE TROPICAL VOLCANOES ON WEATHER AND CLIMATE

EFFECT/MECHANISM	BEGINS	DURATION
6. Ozone depletion, enhanced UV	1 day	1-2 years
Dilution, stratospheric heating, heterogeneous chemistry on aerosols		
7. Global cooling	Immediately	1-3 years
Blockage of shortwave radiation	multiple eruptions:	10-100 years
8. Stratospheric warming	Immediately	1-2 years
Stratospheric absorption of shortwave and longwave radiation		
9. Winter warming of NH continents	½-1½ years	1 or 2 winters
Stratospheric absorption of shortwave and longwave radiation, dynamics		

Alan Robock
Department of Environmental Sciences

EFFECTS OF EXPLOSIVE HIGH-LATITUDE VOLCANOES ON WEATHER AND CLIMATE

EFFECT/MECHANISM	BEGINS	DURATION
High latitude eruptions:		
10. Cooling of continents Blockage of shortwave radiation	Immediately	1-2 years
11. Reduction of Indian summer monsoon Continental cooling, reduction of land-sea temperature contrast	½-1 year	1 or 2 summers
12. Reduction of African summer monsoon Continental cooling, reduction of land-sea temperature contrast	½-1 year	1 or 2 summers
13. Reduction of Nile River flow Reduced monsoon precipitation	½-1 year	1-2 years

RUTGERS
Alan Robock
Department of Environmental Sciences

Major volcanic eruptions of the past 250 years

Volcano	Year	VEI	d.v.i./E_{max}	IVI2
Lakagígar [Laki craters], Iceland	1783	4	2300	93.0
Unknown (El Chichón?)	1809			53.7
Tambora, Sumbawa, Indonesia	1815	7	3000	109.8
Cosiguina, Nicaragua	1835	5	4000	40.2
Askja, Iceland	1875	5	1000	0.0
Krakatau, Indonesia	1883	6	1000	21.9
Okataina [Tarawera], North Island, NZ	1886	5	800	1.9
Santa María, Guatemala	1902	6	600	3.8
Ksudach, Kamchatka, Russia	1907	5	500	0.0
Novarupta [Katmai], Alaska, US	1912	6	500	11.0
Agung, Bali, Indonesia	1963	4	800	20.9
Mt. St. Helens, Washington, US	1980	5	500	0.0
El Chichón, Chiapas, Mexico	1982	5	800	*
Mt. Pinatubo, Luzon, Philippines	1991	6	1000	30.1

Major volcanic eruptions of the past 250 years

Volcano	Year	VEI	d.v.i./E_{max}	IVI2
Lakagígar [Laki craters], Iceland	1783	4	2300	93.0
Unknown (El Chichón?)	1809			53.7
Tambora, Sumbawa, Indonesia	1815	7	3000	109.8
Cosiguina, Nicaragua	1835	5	4000	40.2
Askja, Iceland	1875	5	1000	0.0
Krakatau, Indonesia	1883	6	1000	21.9
Okataina [Tarawera], North Island, NZ	1886	5	800	1.9
Santa María, Guatemala	1902	6	600	3.8
Ksudach, Kamchatka, Russia	1907	5	500	0.0
Novarupta [Katmai], Alaska, US	1912	6	500	11.0
Agung, Bali, Indonesia	1963	4	800	20.9
Mt. St. Helens, Washington, US	1980	5	500	0.0
El Chichón, Chiapas, Mexico	1982	5	800	*
Mt. Pinatubo, Luzon, Philippines	1991	6	1000	30.1

Famous Volcanic Eruptions

Santorini, 1628 BC

Etna, 44 BC

Lakagígar, 1783

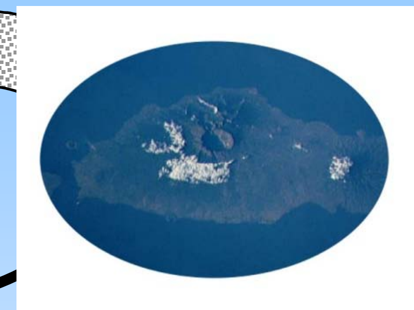

Tambora, 1815

Toba, 74,000 BP

Krakatau, 1883

Pinatubo, 1991

El Chichón, 1982

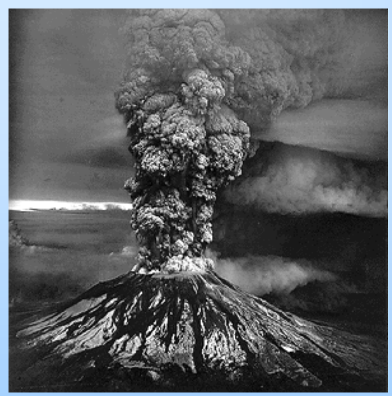

St. Helens, 1980

Agung, 1963

Alan Robock
Department of Environmental Sciences

Santorini, 1628 B.C.

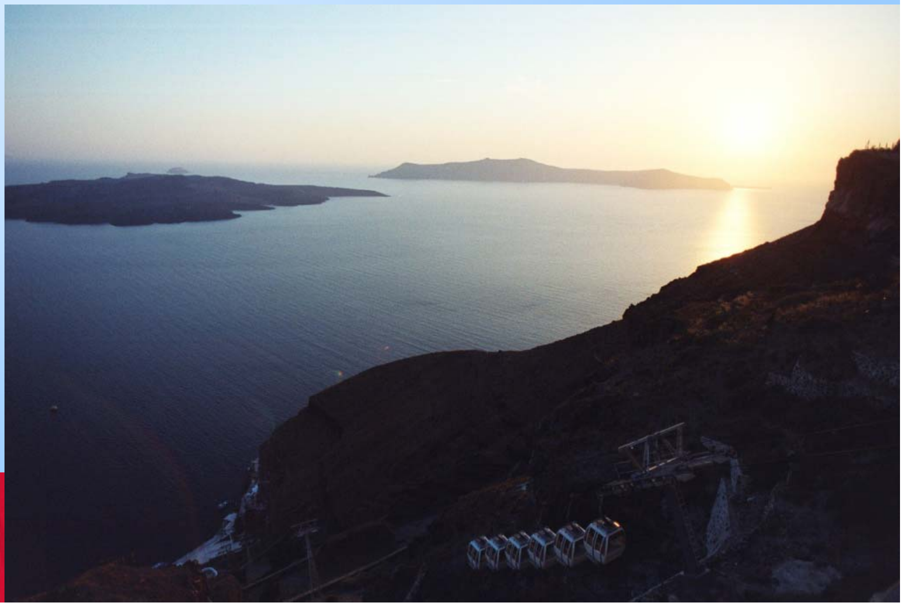

Responsible for the legends of:

- Atlantis (Minoans on Crete)
- Biblical plagues
- Parting of the Red Sea

Etna, 44 B.C.

"The fullest description of the sun in this period is that provided by Plutarch (*Life of Julius Caesar* 69.3-4), who speaks of the rays of the sun being veiled, leaving the face of the sun pale and without radiance and thus furnishing so little heat that fruits never fully ripened, but shriveled instead...'due to the coldness of the atmosphere.'"

(Forsyth, 1988)

Alan Robock
Department of Environmental Sciences


F206 Laki 49
206 Holt 5

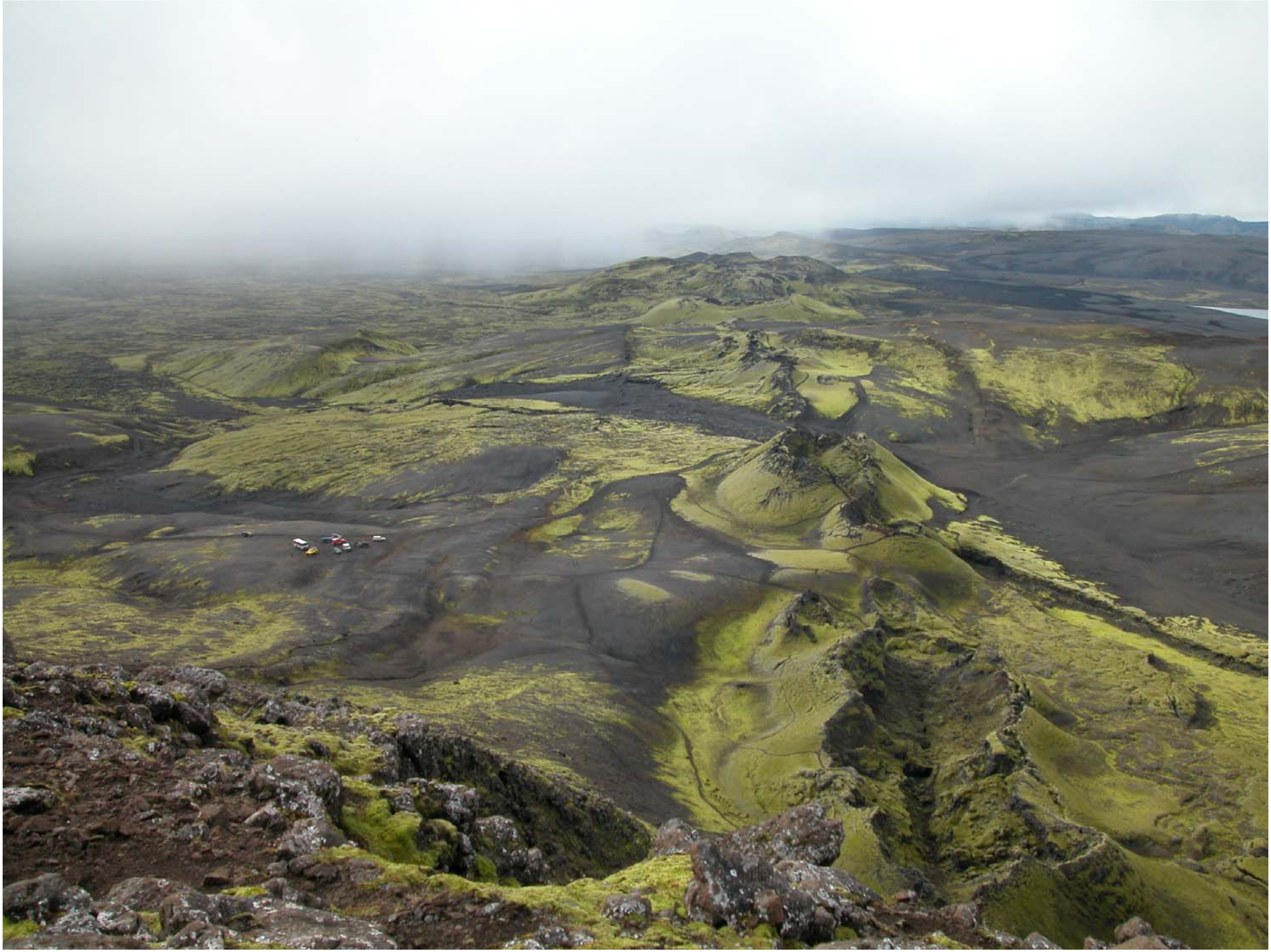

Figure 128. Portrait of Benjamin Franklin by Pierre H. Alix after Charles A.P. van Loo. National Portrait Gallery, Smithsonian Institution, Washington, D.C.

RUTGERS

Franklin (1784)

During several of the summer months of the year 1783, when the effect of the sun's rays to heat the earth in these northern regions should have been greatest, there existed a constant fog over all Europe, and great part of North America. This fog was of a permanent nature; it was dry, and the rays of the sun seemed to have little effect towards dissipating it, as they easily do a moist fog, arising from water. They were indeed rendered so faint in passing through it, that when collected in the focus of a burning glass, they would scarce kindle brown paper. Of course, their summer effect in heating the earth was exceedingly diminished.

Hence the earth was early frozen,

Hence the first snows remained on it unmelted, and received continual additions.

Hence the air was more chilled, and the winds more severely cold.

Hence perhaps the winter of 1783-4, was more severe, than any that had happened for many years.

The cause of this universal fog is not yet ascertained. Whether it was adventitious to this earth, and merely a smoke, proceeding from the consumption by fire of some of those great burning balls or globes which we happen to meet within our rapid course round the sun, and which are sometimes seen to kindle and be destroyed in passing our atmosphere, and whose smoke might be attracted and retained by our earth; or whether it was the vast quantity of smoke, long continuing to issue during the summer from Hecla in Iceland, and that other volcano which arose out of the sea near that island, which smoke might be spread by various winds, over the northern part of the world, is yet uncertain.

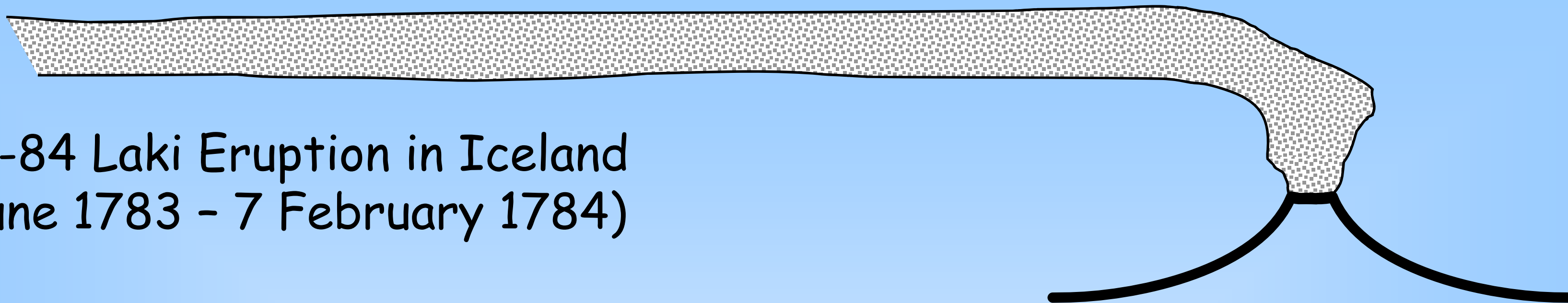

1783-84 Laki Eruption in Iceland
(8 June 1783 – 7 February 1784)

Second largest flood lava eruption in historical time

Iceland's biggest natural disaster

Lava = 14.7 km^3
Tephra = 0.4 km^3

WVZ, EVZ, NVZ are Western, Eastern and Northern Volcanic Zones

Fig. 1 from Thordarson and Self (2003)

RUTGERS
Alan Robock
Department of Environmental Sciences

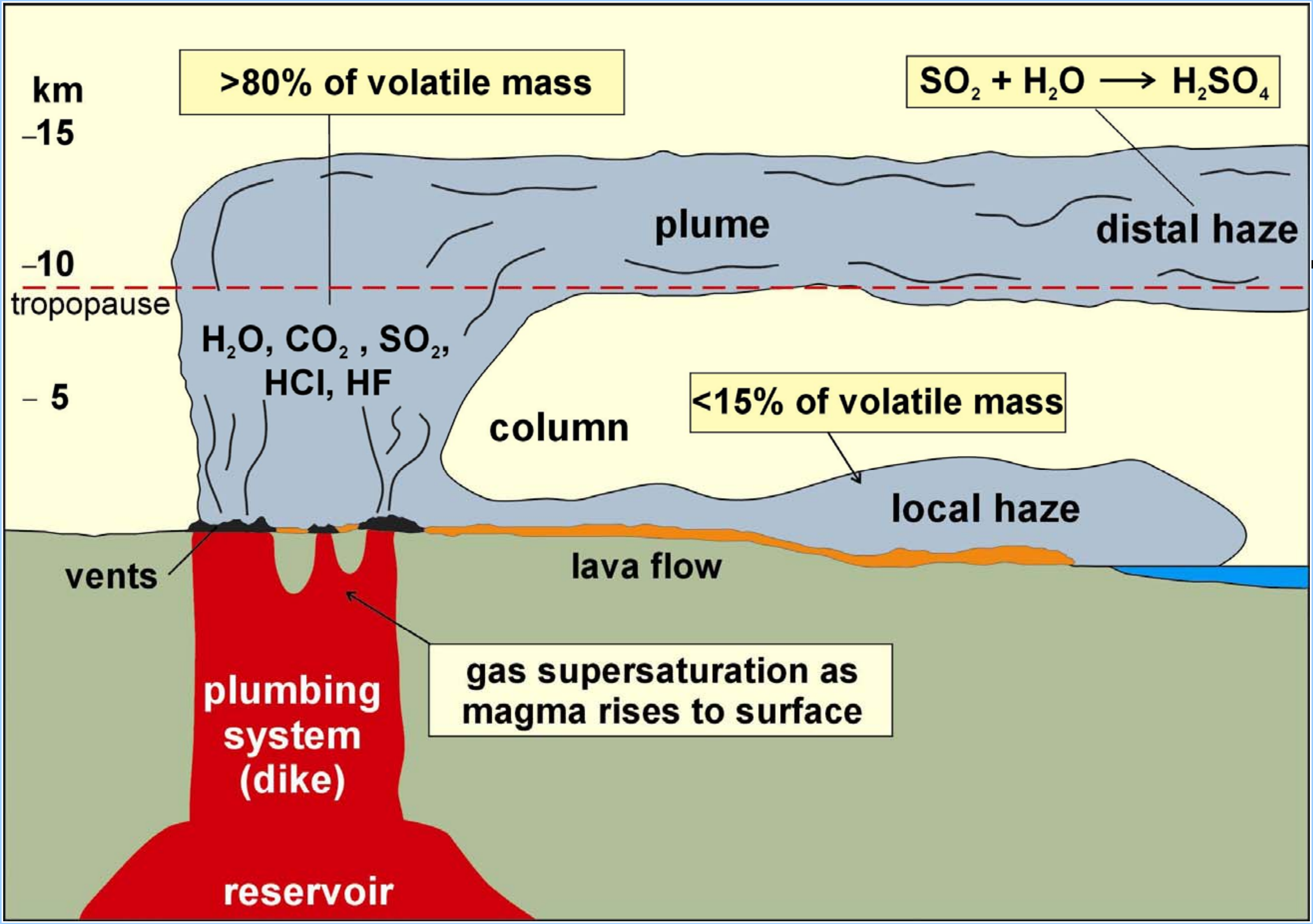

Laki eruption was both tropospheric and stratospheric.

Fig. 3 from Thordarson and Self (2003)

Alan Robock
Department of Environmental Sciences

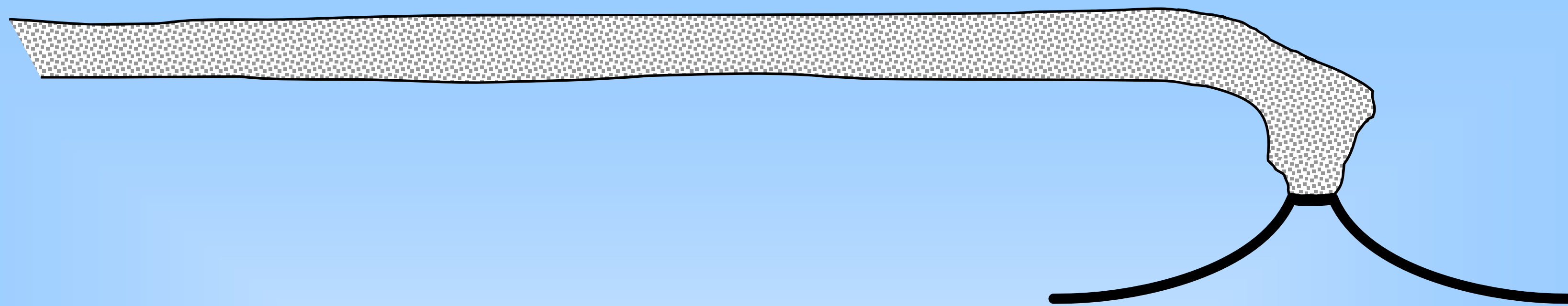

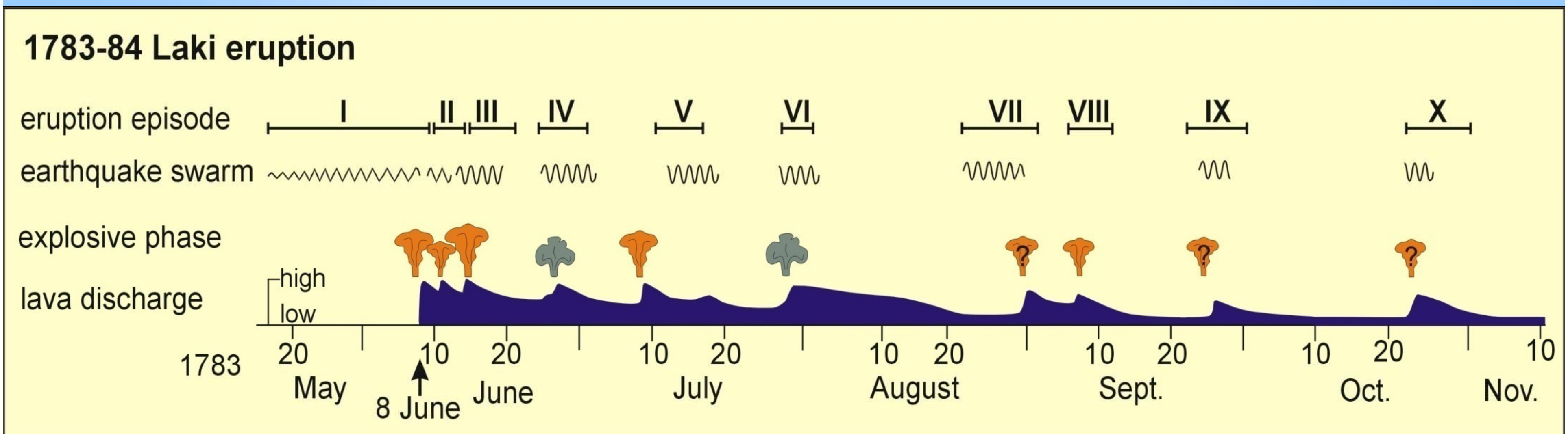

The Laki eruption lasted for 8 months, with continuous effusive emissions into the troposphere, as well as 10 El Chichón-size eruptions to a height of 10-13 km, into the lower stratosphere.

Fig. 2a from Thordarson and Self (2003)

RUTGERS
Alan Robock
Department of Environmental Sciences

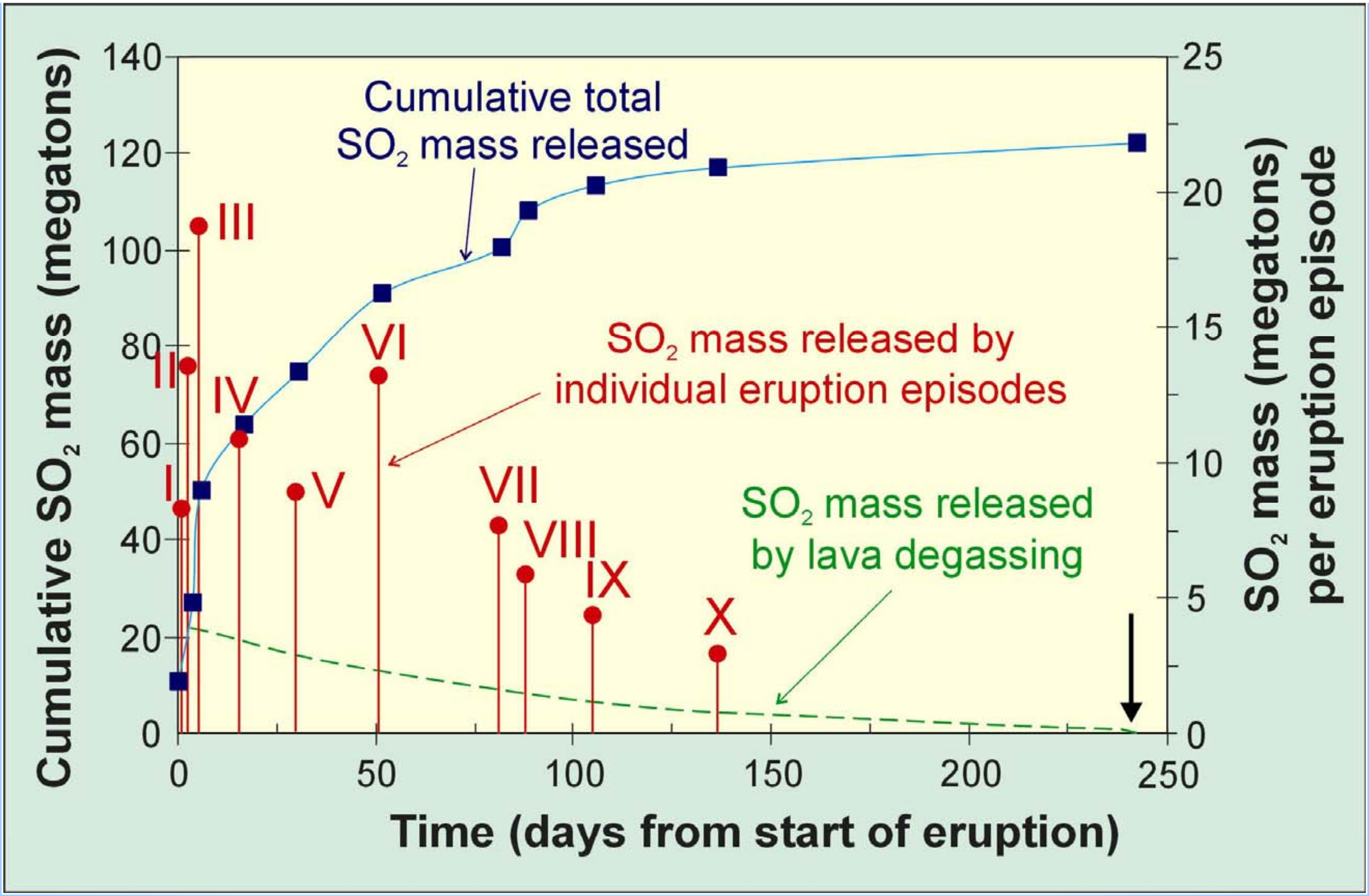

Sulfur mass released

SO_2 total = 122 Mt

SO_2 at vent = 98 Mt

SO_2 by lava = 24 Mt

Fig. 2b from Thordarson and Self (2003)

Other volatiles

H_2O = 235 Mt

CO_2 = 349 Mt

HF = 15 Mt, HCl = 7 Mt

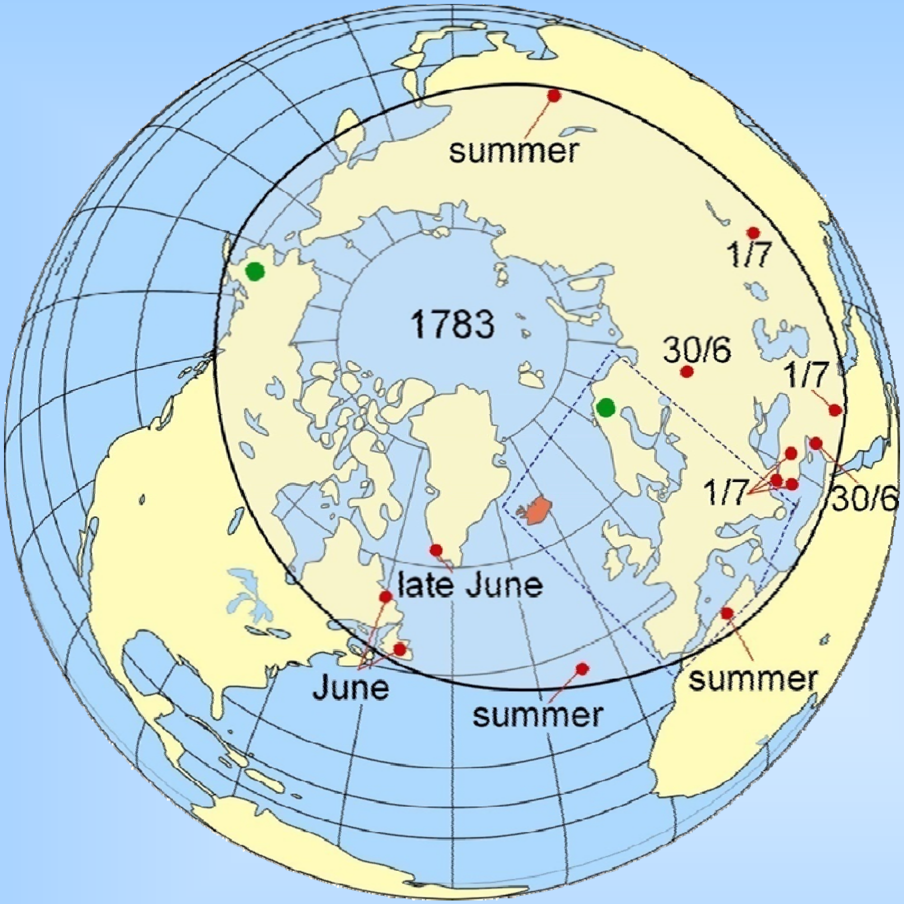

Extent and date of first appearance of Laki haze at surface.

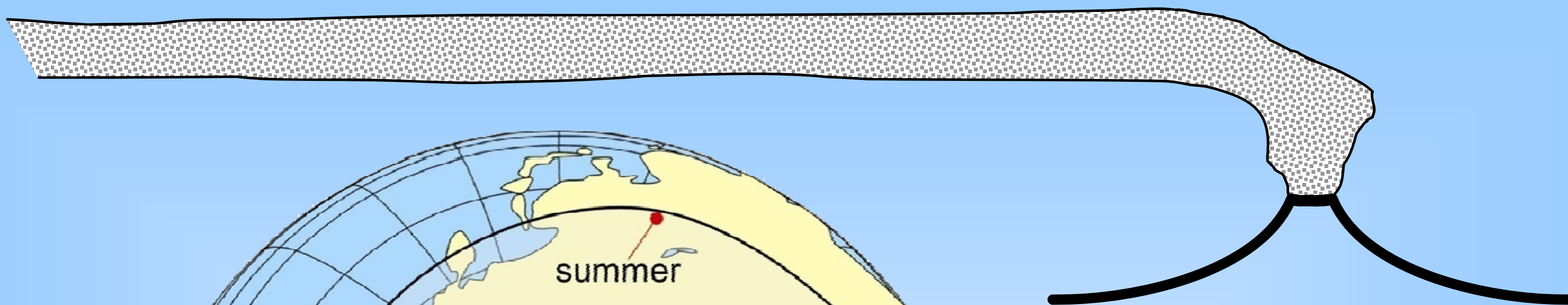

Fig. 4a from Thordarson and Self (2003)

Alan Robock
Department of Environmental Sciences

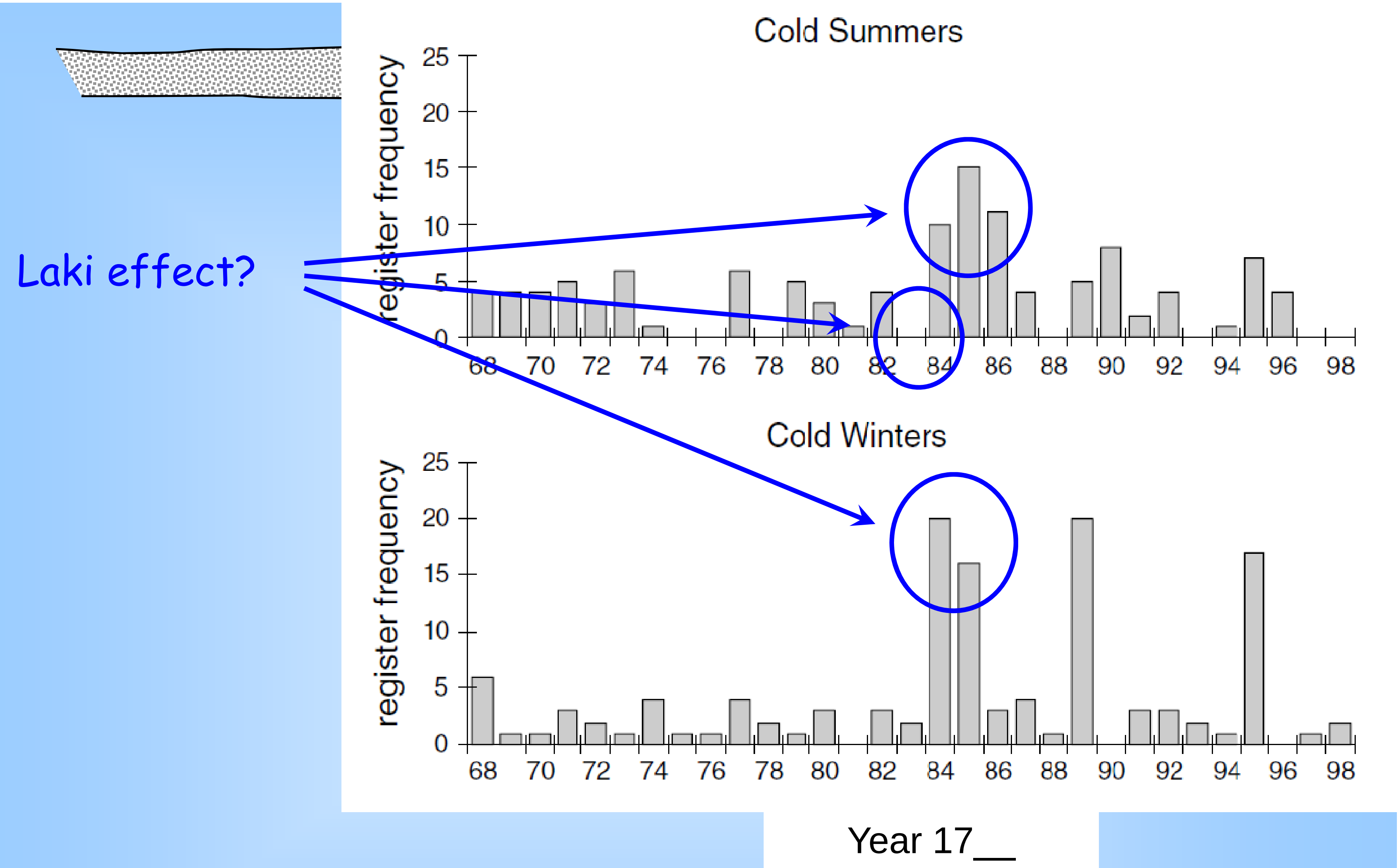

Frequency distribution of cold summers, cold winters, and cold years in Europe and eastern United States during the period 1768 to 1798.

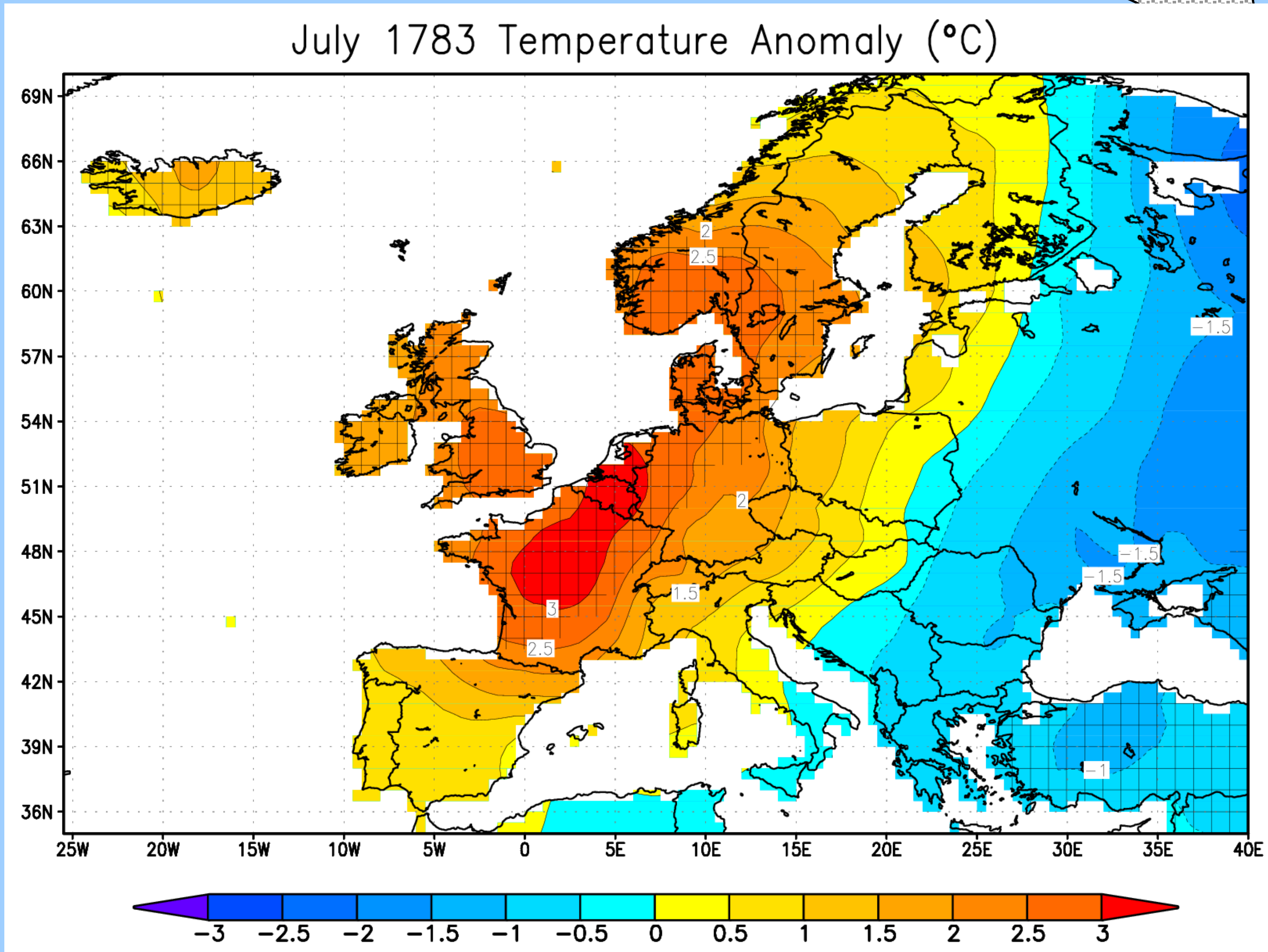

Significant at 90% level

Reconstruction from Luterbacher et al. (2004)

Anomalies based on 31 yr mean, 1770-1800

RUTGERS

Alan Robock
Department of Environmental Sciences

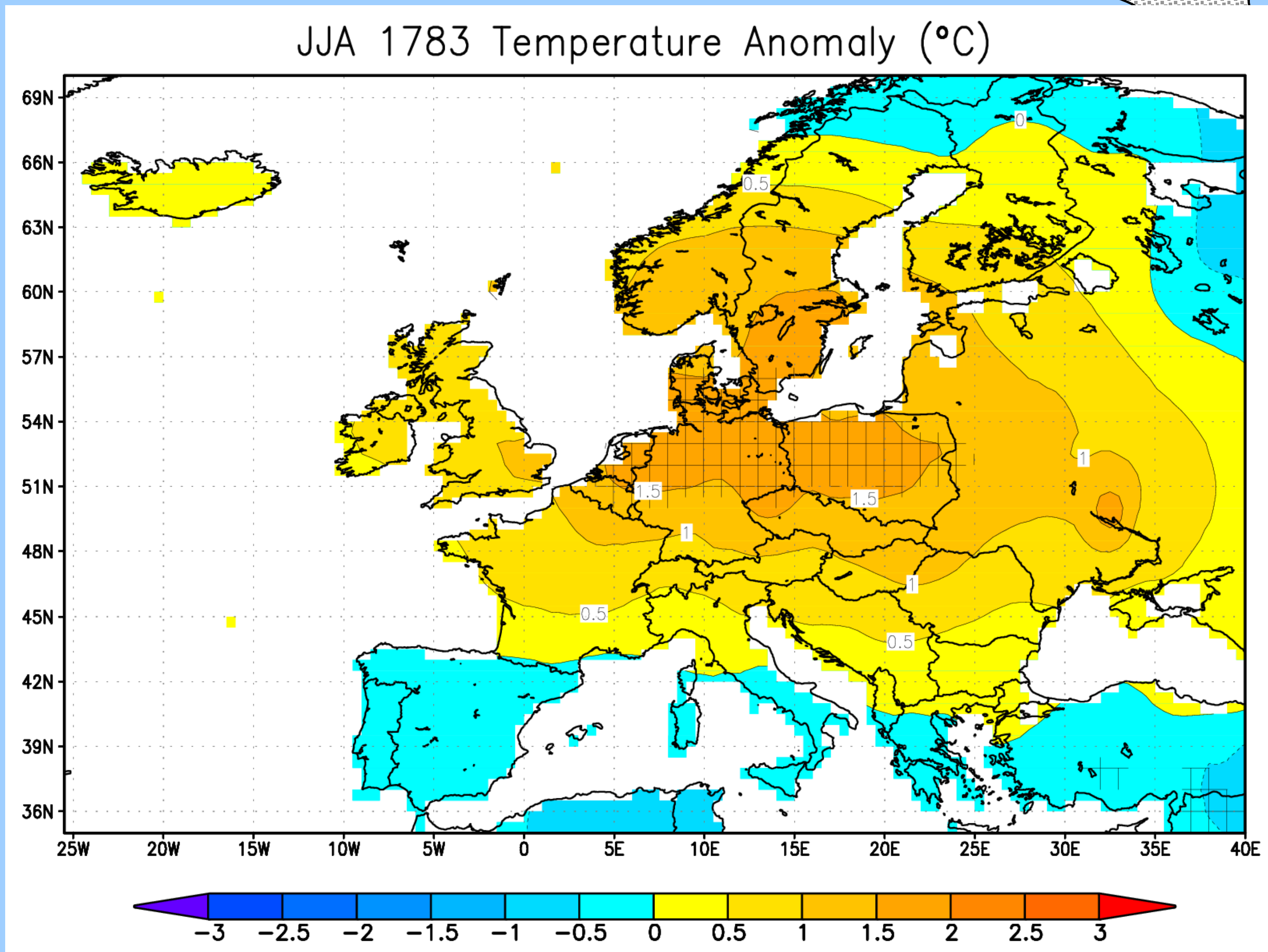

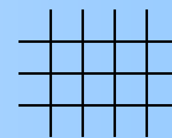

Significant at 90% level

Reconstruction from Luterbacher et al. (2004)

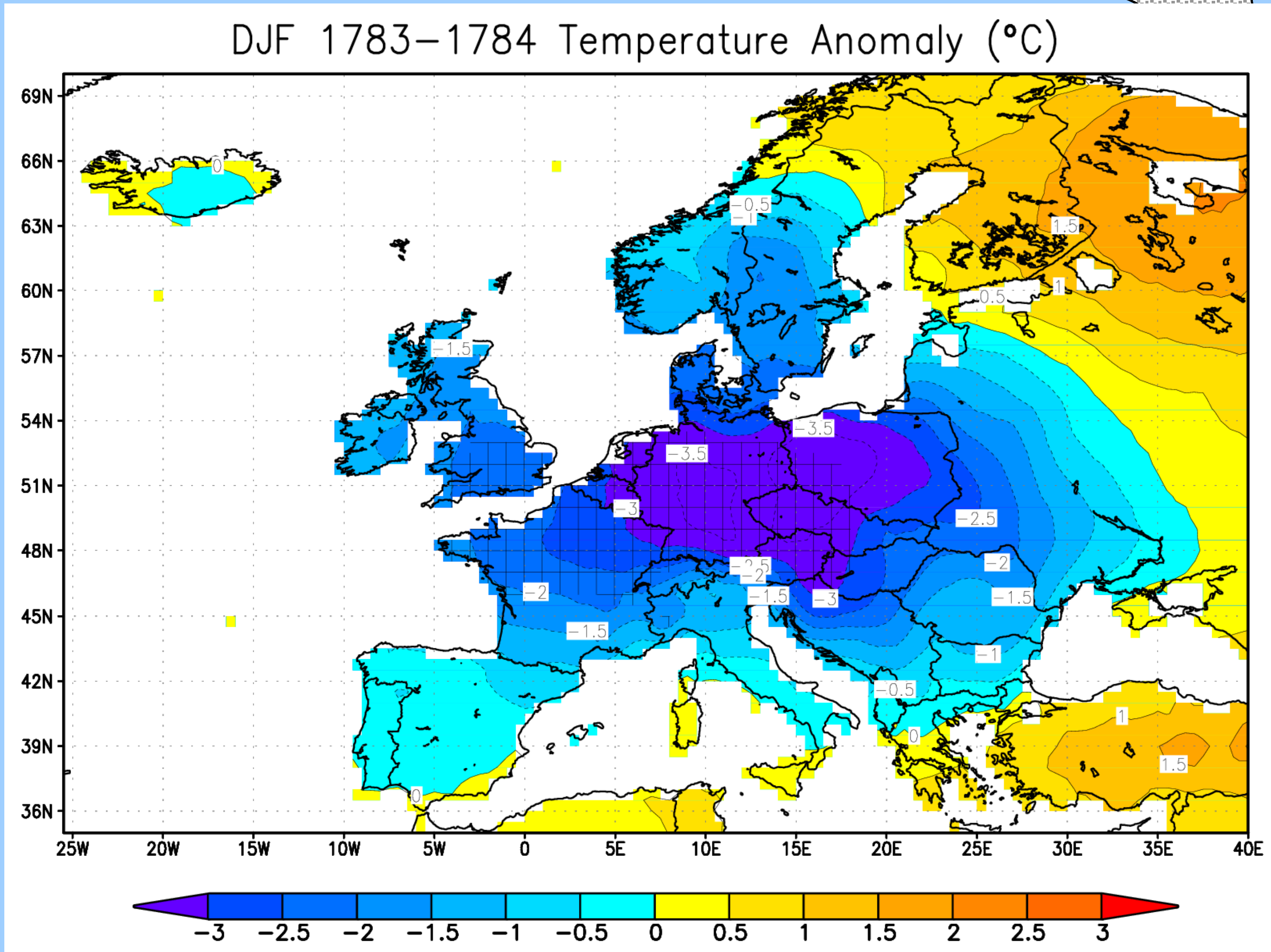

Significant at 90% level

Reconstruction from Luterbacher et al. (2004)

Anomalies based on 31 yr mean, 1770-1800

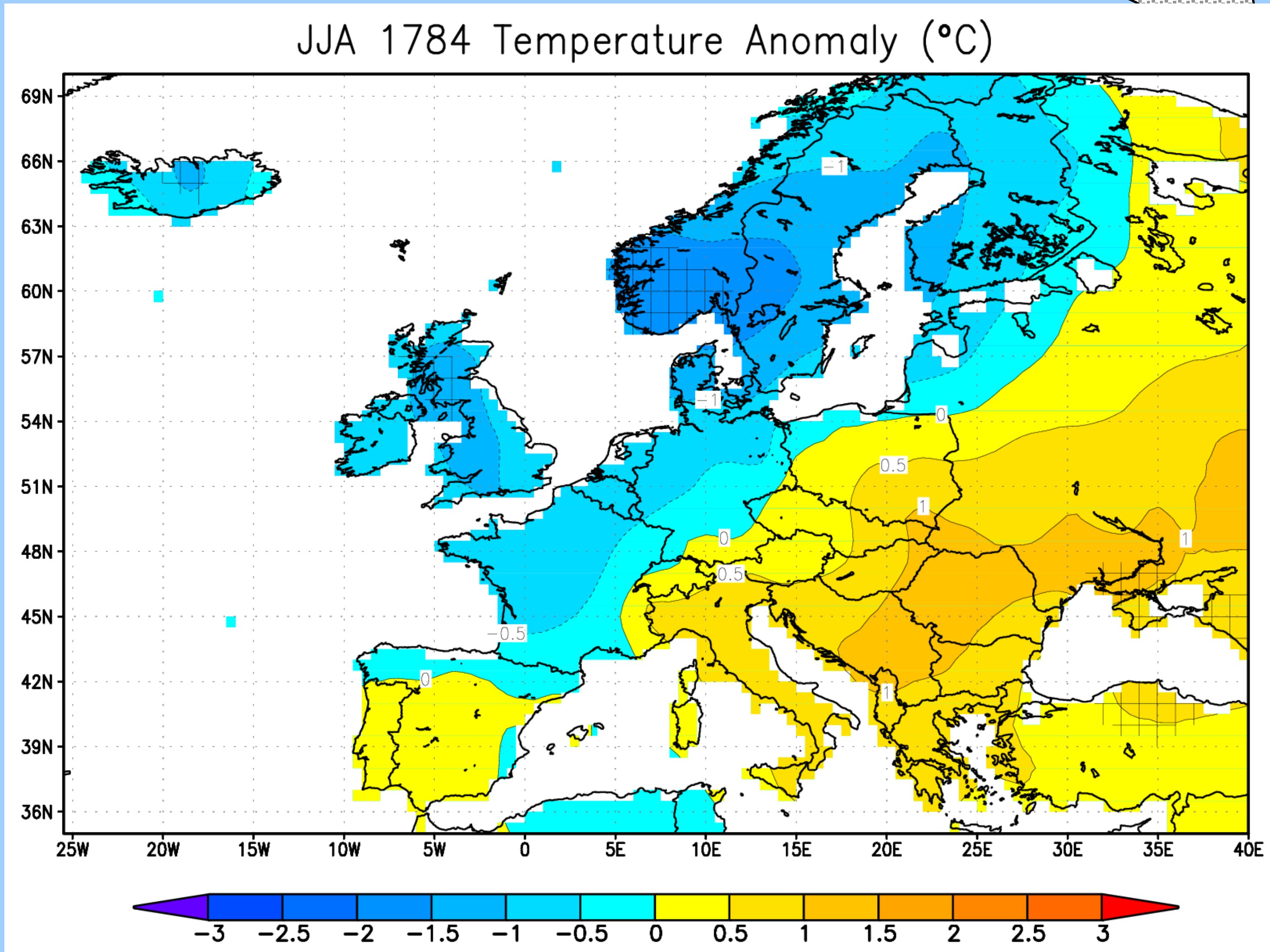

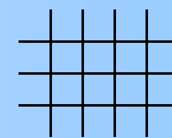

Significant at 90% level

Reconstruction from Luterbacher et al. (2004)

Anomalies based on 31 yr mean, 1770-1800

RUTGERS

Alan Robock
Department of Environmental Sciences

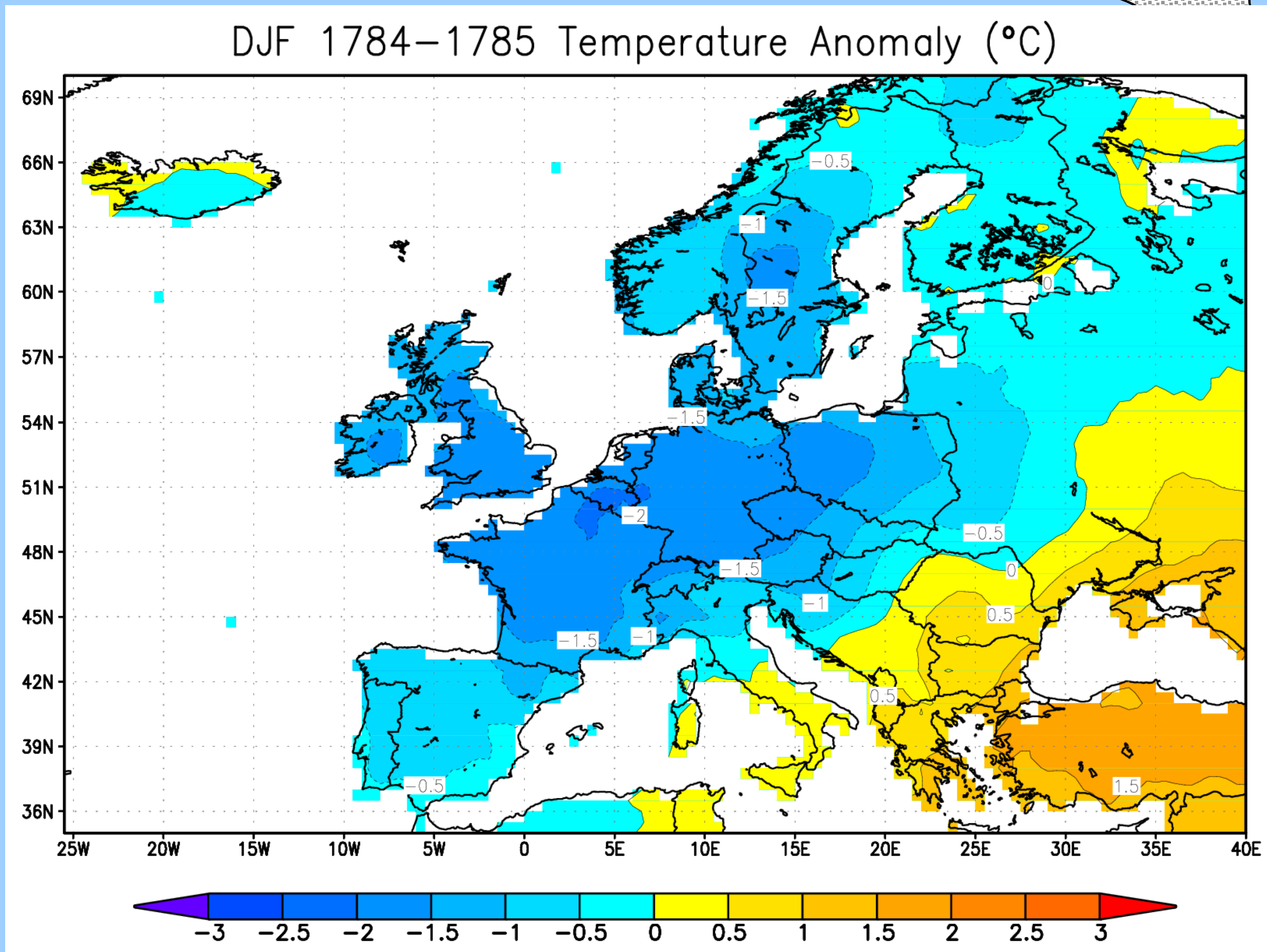

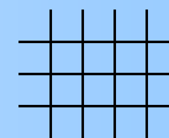

Significant at 90% level

Reconstruction from Luterbacher et al. (2004)

Anomalies based on 31 yr mean, 1770-1800

Alan Robock
Department of Environmental Sciences

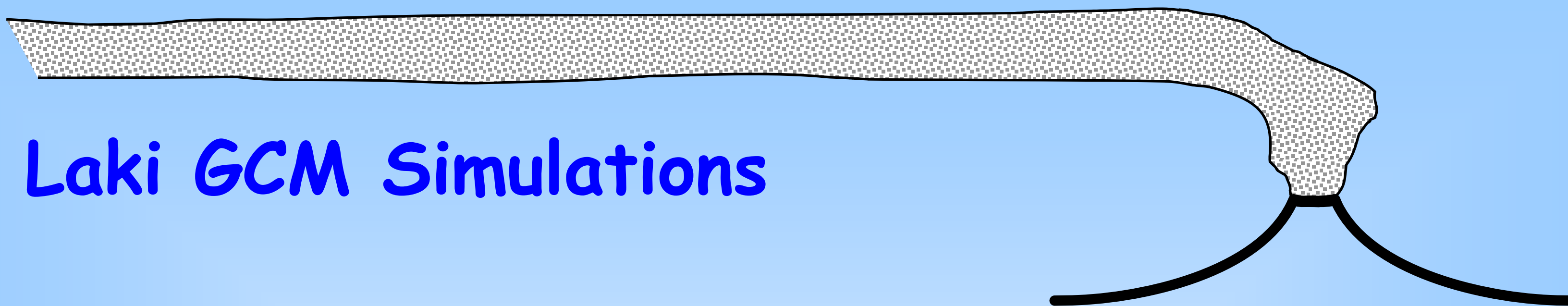

Laki GCM Simulations

- NASA Goddard Institute for Space Studies (GISS) ModelE GCM
- 4°x5° horizontal resolution
- Stratospheric version with 23 vertical levels
- Gravity wave drag scheme
- Fixed climatological SSTs
- Dorothy Koch's sulfur chemistry model, which includes gas-aerosol conversion, transport, and cloud microphysics

Why was the summer of 1783 so warm over Europe?

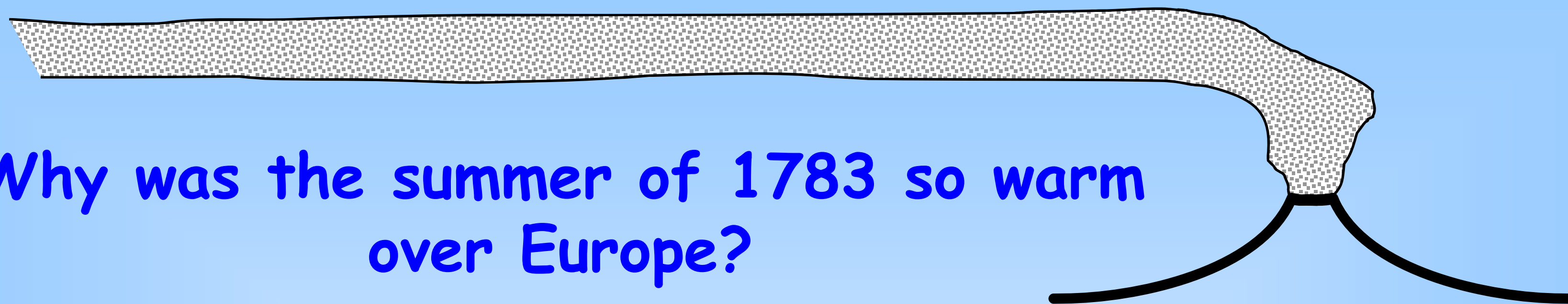

If it was caused by the eruption, there are several possibilities:

1. **Circulation anomalies** induced by radiative forcing from volcanic gases and aerosols.
2. Somehow radiative anomalies from the **sulfate aerosols** caused warming.
3. **SO_2** that had not converted to aerosols acted as a greenhouse gas.

Alan Robock
Department of Environmental Sciences

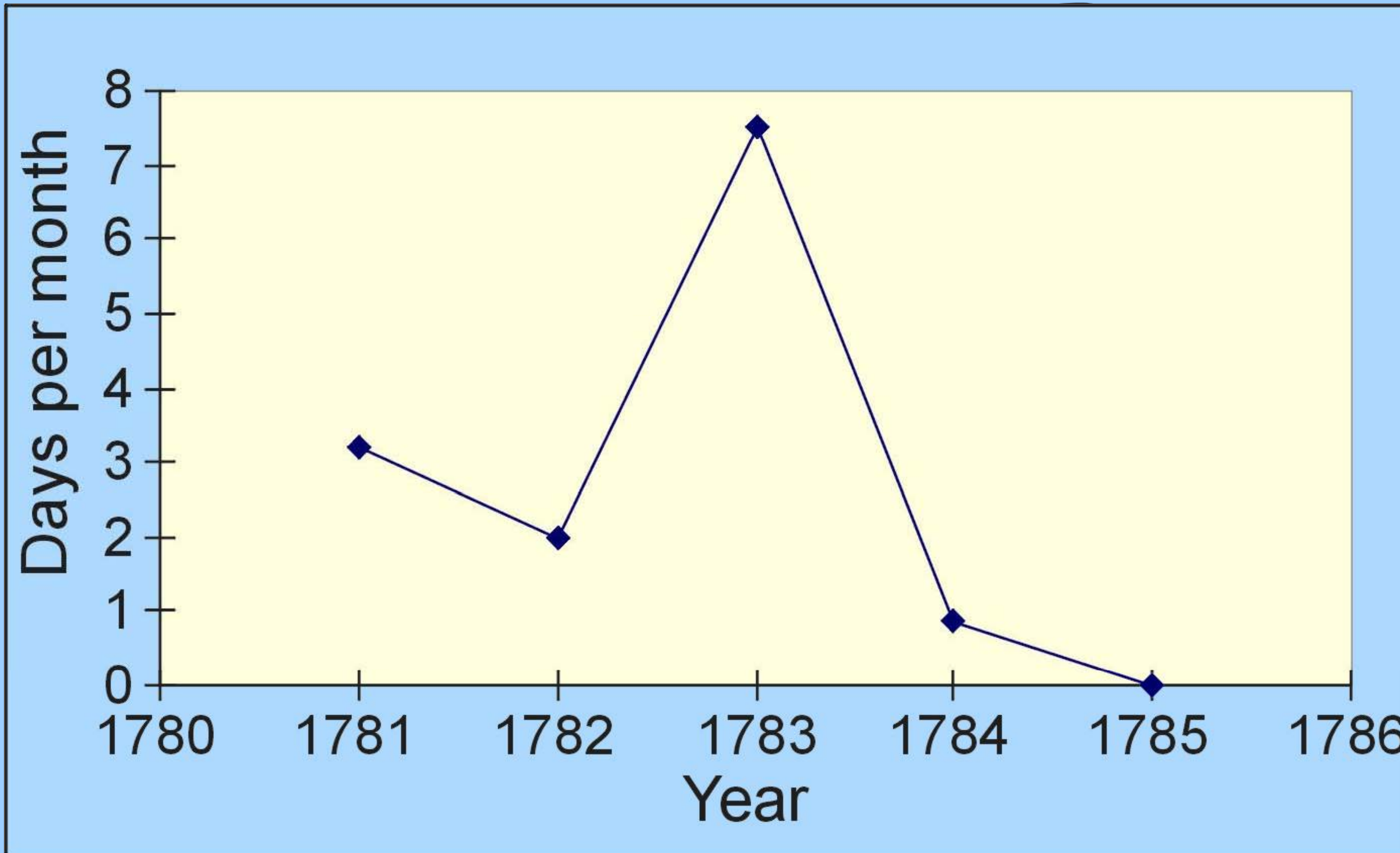

Frequency of southerly weather type in July
for the British Isles. Data from Kington (1988).

Laki SAT Anomaly (°C) JJA 1783 q-flux

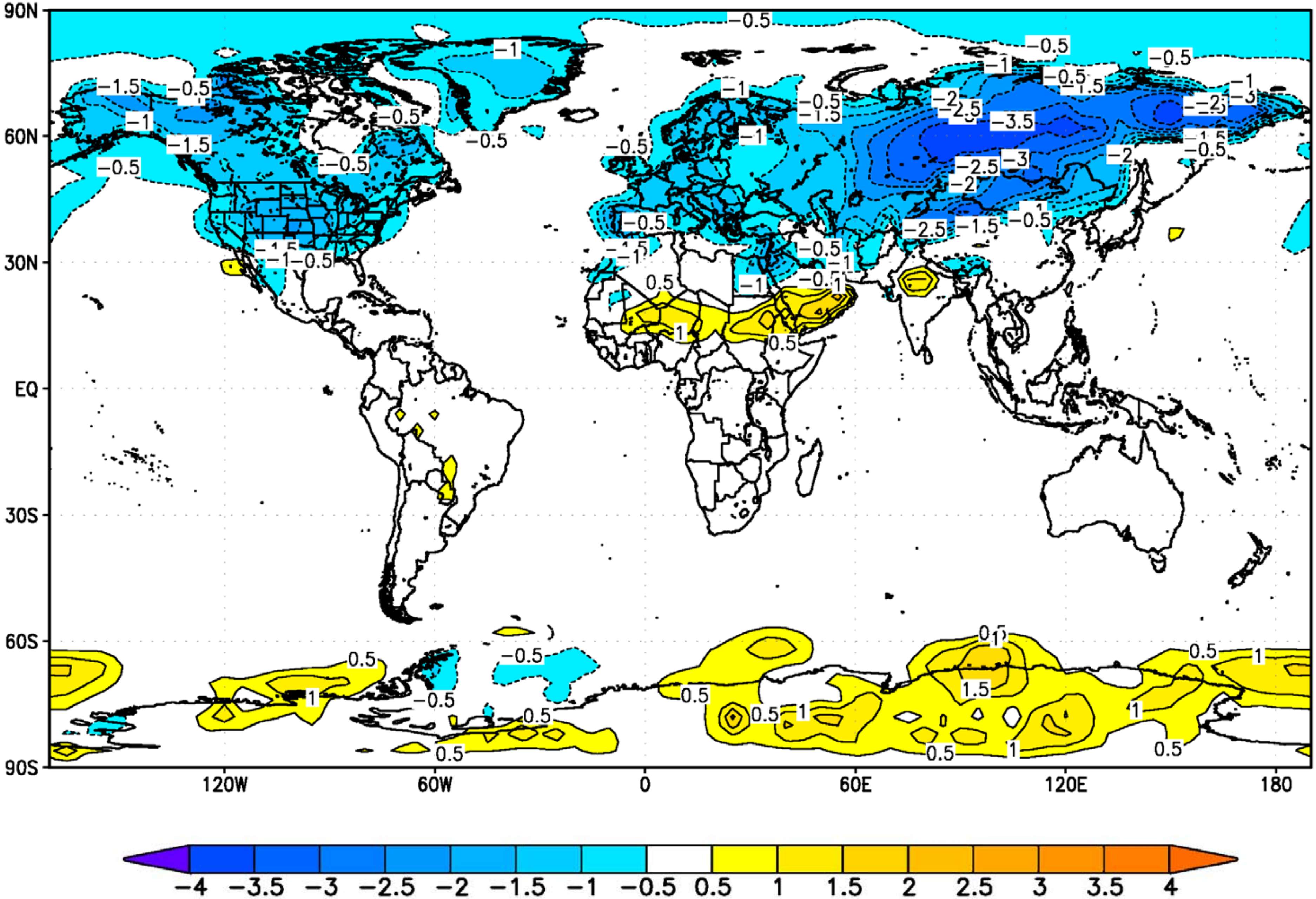

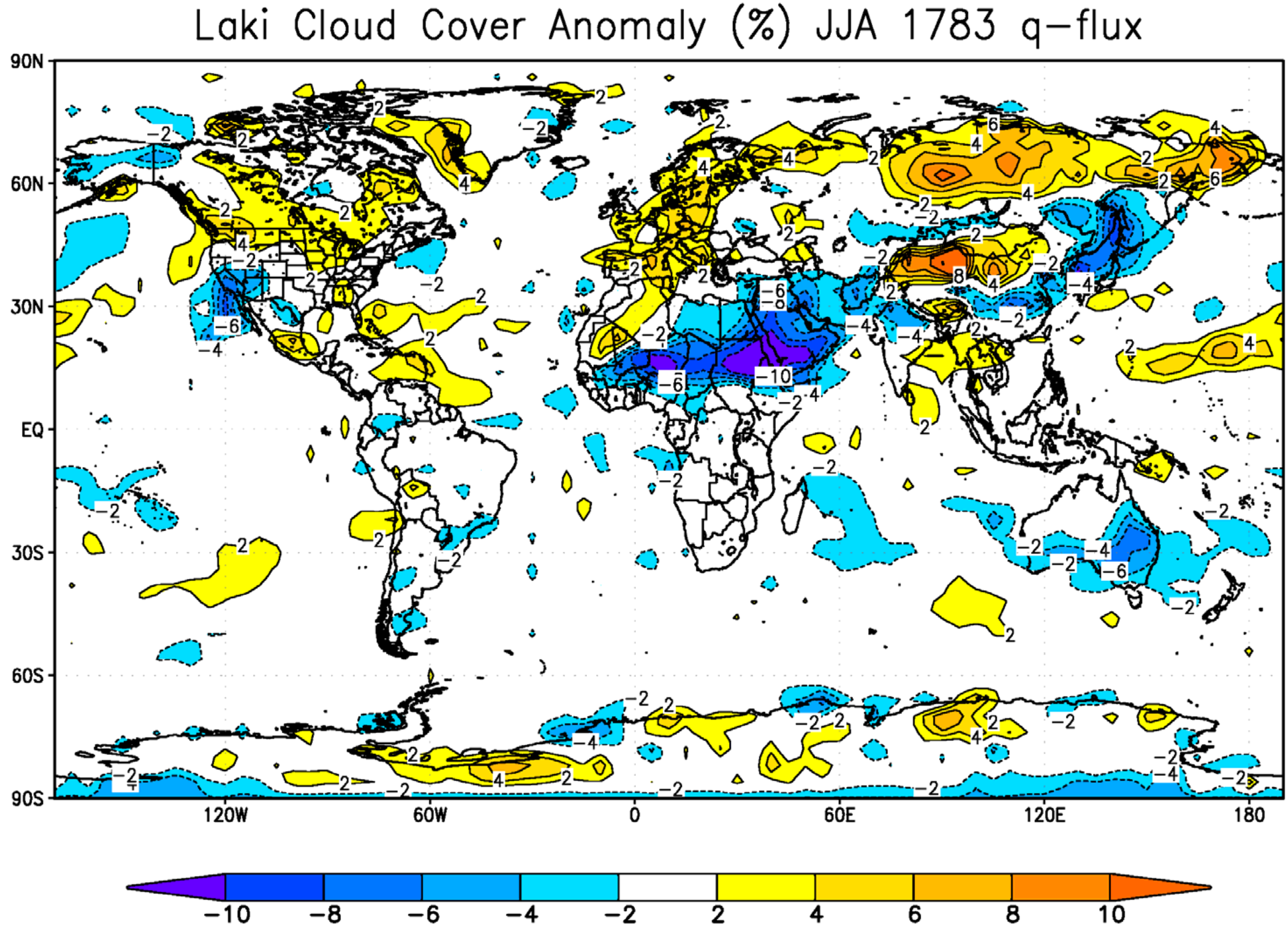

Laki Cloud Cover Anomaly (%) JJA 1783 q-flux
90N
60N
30N
EQ
30S
60S
90S
120W
60W
0
60E
120E
180
−10
−8
−6
−4
−2
2
4
6
8
10

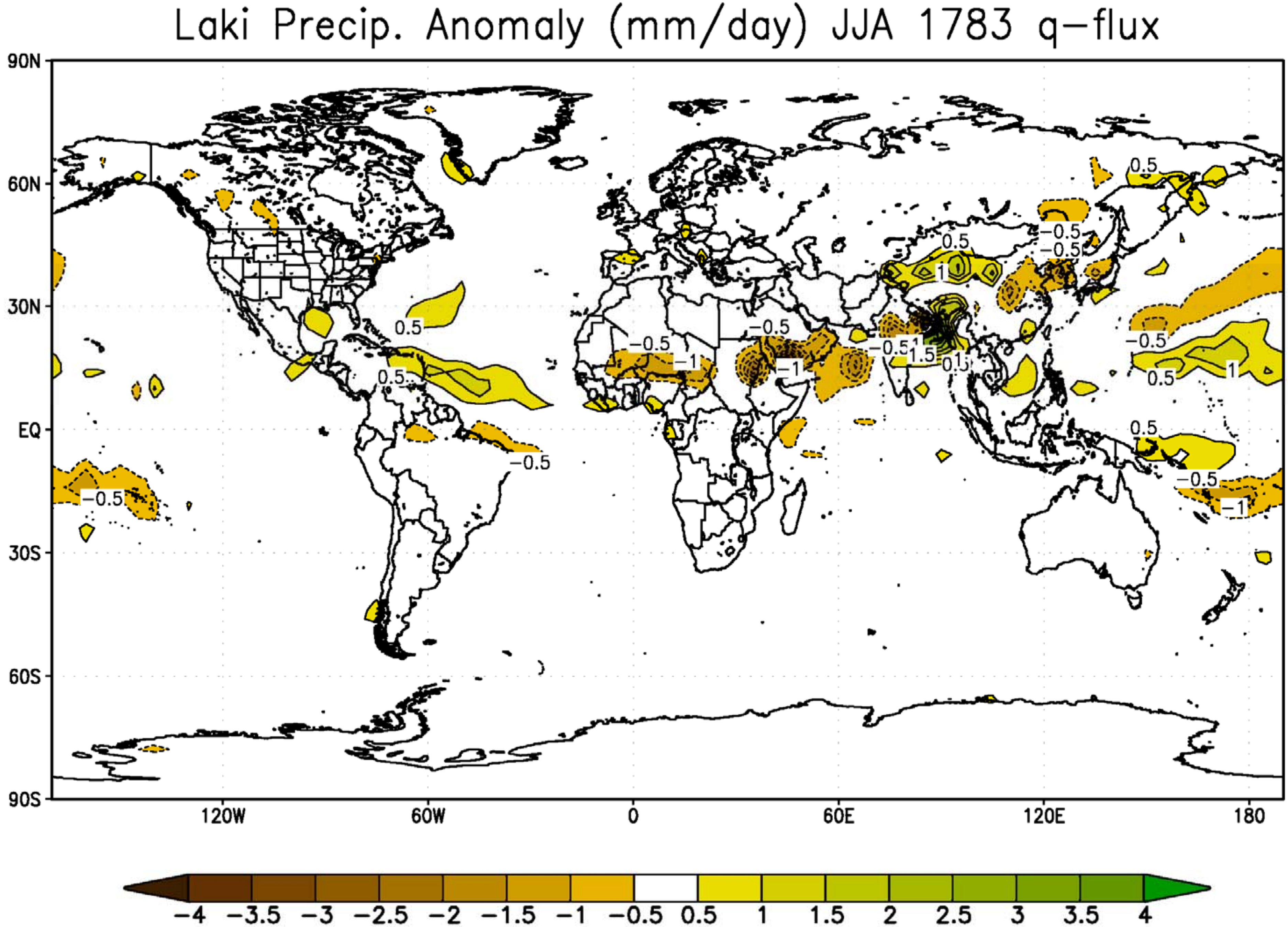

Laki Precip. Anomaly (mm/day) JJA 1783 q-flux
90N
60N
30N
EQ
30S
60S
90S
120W
60W
0
60E
120E
180
−4 −3.5 −3 −2.5 −2 −1.5 −1 −0.5 0.5 1 1.5 2 2.5 3 3.5 4

M. C-F. Volney, *Travels through Syria and Egypt, in the years 1783, 1784, and 1785, Vol. I*, Dublin, 258 pp. (1788) reports on the famine in Cairo and the annual flood (inundation) of the Nile River.

"The inundation of 1783 was not sufficient, great part of the lands therefore could not be sown for want of being watered, and another part was in the same predicament for want of seed. In 1784, the Nile again did not rise to the favorable height, and the dearth immediately became excessive. Soon after the end of November, the famine carried off, at Cairo, nearly as many as the plague; the streets, which before were full of beggars, now afforded not a single one: all had perished or deserted the city."

By January 1785, 1/6 of the population of Egypt had either died or left the country in the previous two years.

http://www.academie-francaise.fr/images/immortels/portraits/volney.jpg

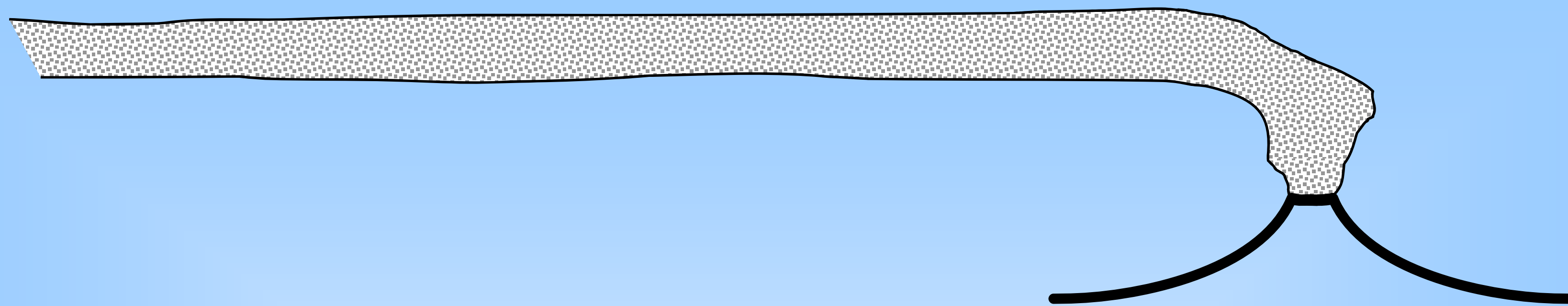

FAMINE IN INDIA AND CHINA IN 1783

The Chalisa Famine devastated India as the monsoon failed in the summer of 1783.

There was also the Great Tenmei Famine in Japan in 1783-1787, which was locally exacerbated by the Mount Asama eruption of 1783.

Alan Robock
Department of Environmental Sciences

Photo by George C. Martin

KATMAI VILLAGE, LOOKING NORTH TOWARD KATMAI VOLCANO, WHICH IS CONCEALED IN THE CLOUD BEYOND THE HILLS
AUGUST 13, 1912

The eruption of Katmai Volcano, though one of the most violent explosions recorded, did not cause the loss of a single life, owing to the sparse settlement of the neighborhood. The town of Katmai was deserted at the time of the eruption, most of the inhabitants being away, engaged in the summer fishing.

Katmai village, buried by ash from the June 6, 1912 eruption
Katmai volcano in background covered by cloud

Simulations showed same reduction in African summer precipitation.

Alan Robock
Department of Environmental Sciences

Niger Basin

http://www.festivalsegou.org

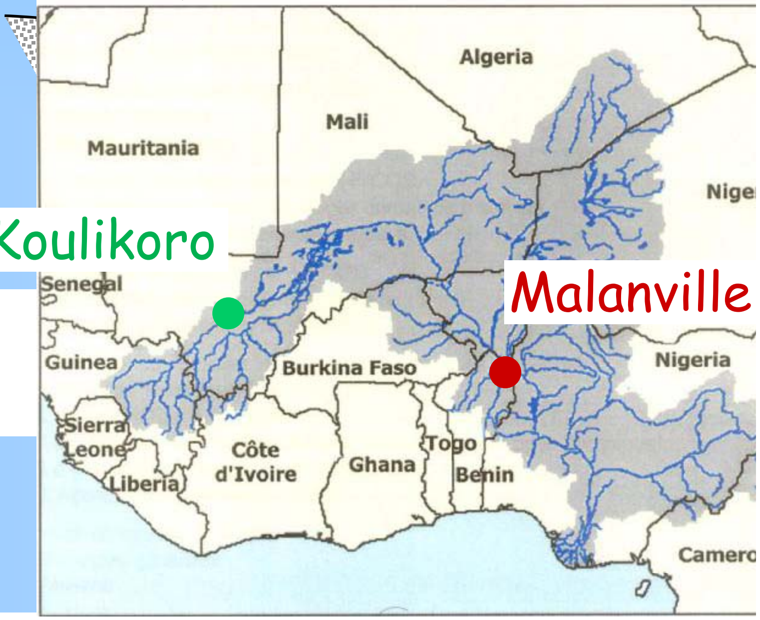

Annual rainfall & runoff deficit for the Niger river

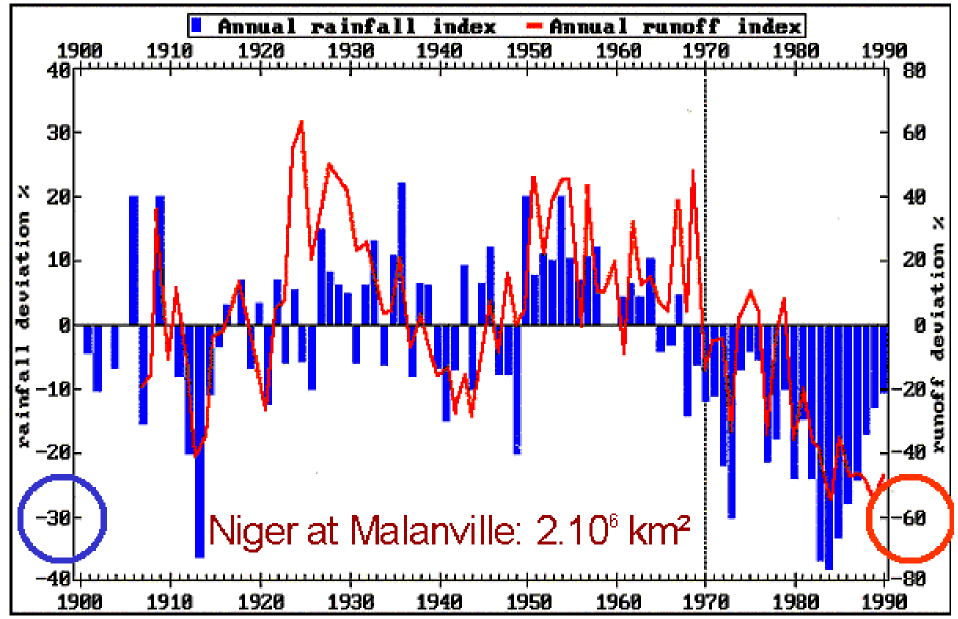

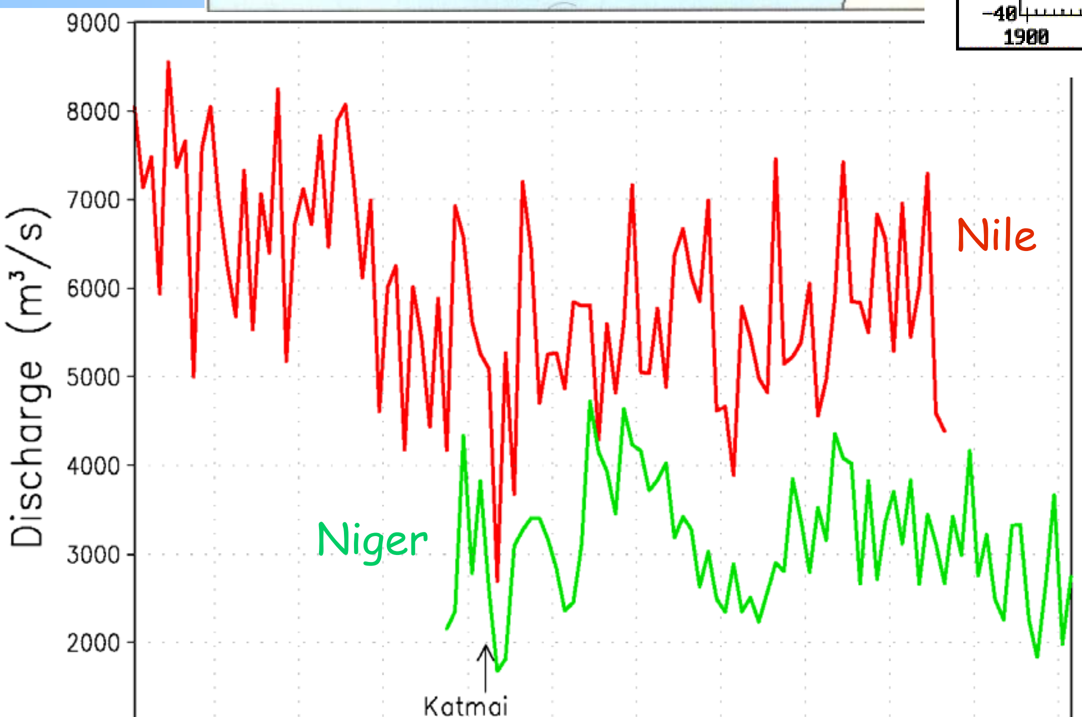

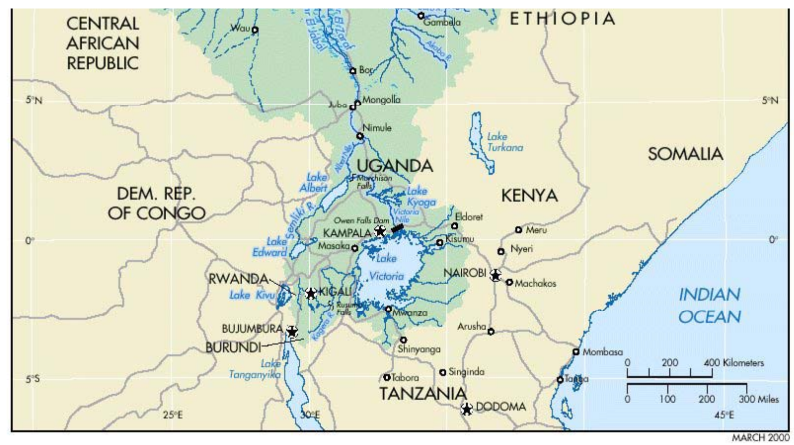

http://www.isiimm.agropolis.org

Alan Robock
Department of Environmental Sciences

Tambora in 1815, together with an eruption from an unknown volcano in 1809, produced the "Year Without a Summer" (1816)

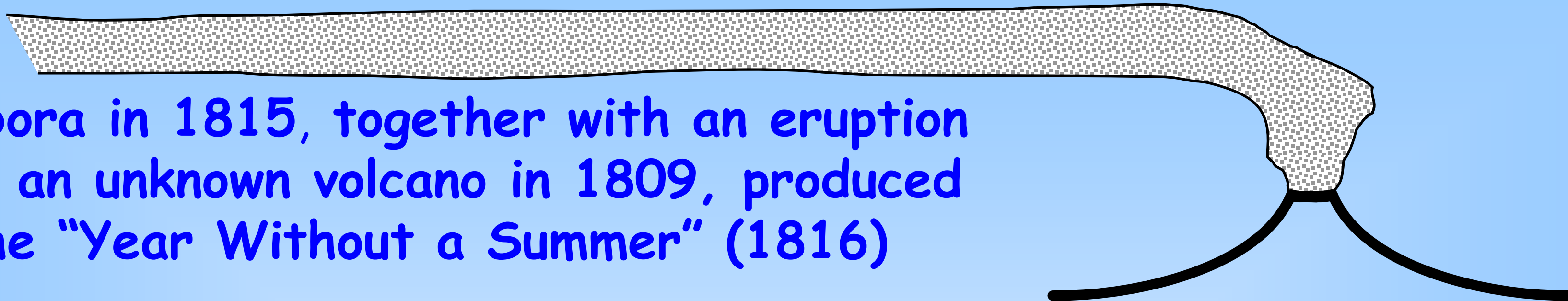

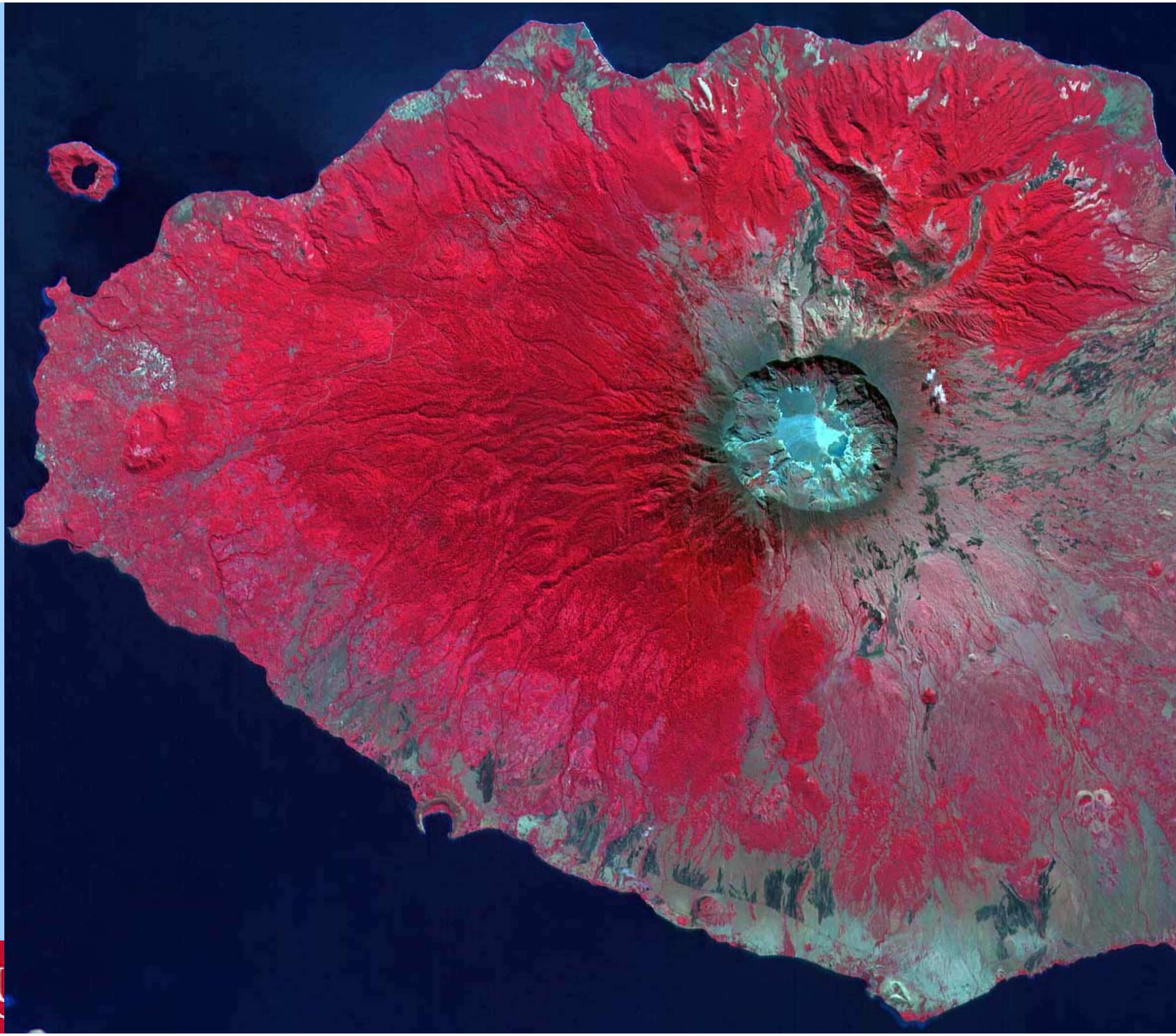

Tambora in 1815, together with an eruption from an unknown volcano in 1809, produced the "Year Without a Summer" (1816)

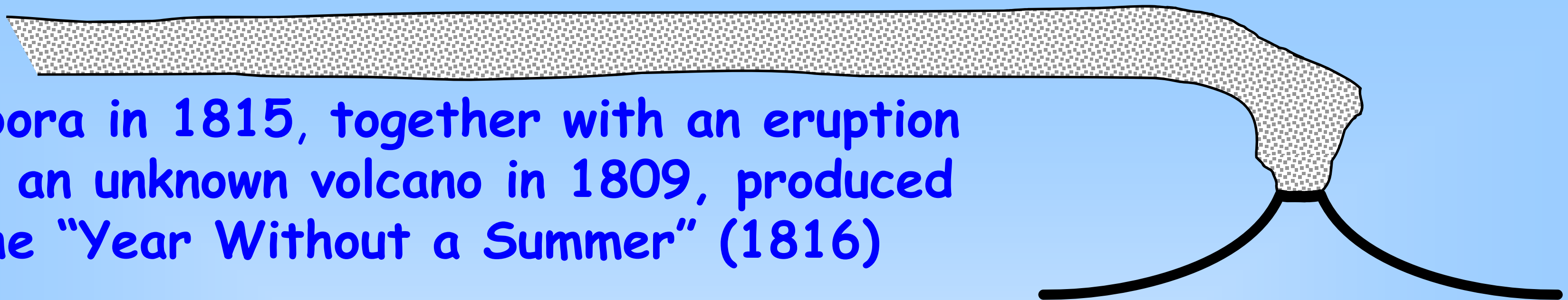

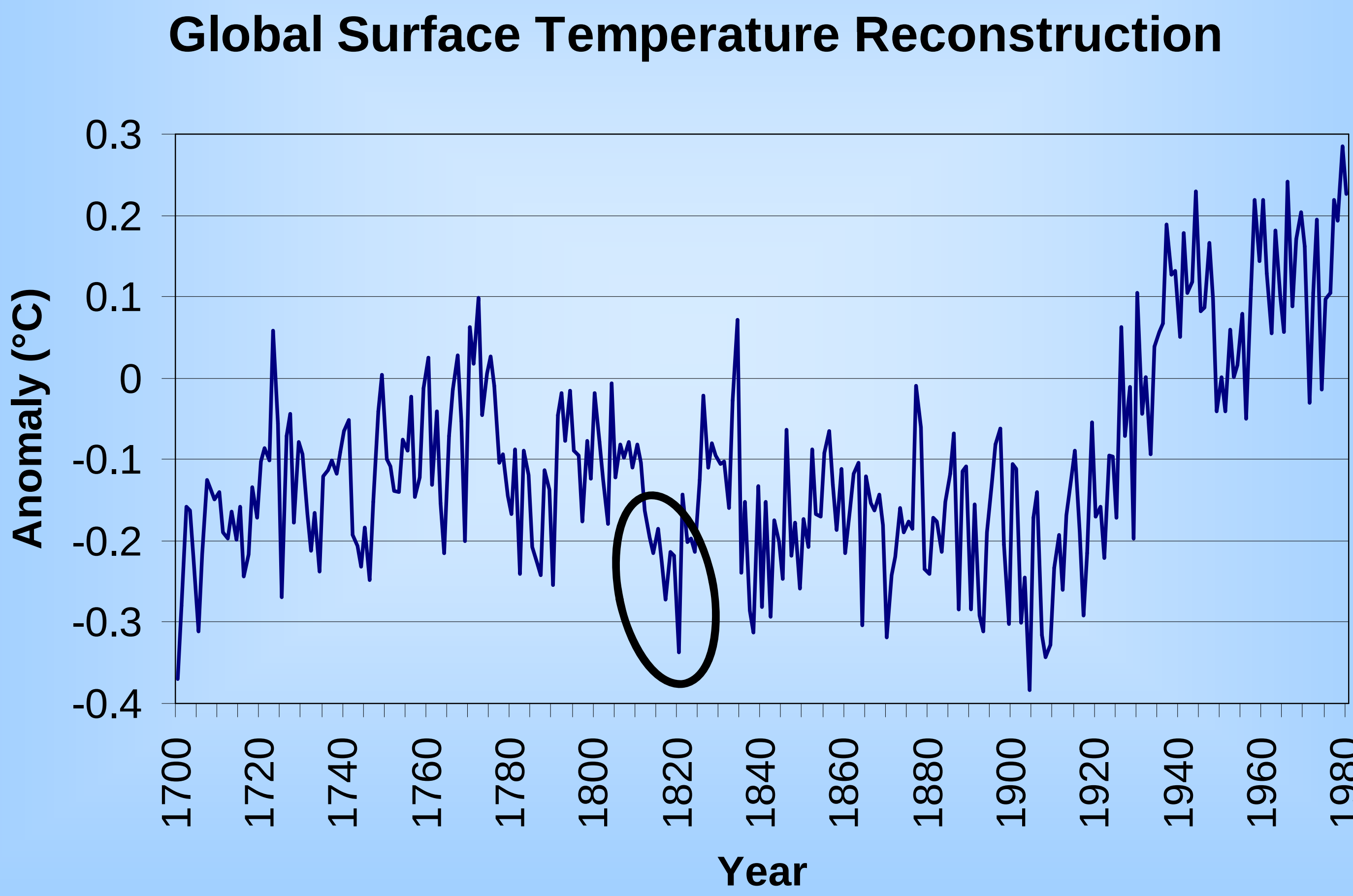

Mann et al. (2000)


LORD BYRON
POÊTE ANGLAIS
AUTEUR DU
PRISONER of CHILLON
HABITA LA
VILLA DIODATI
EN 1816
YCOMPOSA LE 3me CHANT
DE
CHILDE HAROLD

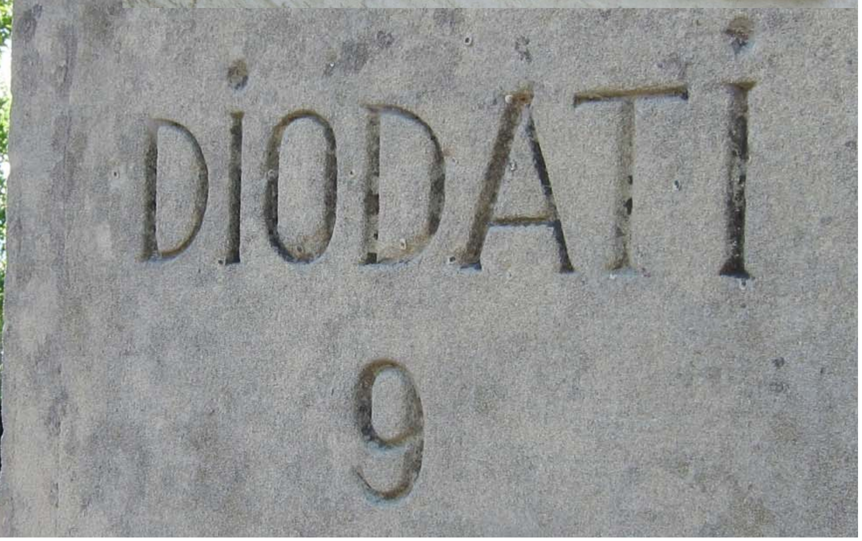
DiODATi
9

During the summer of 1816, the weather was atrocious, cold and rainy spells alternating with violent thunder storms. At that time Byron, a 28 years old poet, was renting the villa Diodati situated to the left of this meadow.

Mary Shelley was also spending the summer in Cologny, at Jacob Chappuis' home situated at the lower end of Montalègre, below where you are now standing.

RUTGERS

Alan Robock
Department of Environmental Sciences

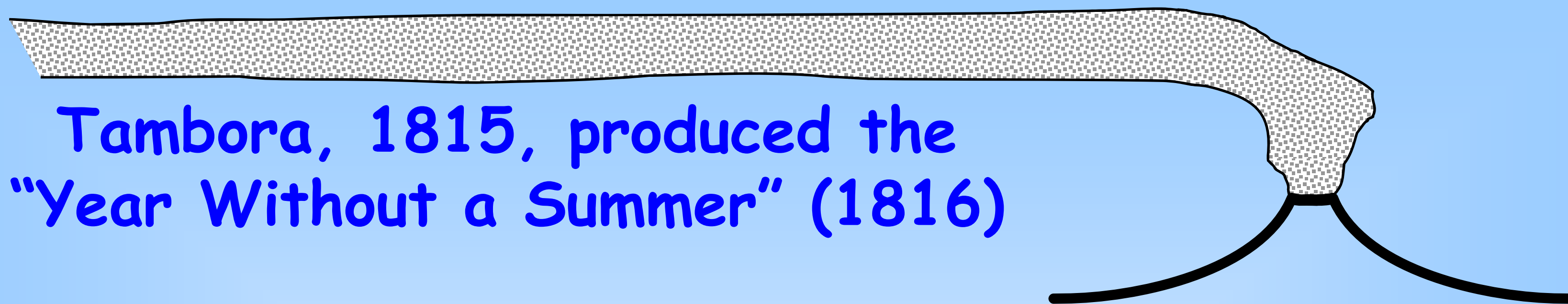

Tambora, 1815, produced the "Year Without a Summer" (1816)

"Darkness"
by Byron

I had a dream, which was not all a dream.
The bright sun was extinguish'd, and the stars
Did wander darkling in the eternal space,
Rayless, and pathless, and the icy earth
Swung blind and blackening in the moonless air;
Morn came and went—and came, and brought no day,
And men forgot their passions in the dread
Of this their desolation; and all hearts
Were chill'd into a selfish prayer for light:
And they did live by watchfires—and the thrones,
The palaces of crowned kings—the huts,
The habitations of all things which dwell,
Were burnt for beacons; cities were consumed,
And men were gather'd round their blazing homes
To look once more into each other's face; . . .

Alan Robock
Department of Environmental Sciences

Photo by George C. Martin

KATMAI VILLAGE, LOOKING NORTH TOWARD KATMAI VOLCANO, WHICH IS CONCEALED IN THE CLOUD BEYOND THE HILLS
AUGUST 13, 1912

The eruption of Katmai Volcano, though one of the most violent explosions recorded, did not cause the loss of a single life, owing to the sparse settlement of the neighborhood. The town of Katmai was deserted at the time of the eruption, most of the inhabitants being away, engaged in the summer fishing.

Katmai village, buried by ash from the June 6, 1912 eruption
Katmai volcano in background covered by cloud

GISS ModelE GCM

- NASA Goddard Institute for Space Studies (GISS) ModelE GCM
- 4°x5° horizontal resolution
- Stratospheric version with 23 vertical levels
- Gravity wave drag scheme
- Fixed climatological SSTs
- 40-year control run
- 20 ensemble members for each case

NH Summer Surface Air Temperature Anomalies

Significant cooling over most NH land masses especially Asia

Warming over Northern India in 3x Katmai case from reduced monsoon circulation

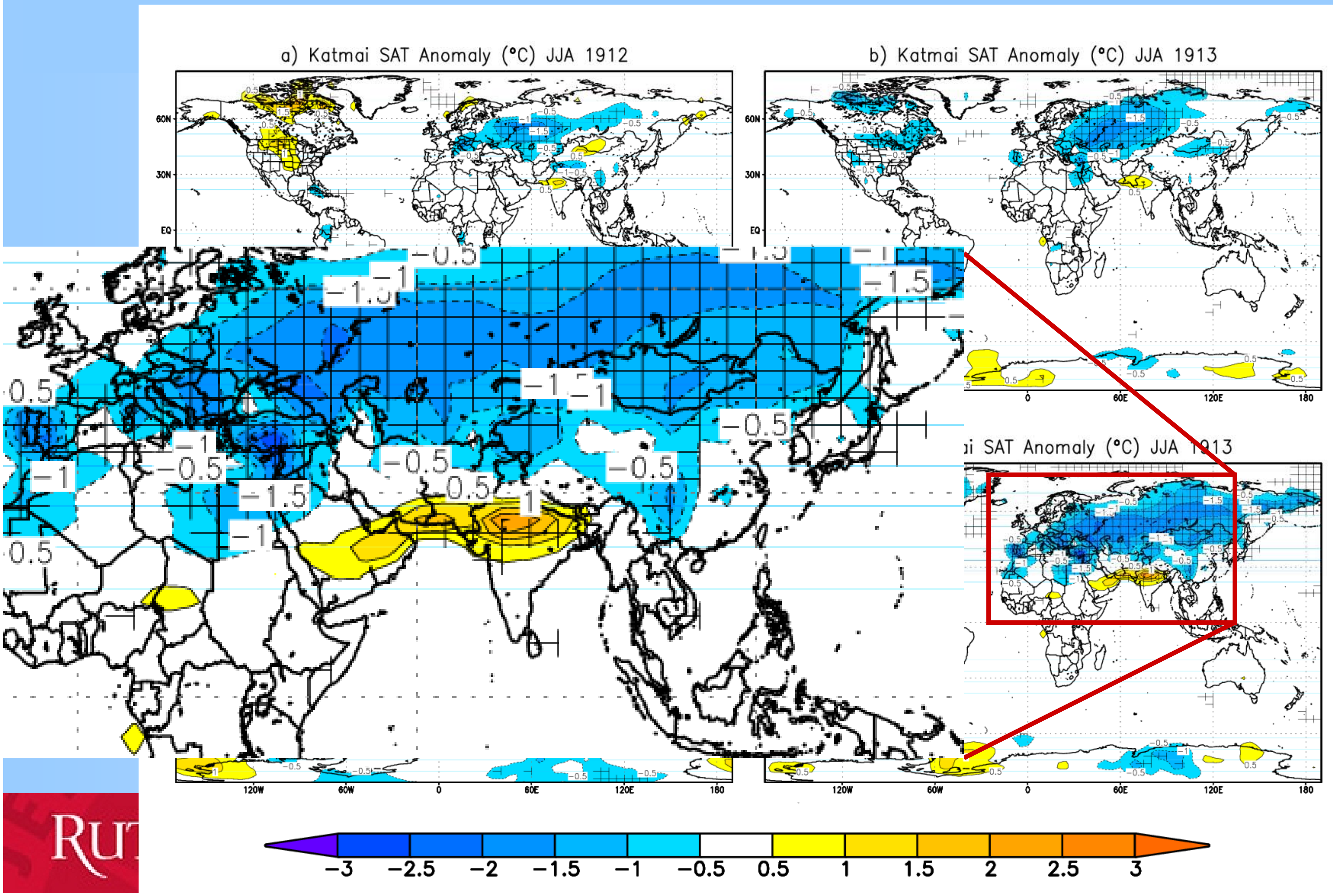

an Robock
Sciences

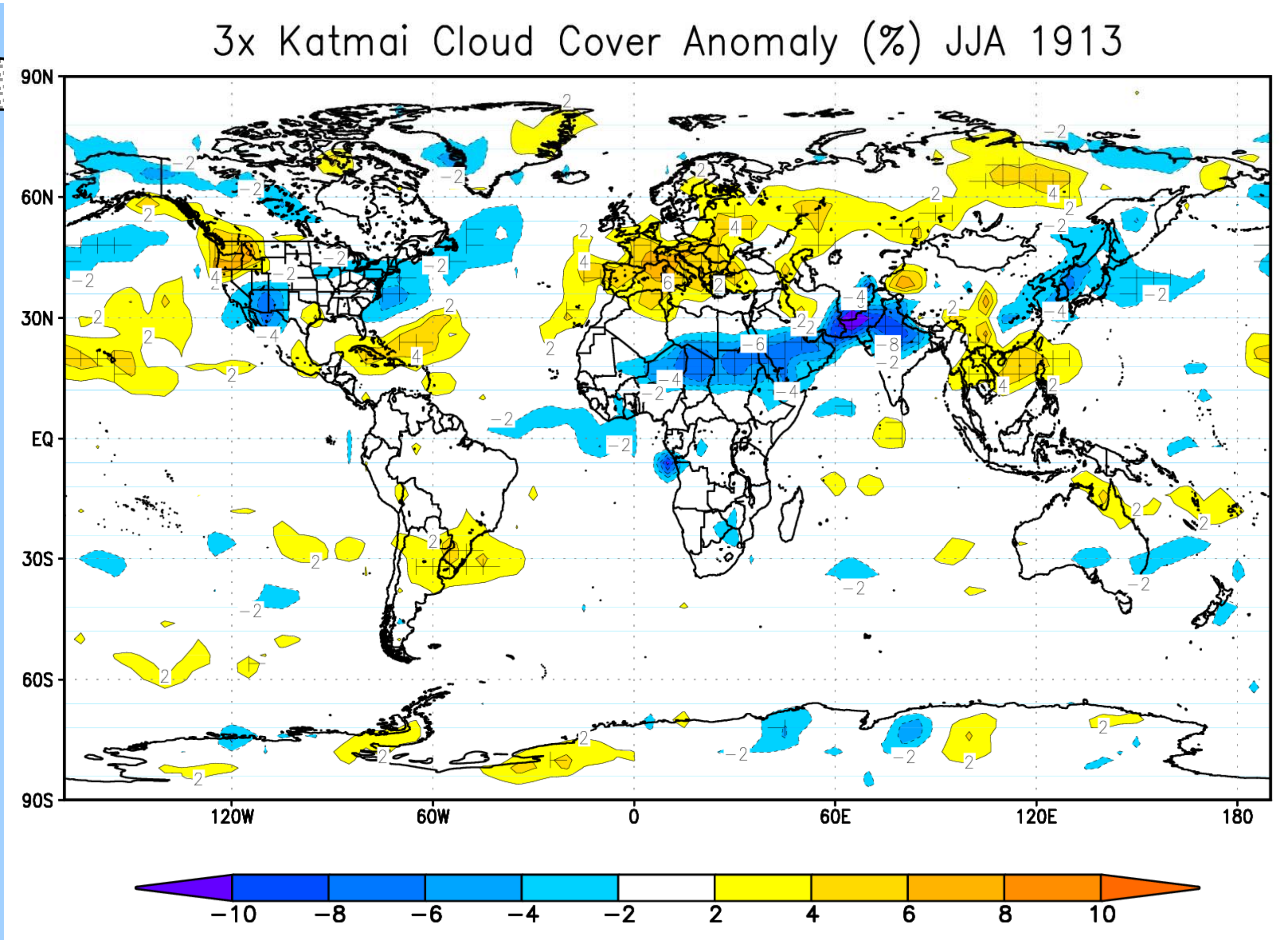

3x Katmai produced less cloud cover over the monsoon region and increased cloud cover over southern Europe

Consistent with a reduced Indian monsoon circulation

Alan Robock
Department of Environmental Sciences

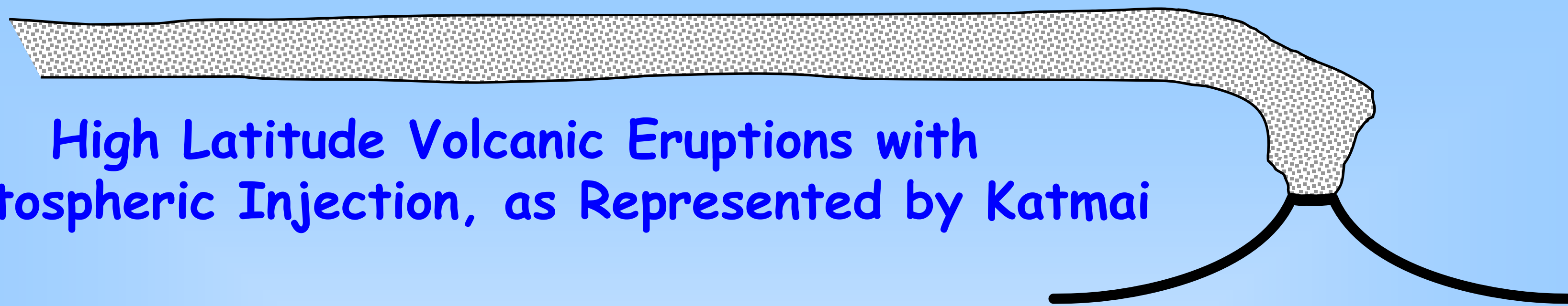

High Latitude Volcanic Eruptions with Stratospheric Injection, as Represented by Katmai

- Radiative impact appears to be larger than dynamic
- High latitude eruptions appear to weaken Indian monsoon
- High latitude eruptions do not cause enhanced negative AO response
- Similar response was seen in first winter following Katmai and second winter following 3x Katmai in 70 mb geopotential and surface pressure
- A large number of ensemble simulations are needed
- Future simulations could include a mixed layer ocean to see its impact

Alan Robock
Department of Environmental Sciences

Agung, 1963

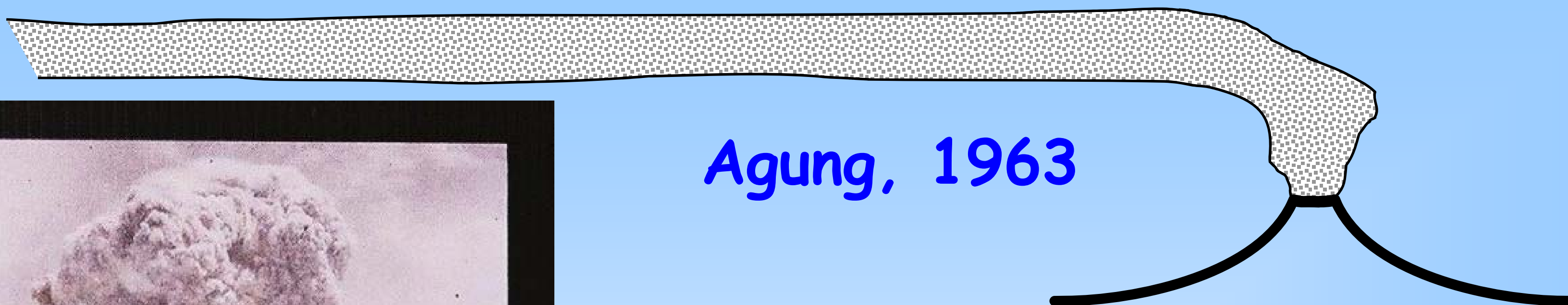


LETUSAN G. AGUNG, 12 MARET 1963


Bangunan rumah terkubur endapan lahar

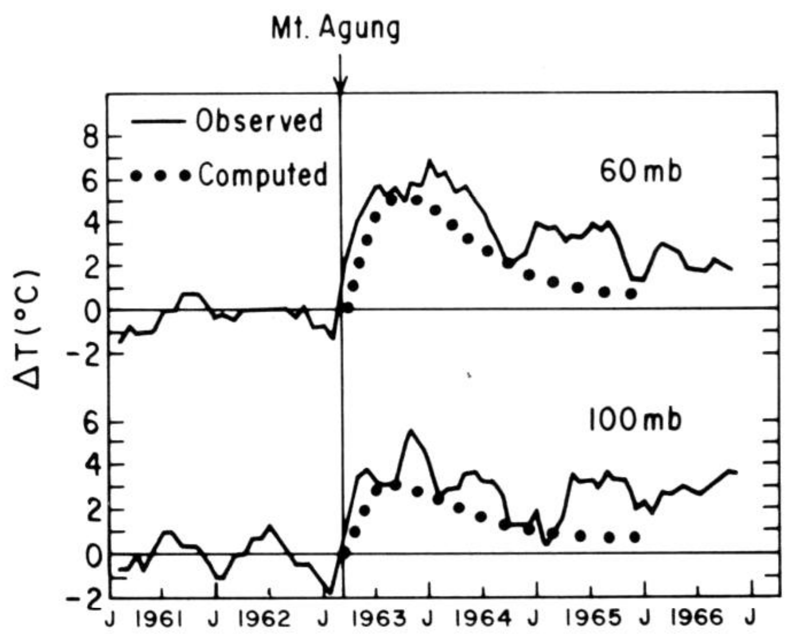

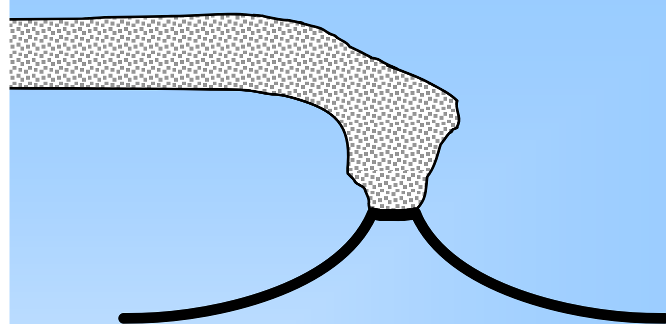

Hansen et al. (1978)

RCM

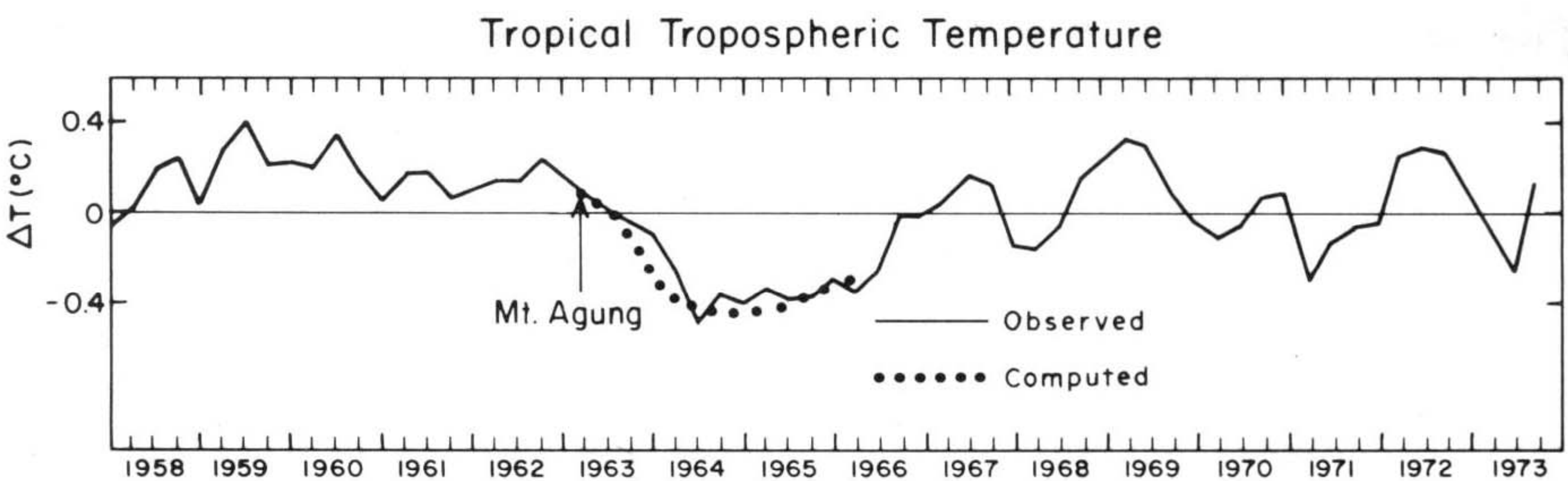

Fig. 2. Observed tropospheric temperatures between 30°N and 30°S (*19*) and computed temperatures after the eruption of Mount Agung, assuming that the added stratospheric aerosols are sulfuric acid and the average depth of the mixed layer of the ocean is 70 m.

Mt. St. Helens, May 18, 1980

Cliff Mass and Alan Robock
in the Mount St. Helens crater, summer 1980

Mt. St. Helens, 1980

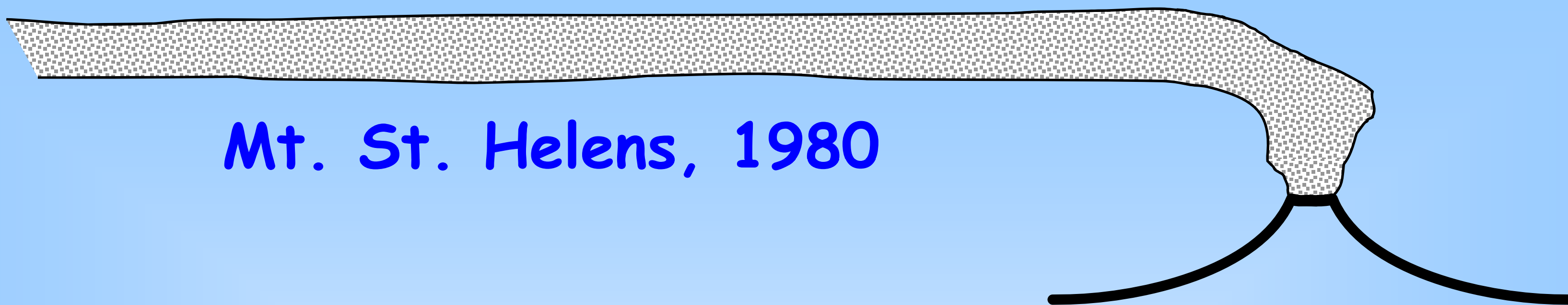

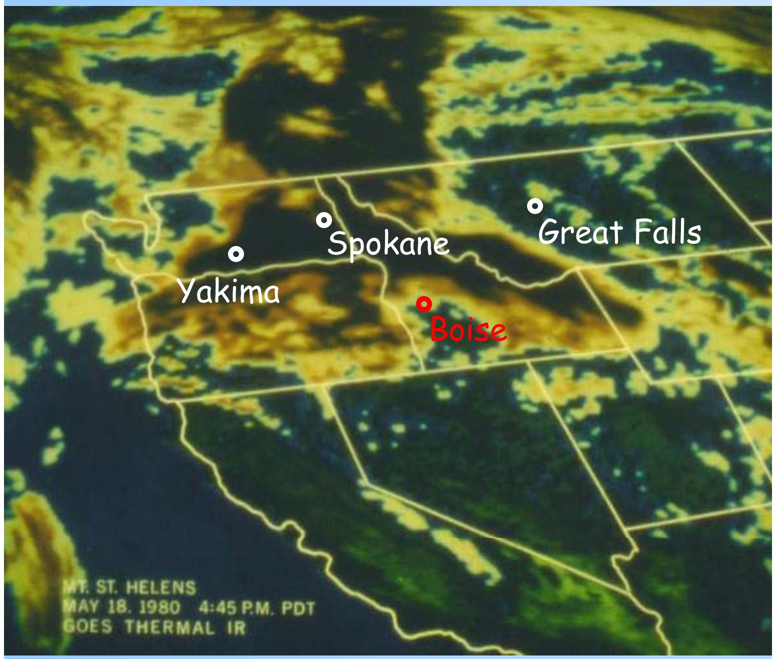

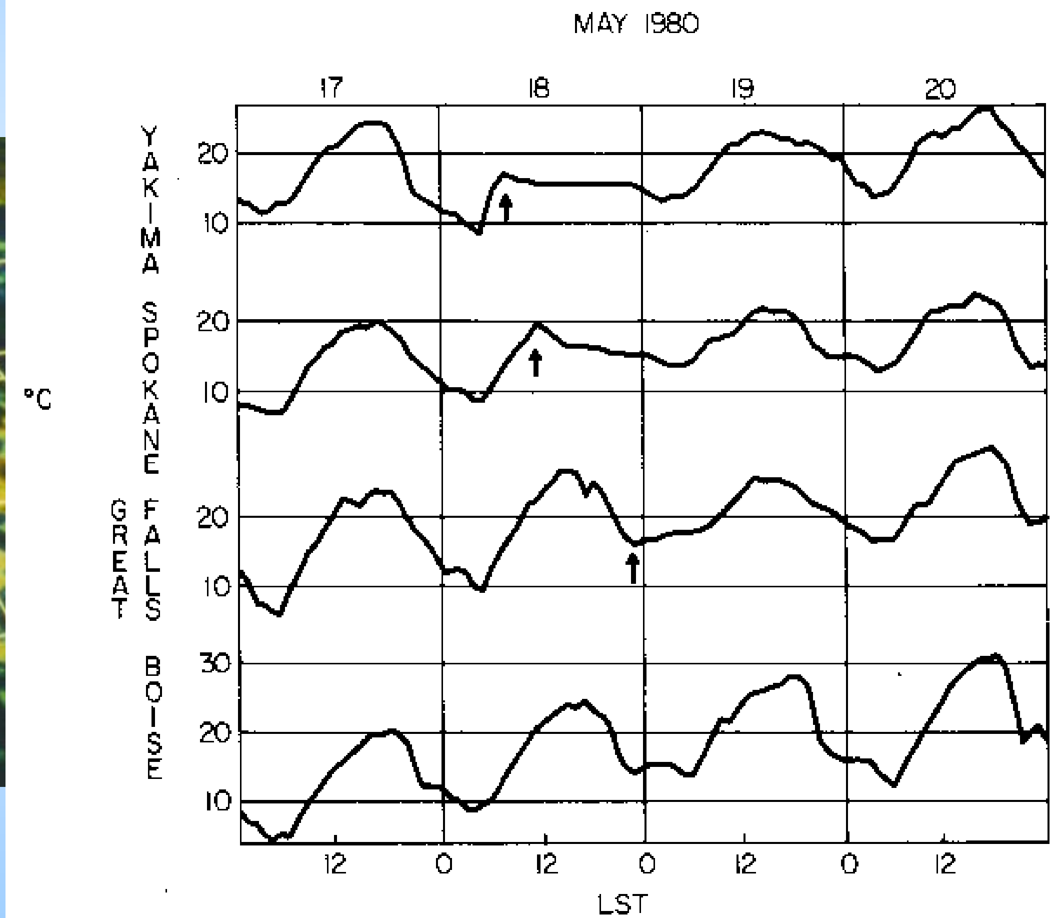

Robock and Mass (1982)

Alan Robock
Department of Environmental Sciences

El Chichón, 1982

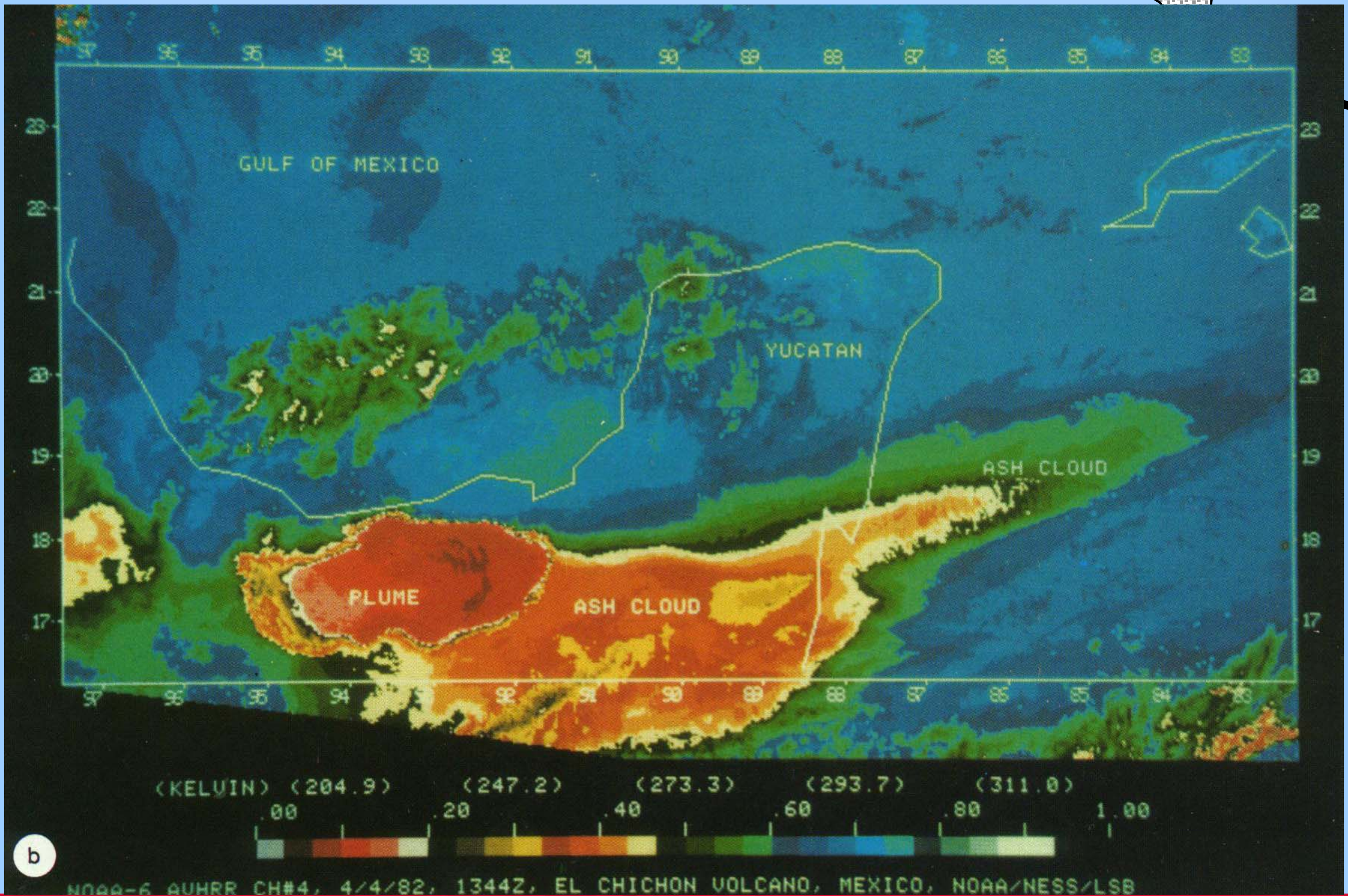

Matson (1984)

Alan Robock
Department of Environmental Sciences

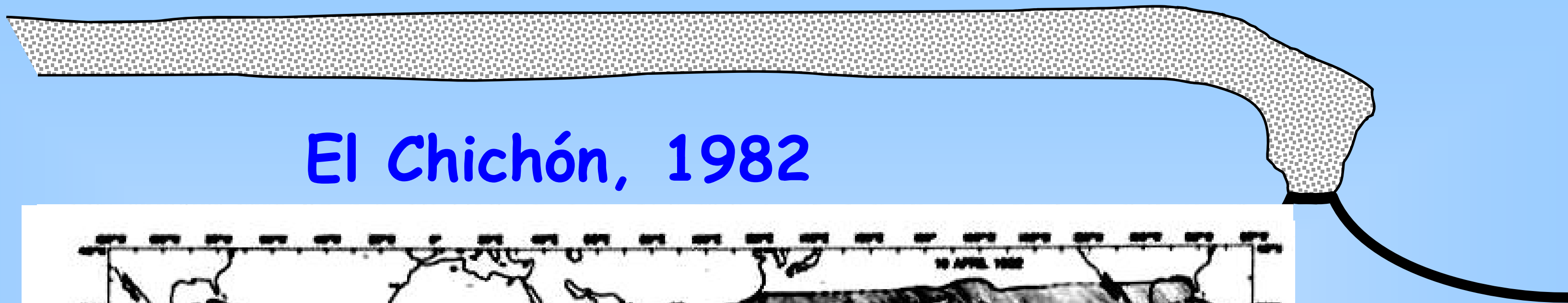

El Chichón, 1982

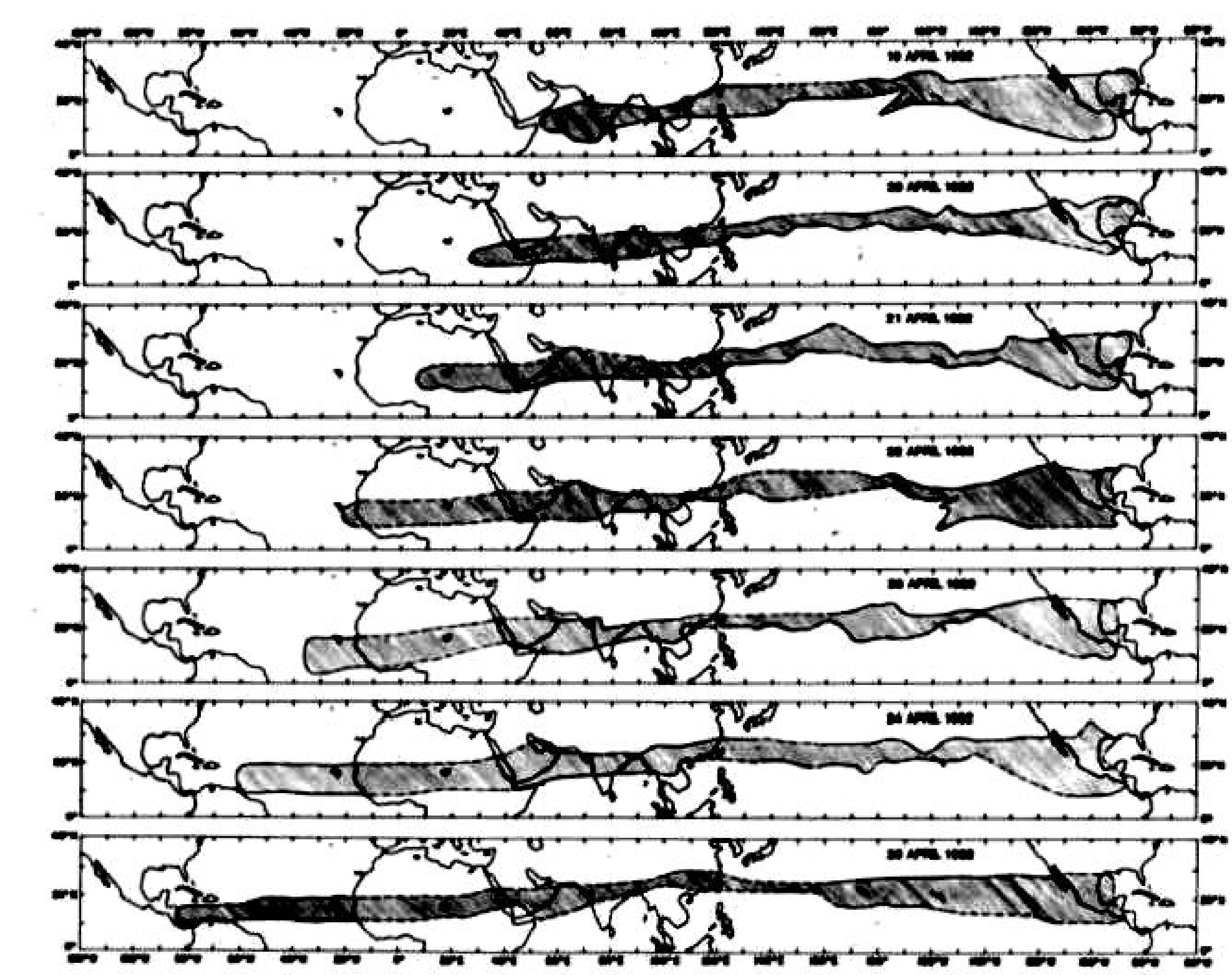

(Robock and Matson, 1983)

El Chichón, 1982

Sunset

Madison, Wisconsin

July, 1982

Photograph by Alan Robock

Alan Robock
Department of Environmental Sciences

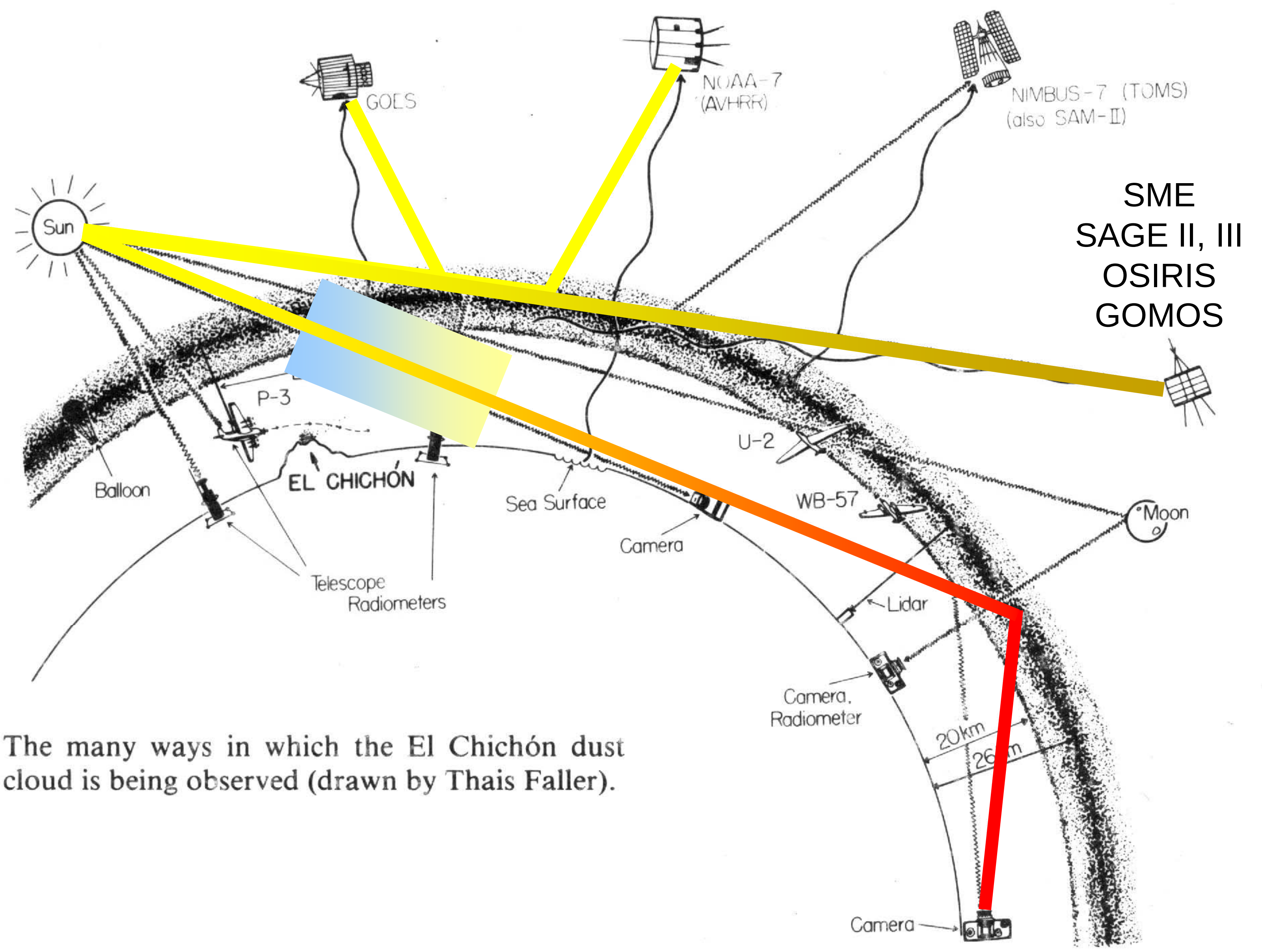

The many ways in which the El Chichón dust cloud is being observed (drawn by Thais Faller).

Robock (1983)

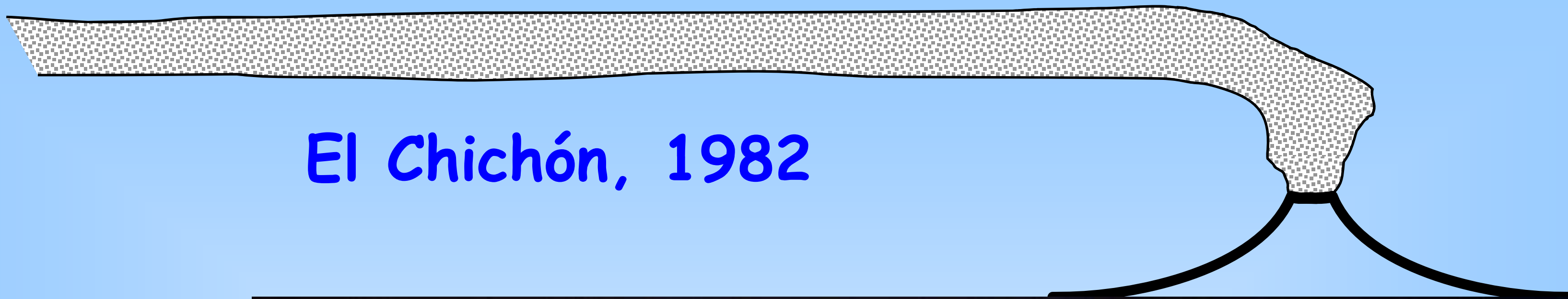

El Chichón, 1982

Sunset

Madison, Wisconsin

May, 1983

Photograph by Alan Robock

Krakatau, 1883
Watercolor by William Ascroft

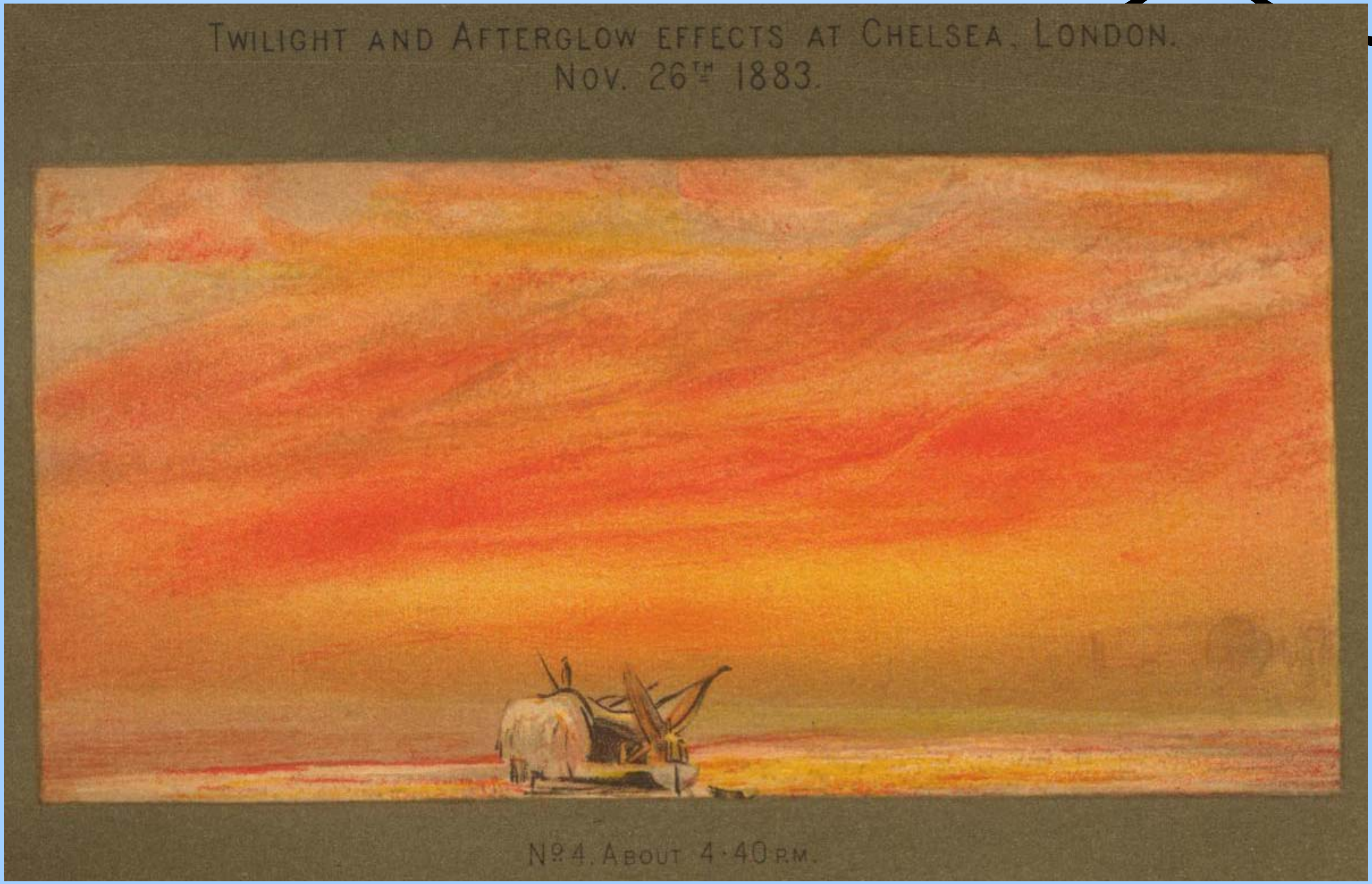

Figure from Symons (1888)

"The Scream"

Edvard Munch

Painted in 1893 based on Munch's memory of the brilliant sunsets following the 1883 Krakatau eruption.

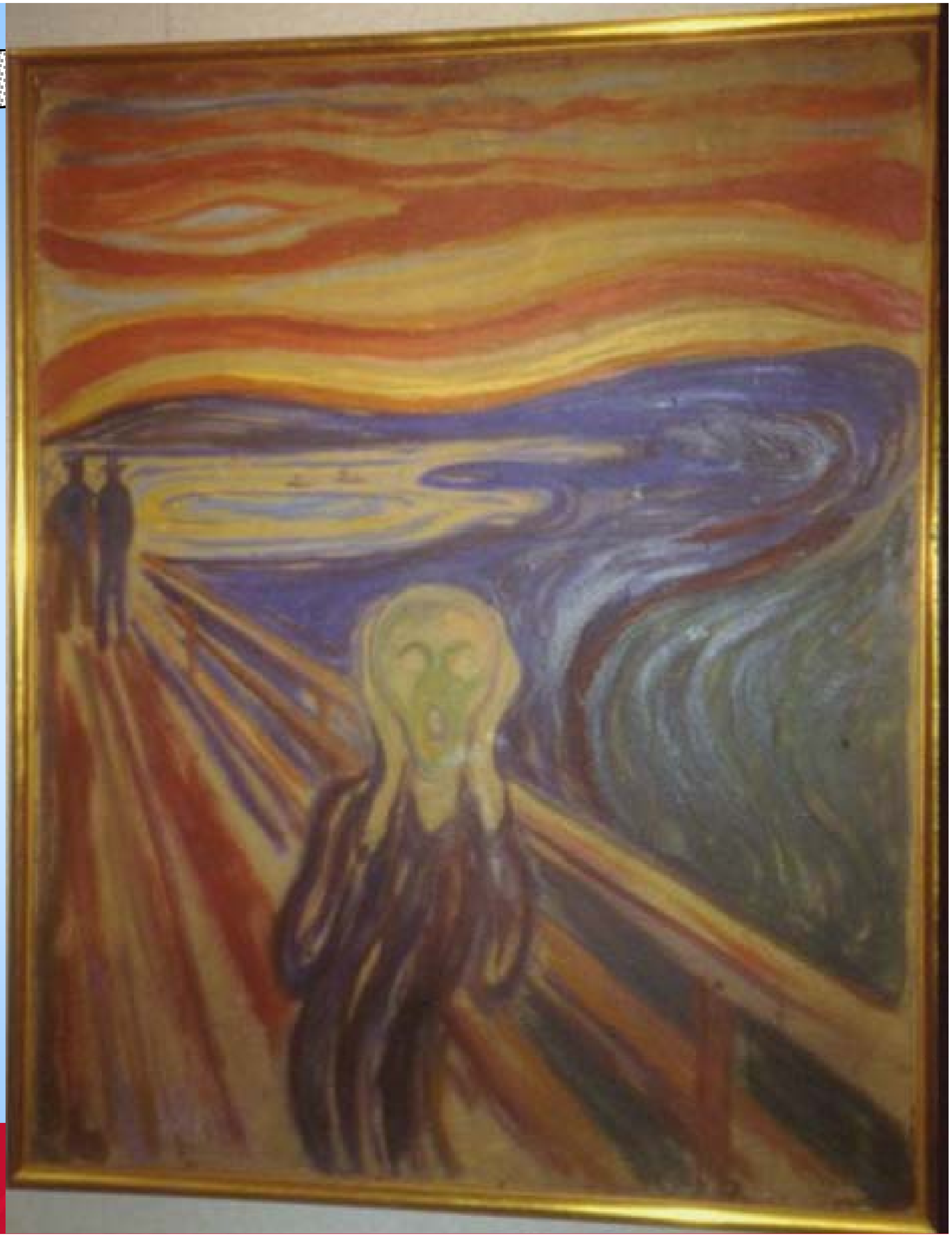

RUTGERS

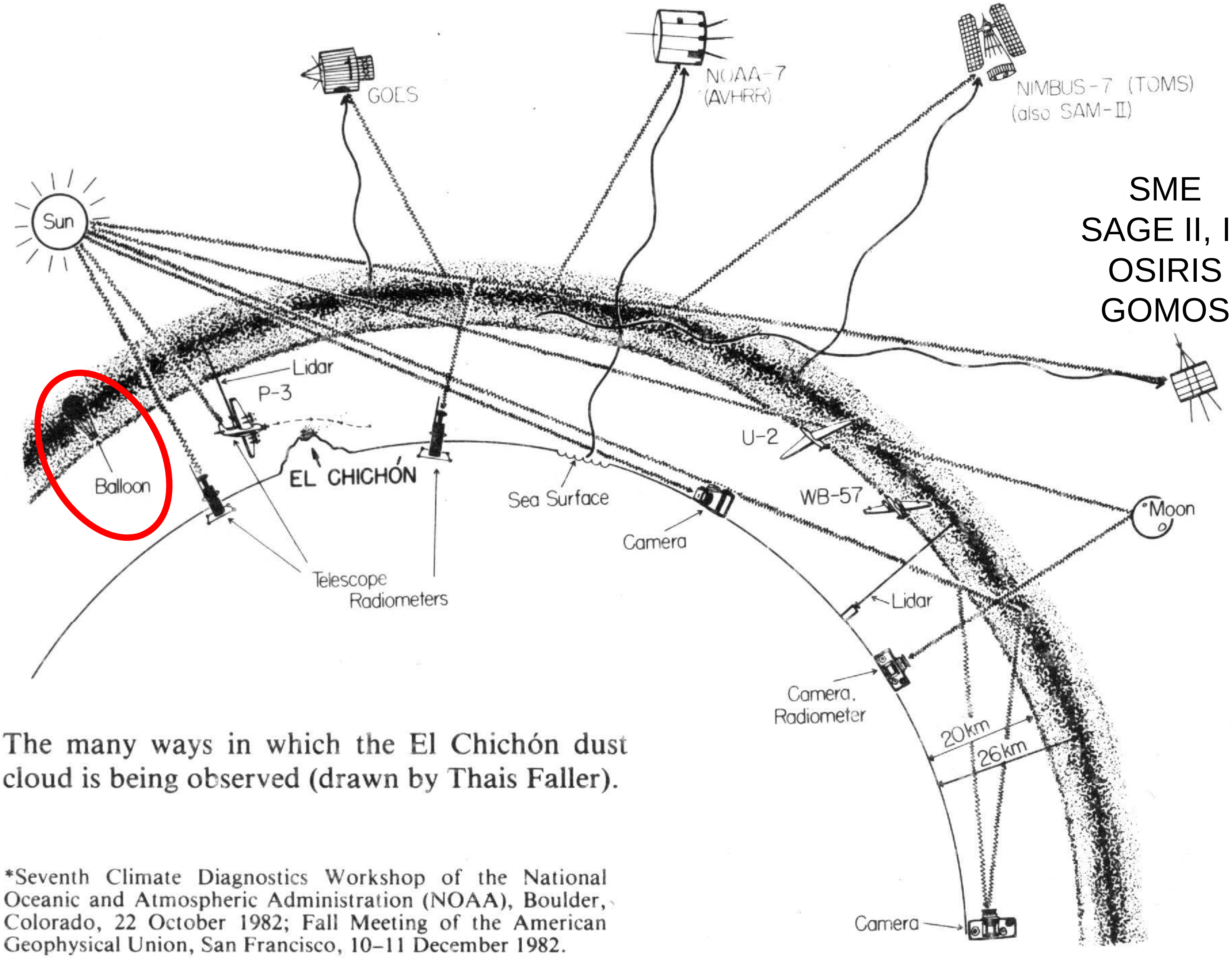

The many ways in which the El Chichón dust cloud is being observed (drawn by Thais Faller).

*Seventh Climate Diagnostics Workshop of the National Oceanic and Atmospheric Administration (NOAA), Boulder, Colorado, 22 October 1982; Fall Meeting of the American Geophysical Union, San Francisco, 10–11 December 1982.

Robock (1983)

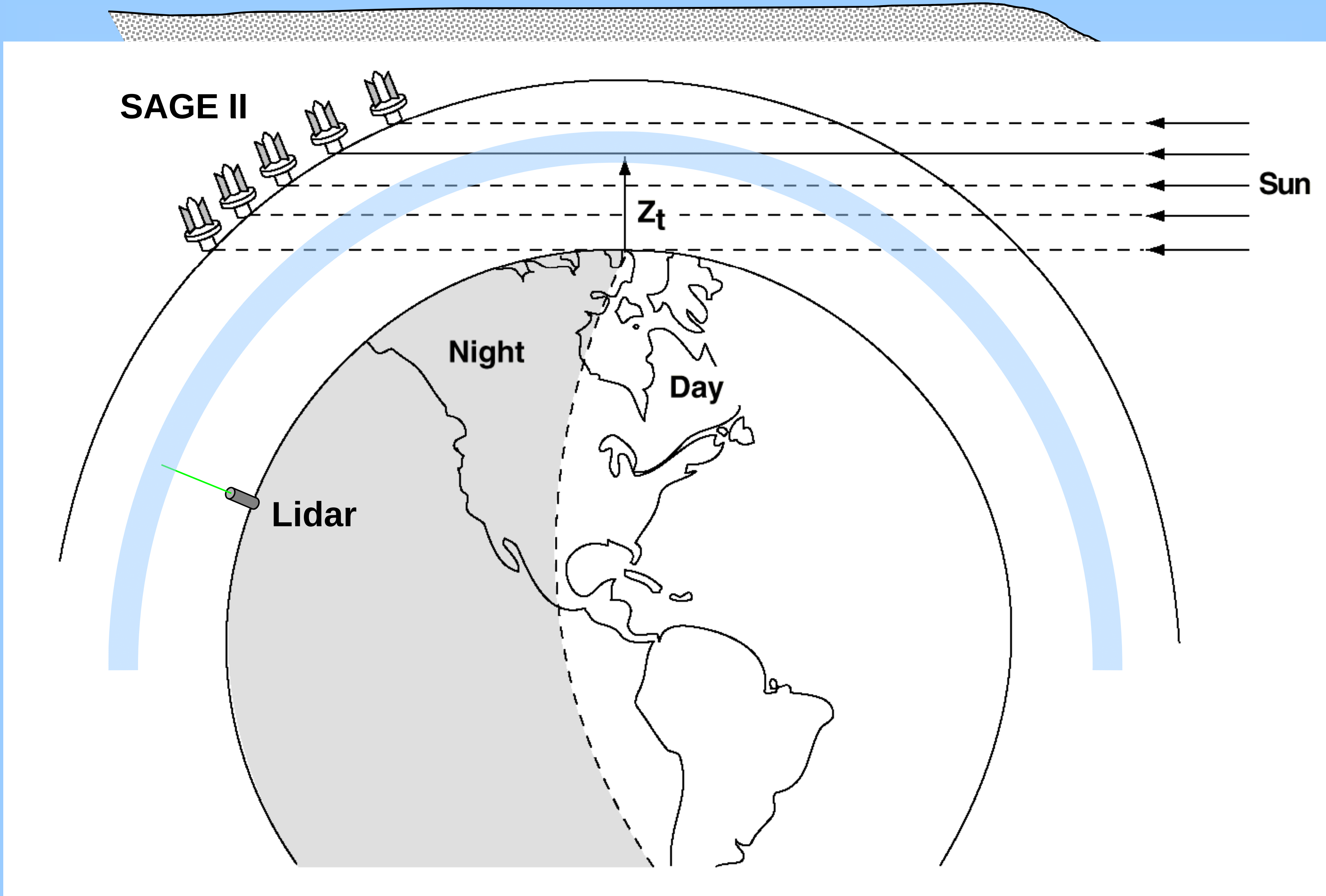
SAGE II
Sun
Zt
Night
Day
Lidar

One month of SAGE II coverage

Hampton

Mauna Loa

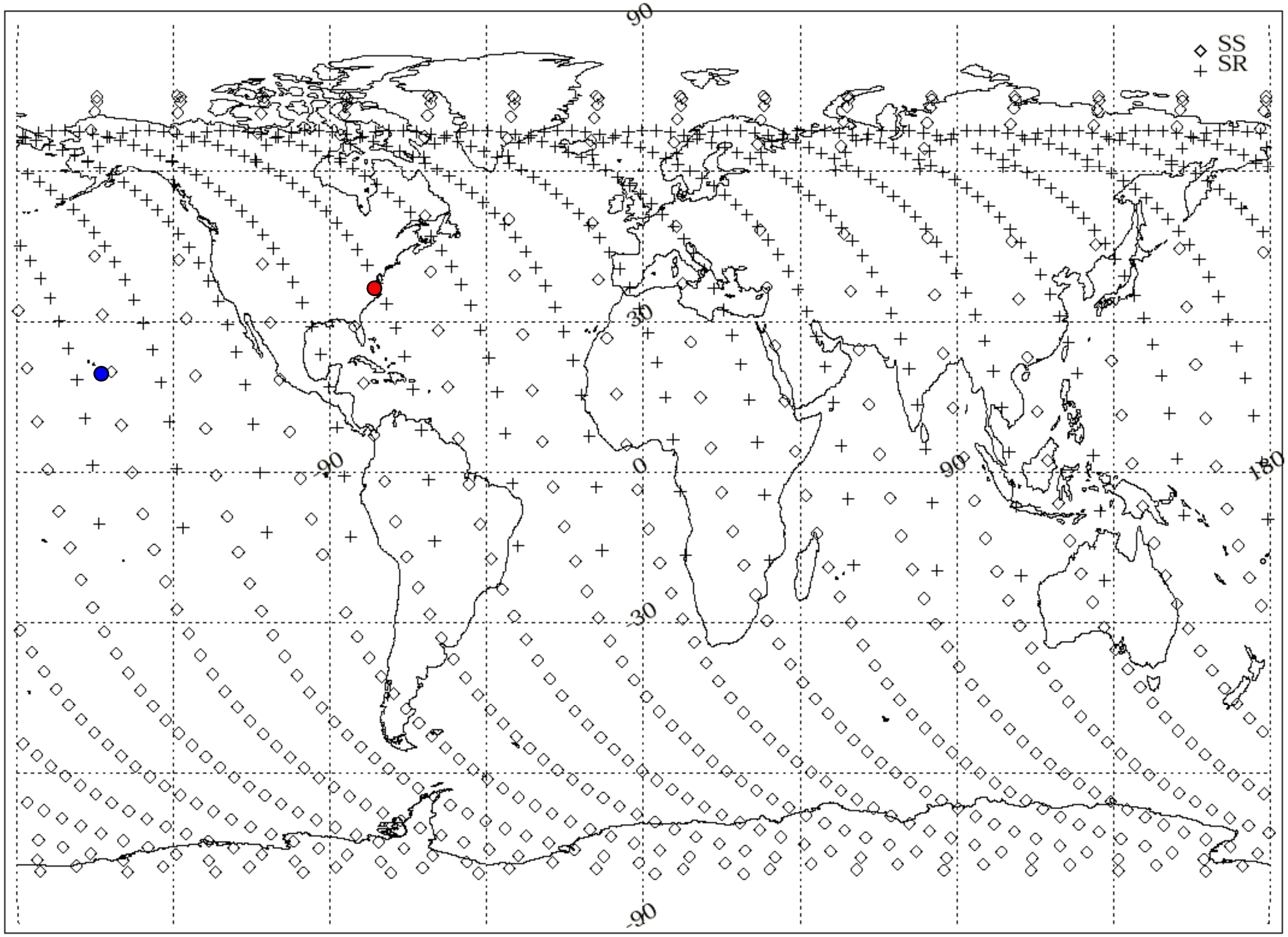

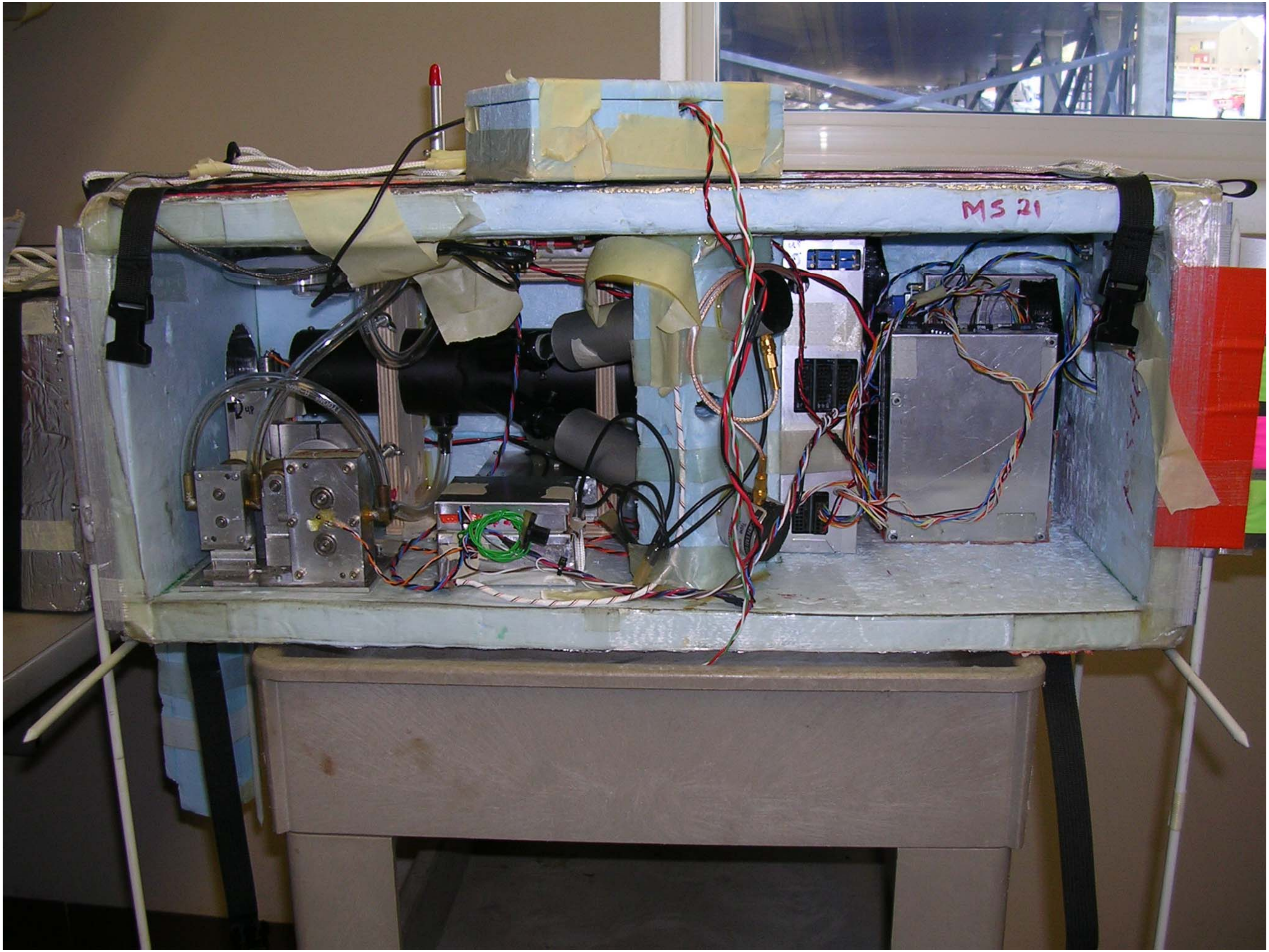
MS 21

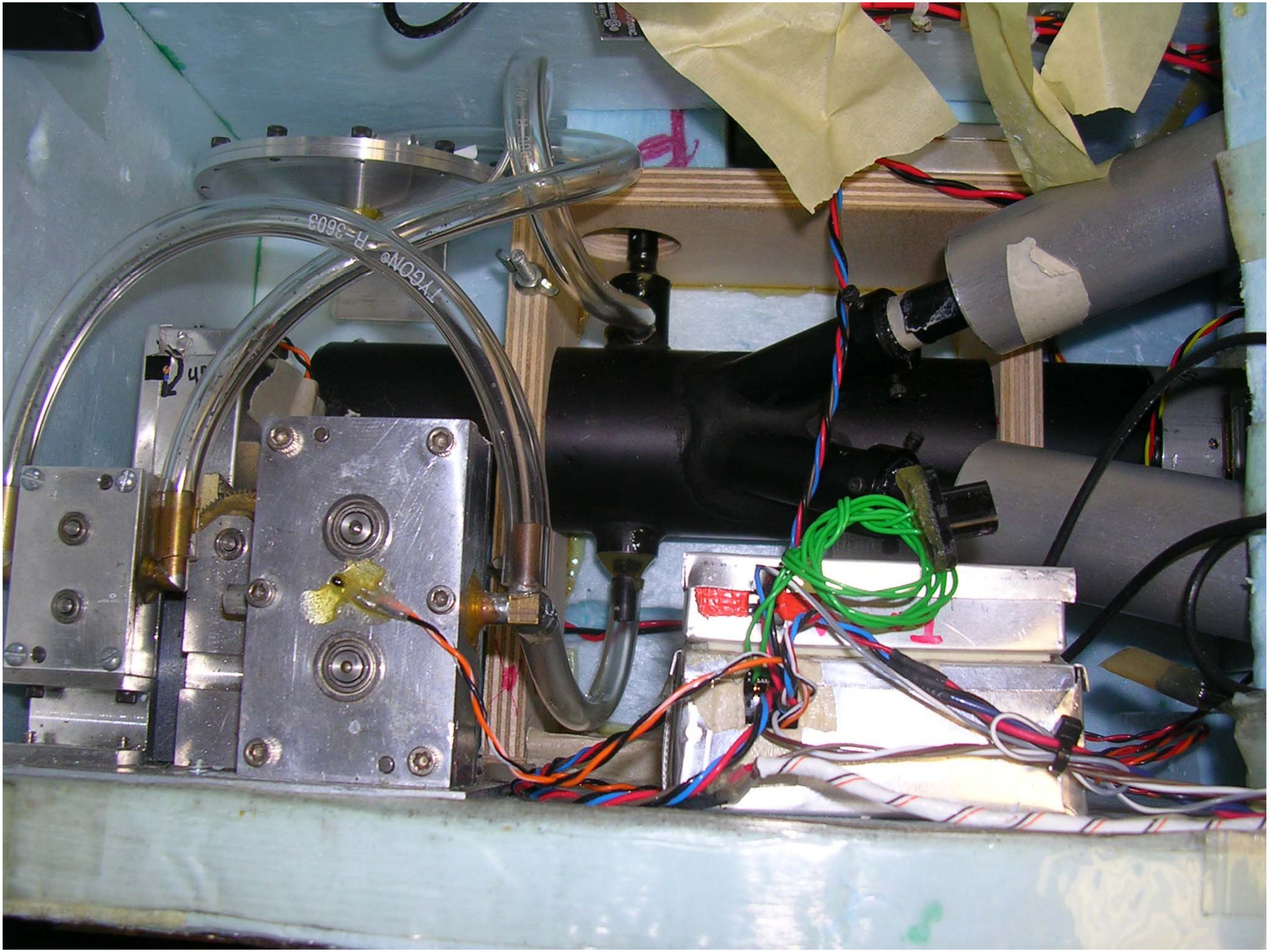
TYGON® R-3603

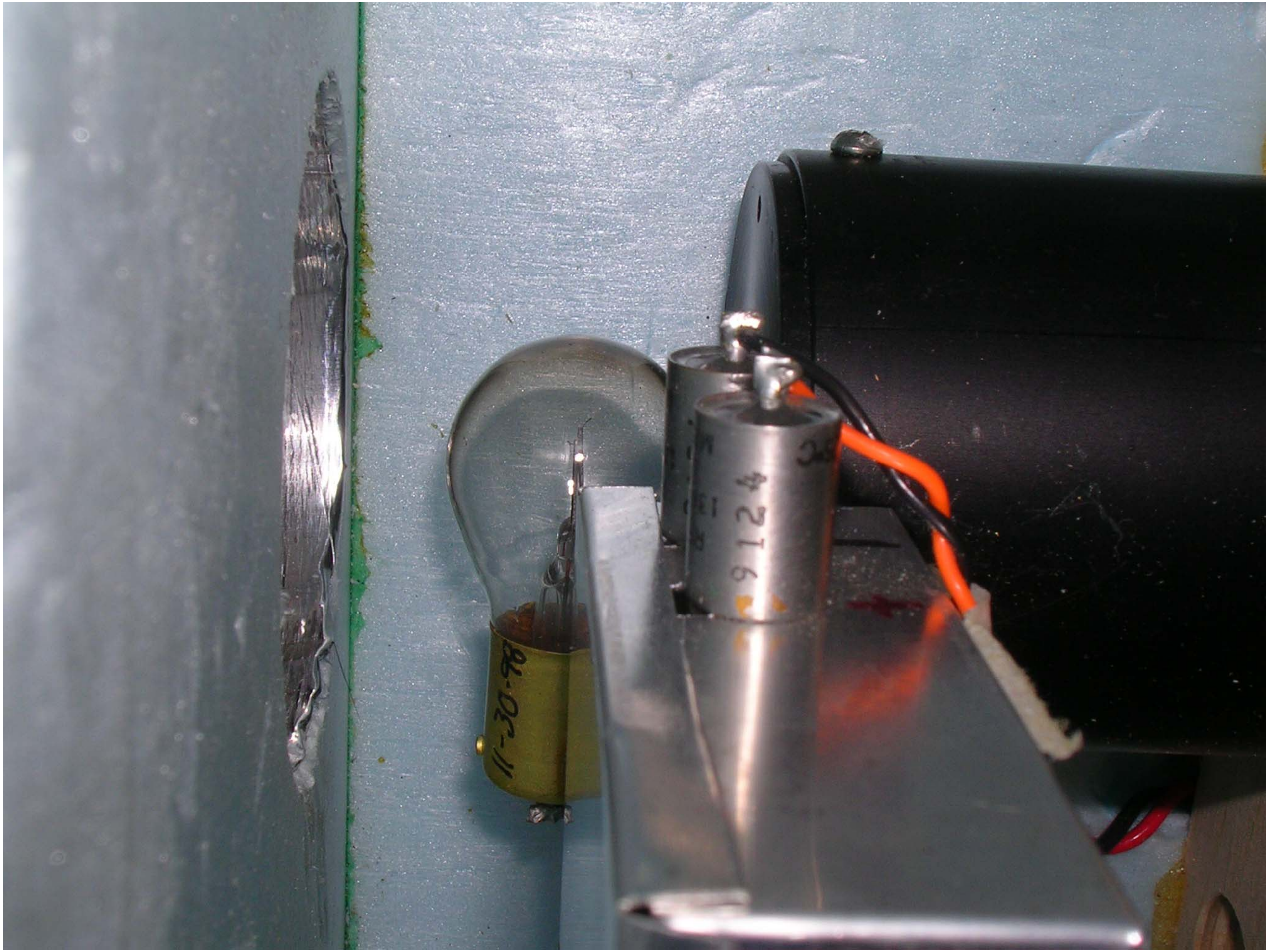
11-30-98

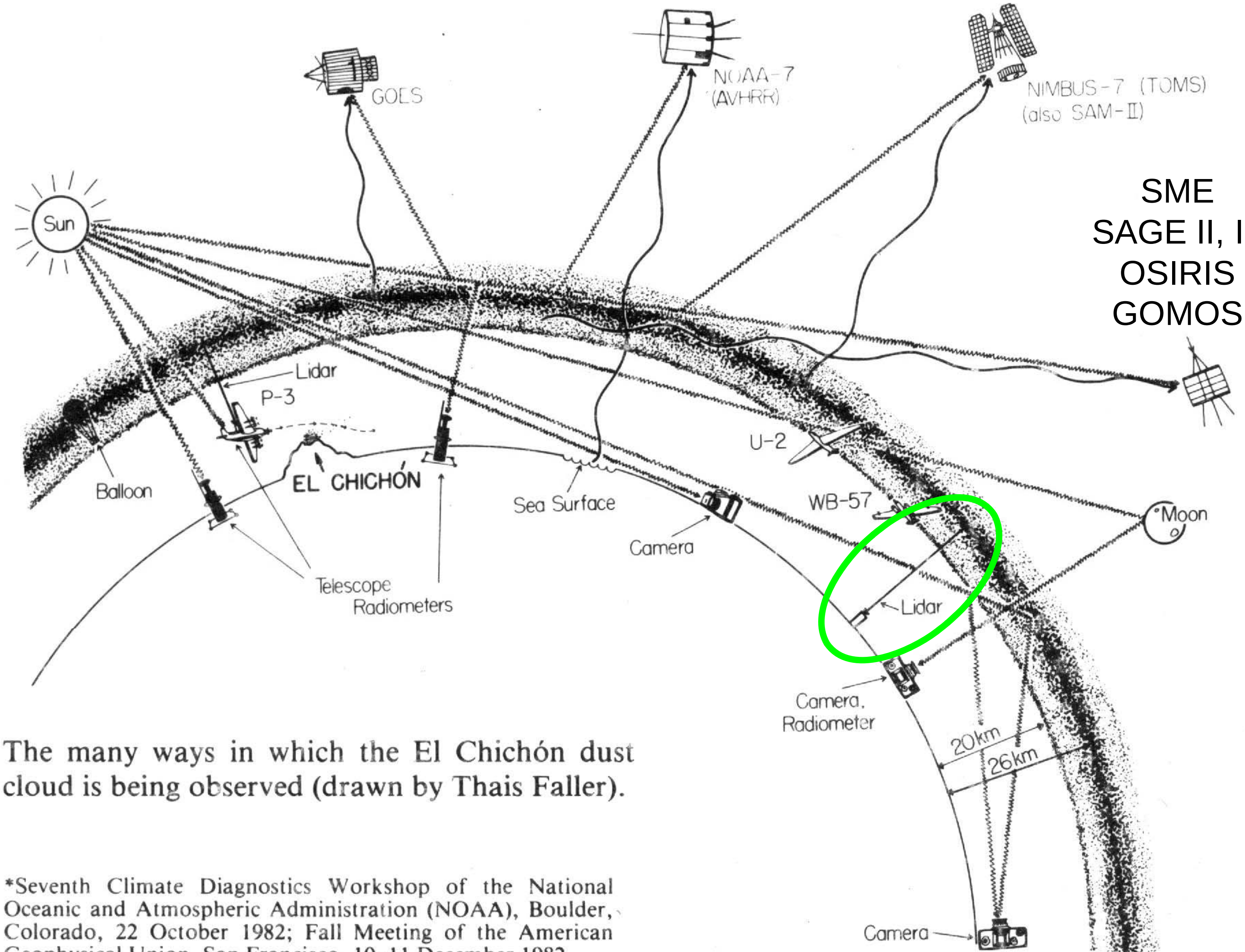

The many ways in which the El Chichón dust cloud is being observed (drawn by Thais Faller).

*Seventh Climate Diagnostics Workshop of the National Oceanic and Atmospheric Administration (NOAA), Boulder, Colorado, 22 October 1982; Fall Meeting of the American Geophysical Union, San Francisco, 10–11 December 1982.

RUTGERS

Robock (1983)

Alan Robock
Department of Environmental Sciences


CELESTRON
RADIANT
HEATER

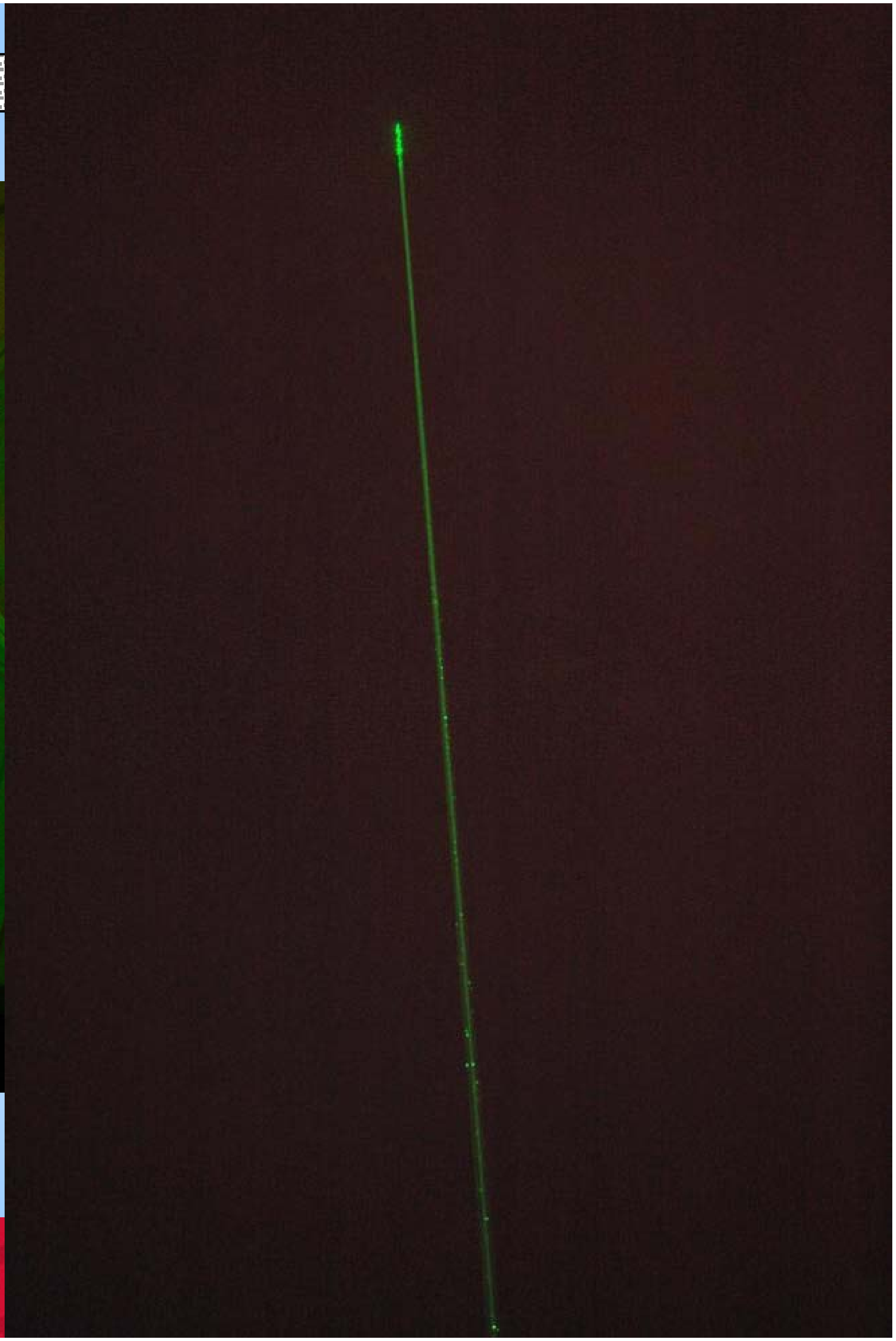

RUTGERS

Pinatubo
June 12, 1991

Three days before major eruption of June 15, 1991

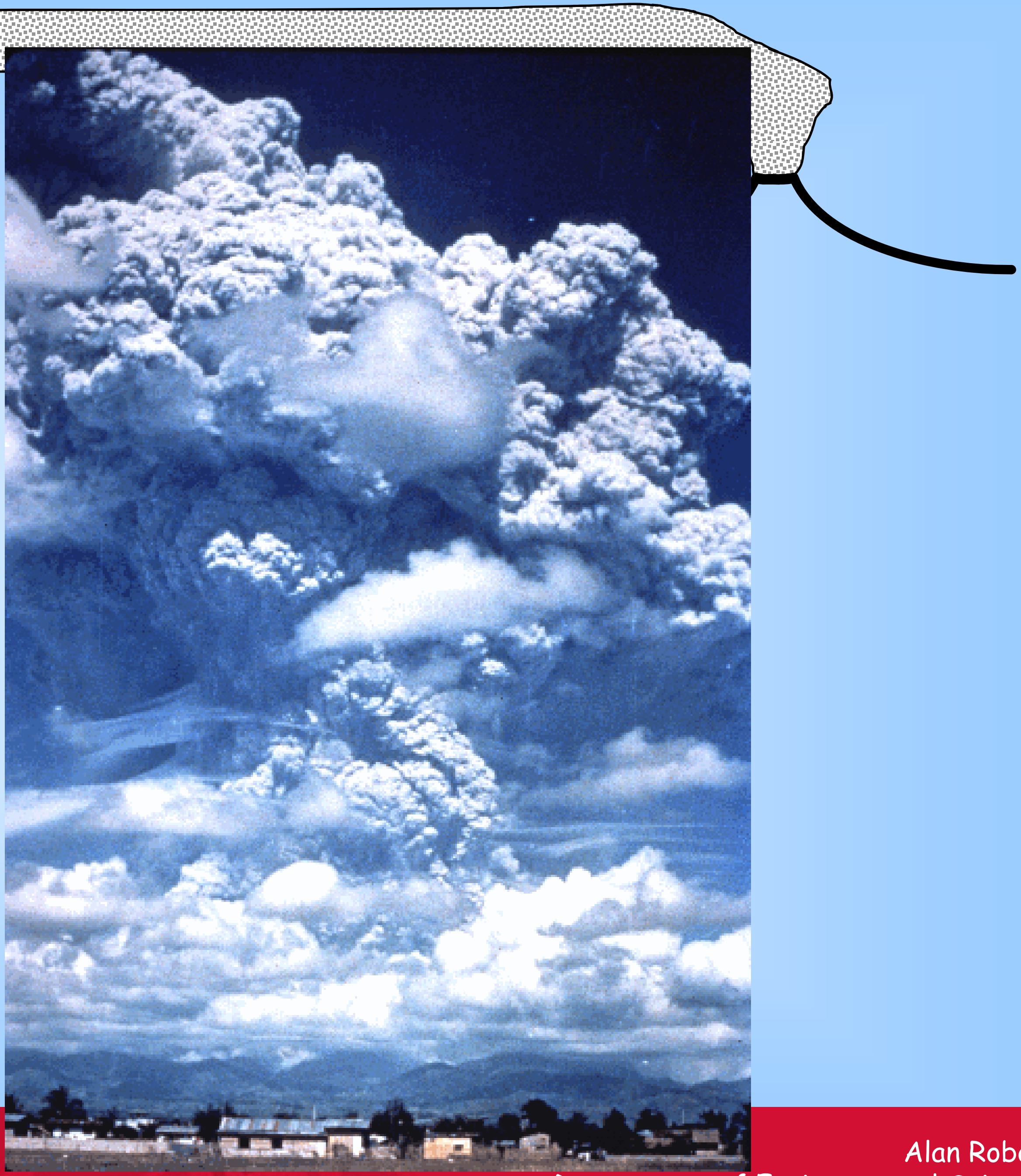

Alan Robock
Department of Environmental Sciences

August 30, 1984

August 8, 1991

These two photos show the Earth's limb at sunset before and after the Mt. Pinatubo eruption. The first view (STS41D-32-14) shows a relatively clear atmosphere, taken August 30, 1984. Astronauts were looking at the profiles of high thunderstorms topping out at the tropopause at sunset; different atmospheric layers absorbed the last rays of light from the sun as the spacecraft moved eastward.

The same type of photograph (STS043-22-23) was taken August 8, 1991, less than two months after the Pinatubo eruption. Two dark layers of aerosols make distinct boundaries in the atmosphere. The estimated altitude of aerosol layers in this view is 20 to 25 km.

Alan Robock
Department of Environmental Sciences

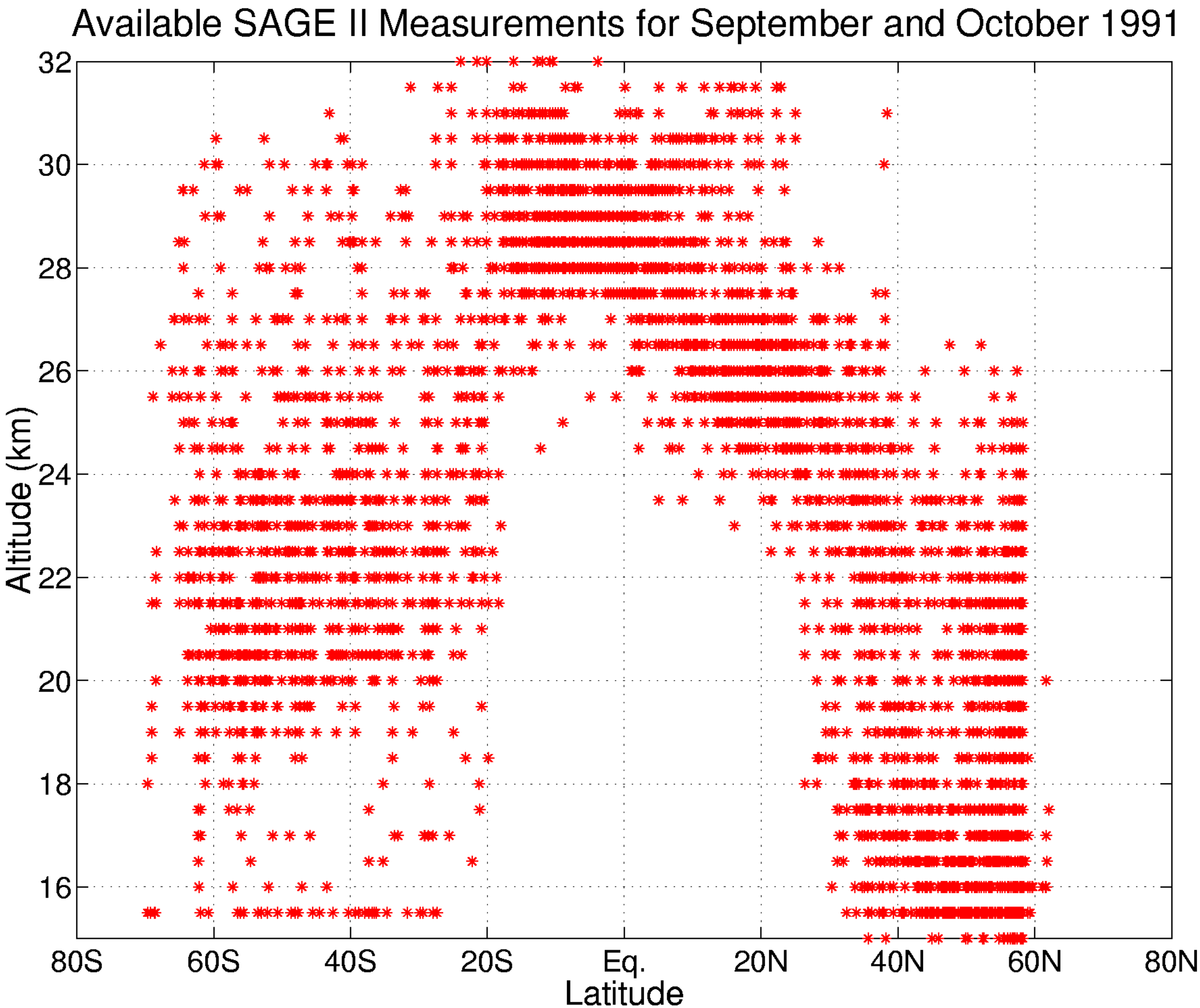

Available SAGE II Measurements for September and October 1991
Altitude (km)
32
30
28
26
24
22
20
18
16
80S
60S
40S
20S
Eq.
20N
40N
60N
80N
Latitude

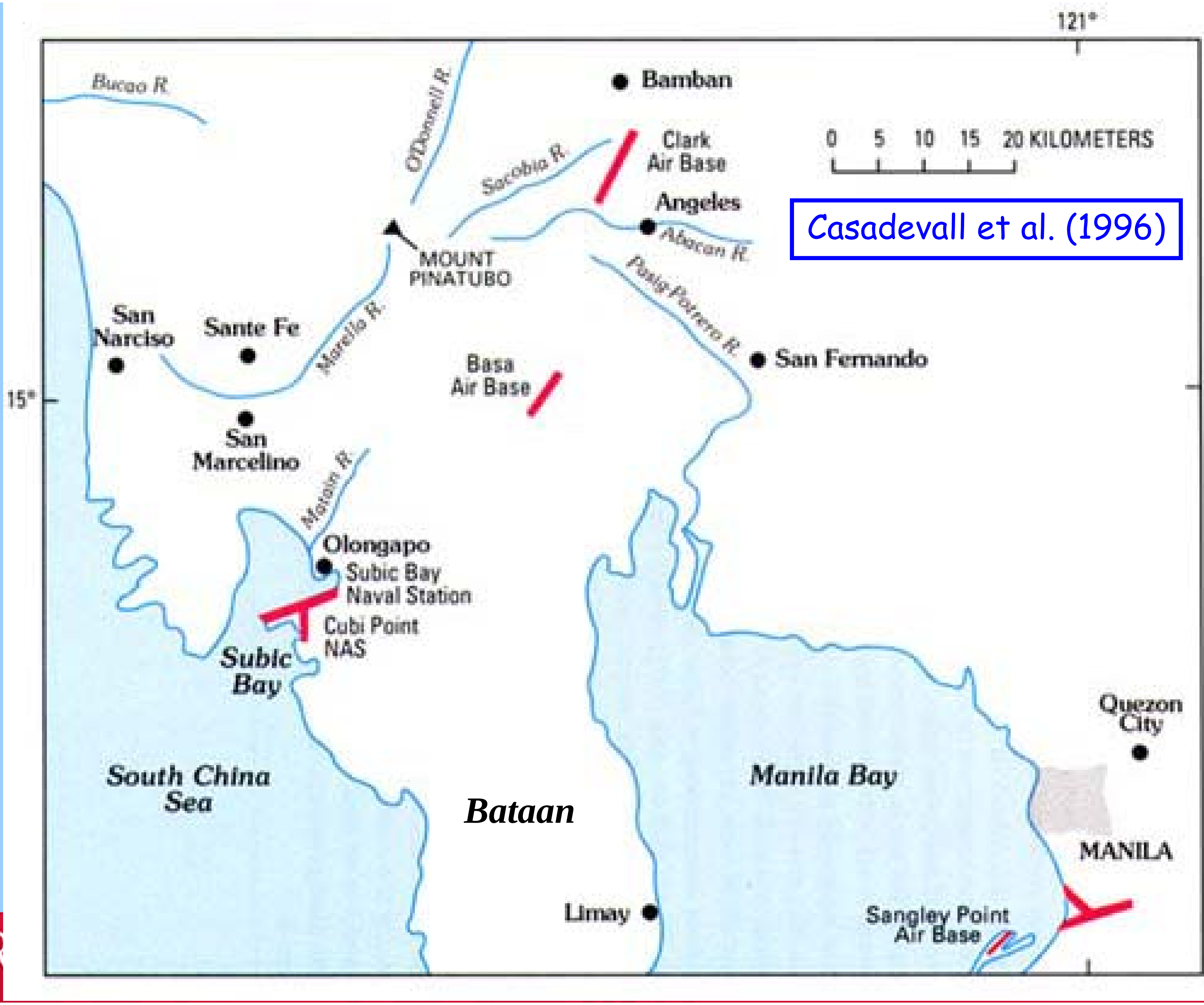

Casadevall et al. (1996)

After Pinatubo, Clark Air Force Base
25 km from volcano

Photo by R. P. Hoblitt, June 15, 1991

RUTGERS
Alan Robock
Department of Environmental Sciences

After Pinatubo, Cubi Point Naval Air Station, 40 km from volcano

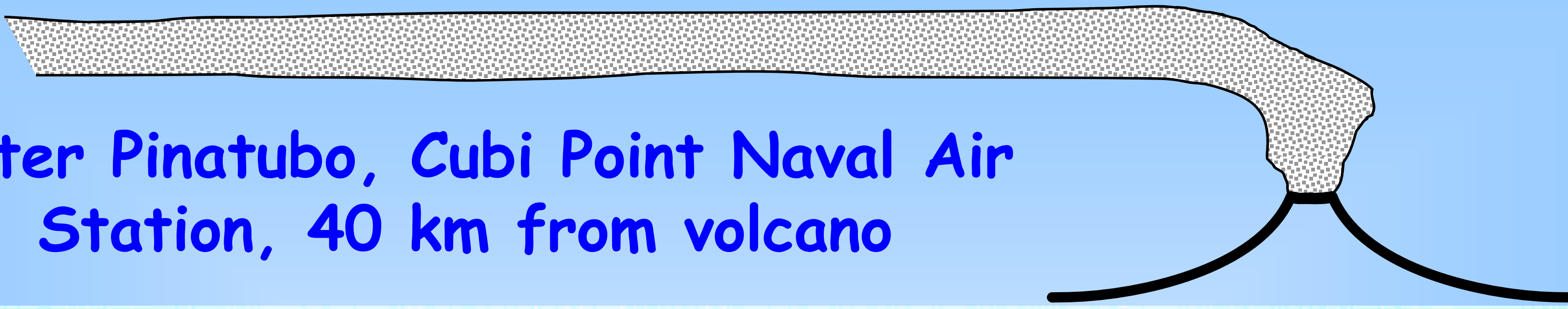

U.S. Navy photograph by R. L. Rieger

Alan Robock
Department of Environmental Sciences

After Pinatubo, Subic Bay Naval Base
35 km from volcano

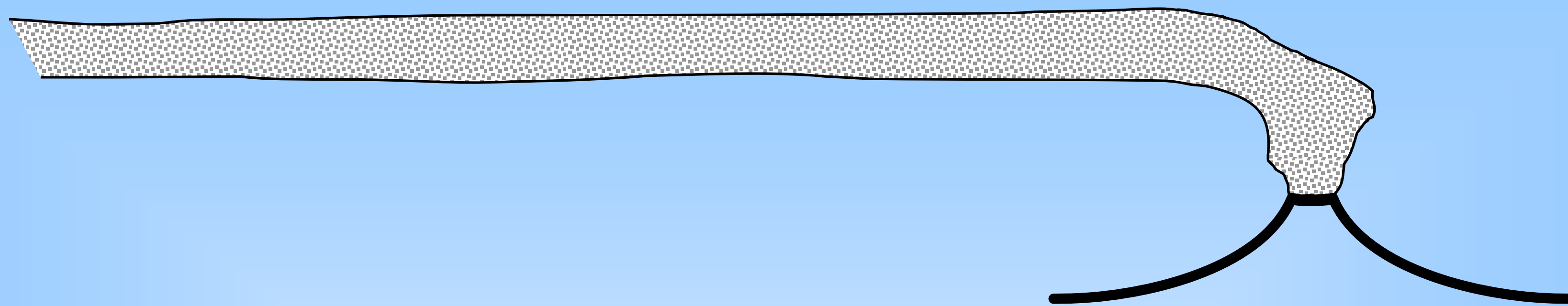

Radiative Effects

RUTGERS
Alan Robock
Department of Environmental Sciences

Diffuse Radiation from Pinatubo Makes a White Sky

Photographs by Alan Robock

RUTGERS

Alan Robock
Department of Environmental Sciences

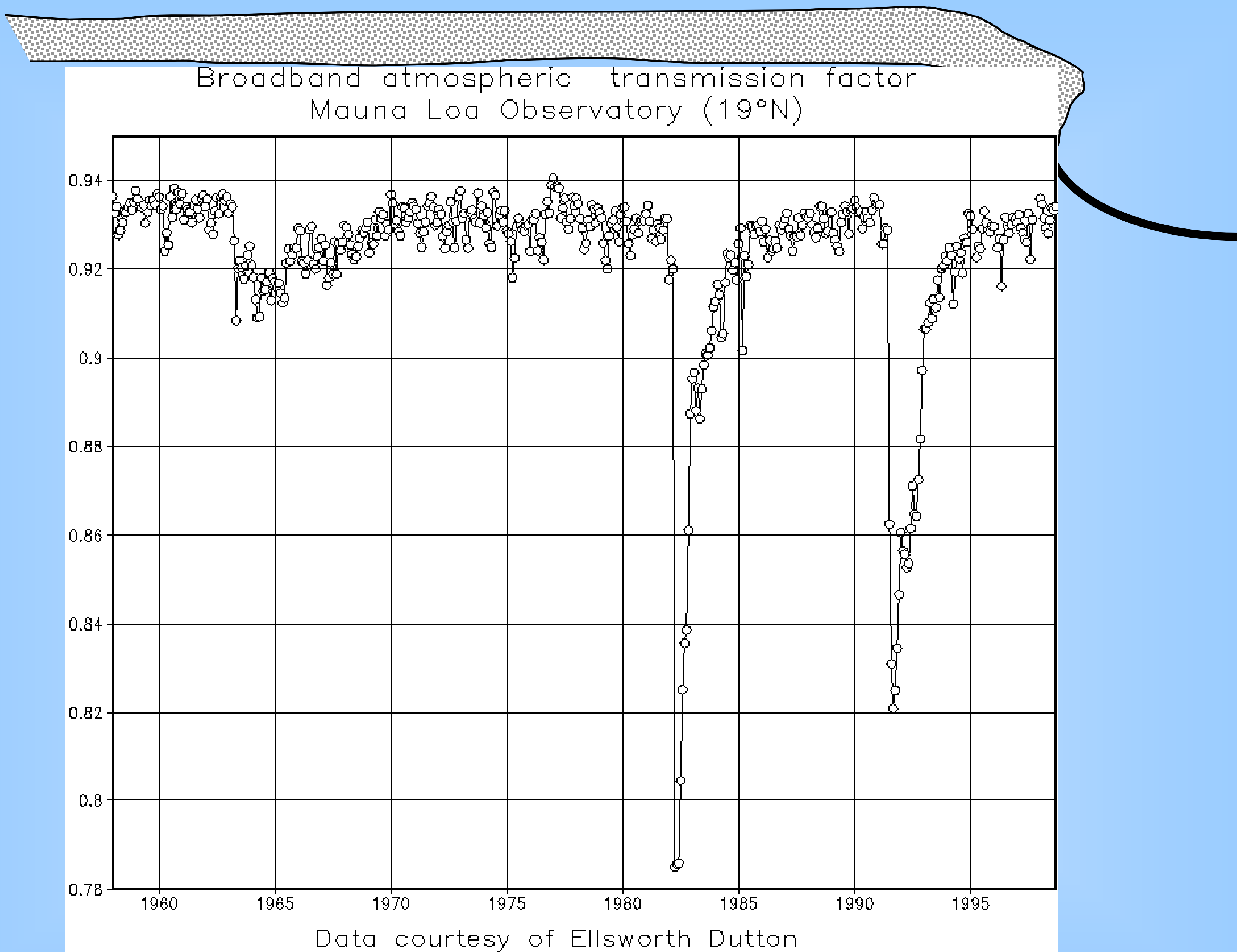
Broadband atmospheric transmission factor
Mauna Loa Observatory (19°N)
0.94
0.92
0.9
0.88
0.86
0.84
0.82
0.8
0.78
1960
1965
1970
1975
1980
1985
1990
1995
Data courtesy of Ellsworth Dutton

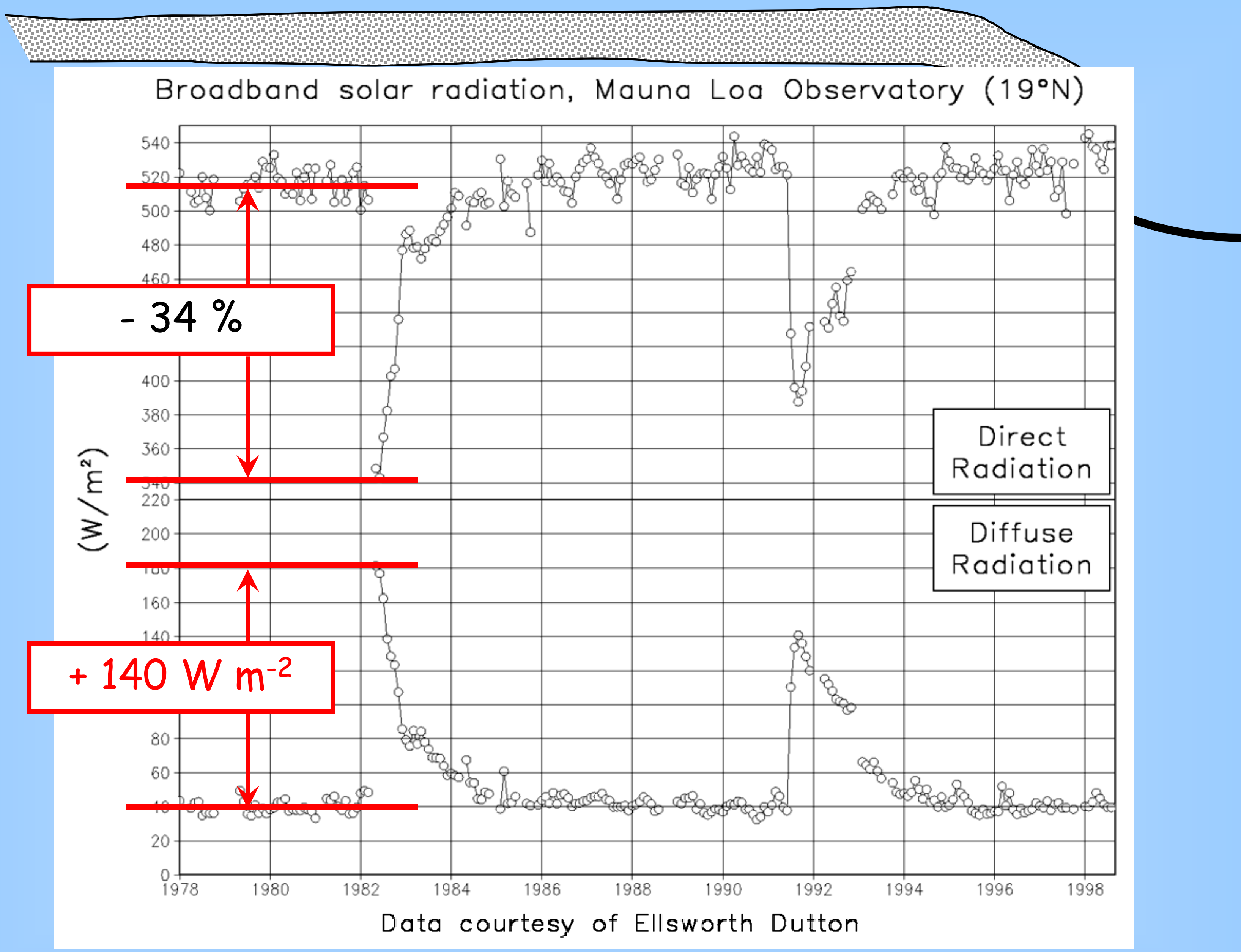

Robock (2000), Dutton and Bodhaine (2001)

Nevada Solar One
64 MW

Solar steam generators requiring direct solar

Seville, Spain
Solar Tower
11 MW

http://www.electronichealing.co.uk/articles/solar_power_tower_spain.htm

http://judykitsune.wordpress.com/2007/09/12/solar-seville/

Alan Robock
Department of Environmental Sciences

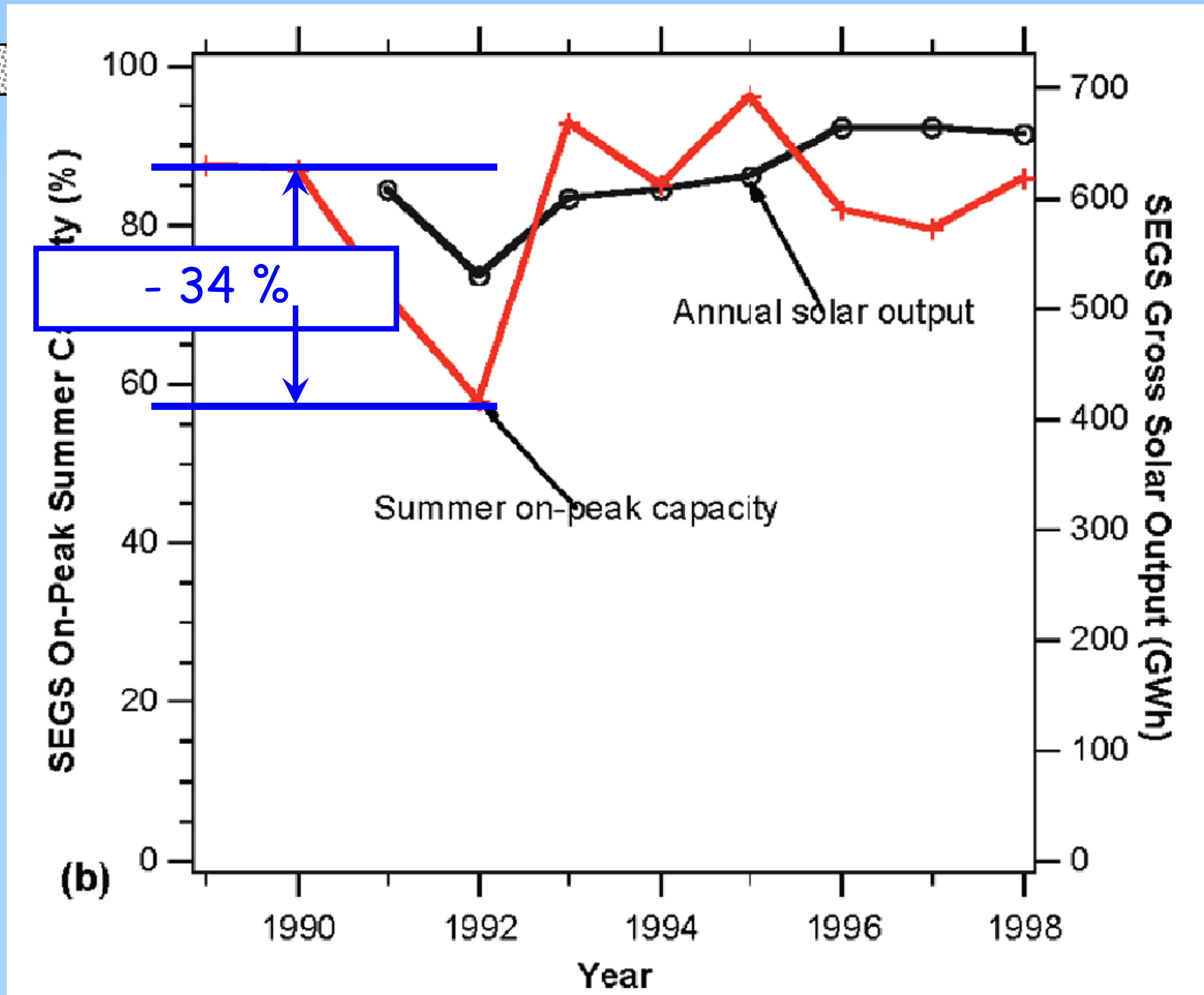

Output of solar electric generating systems (SEGS) solar thermal power plants in California (9 with a combined capacity of 354 peak MW). (Murphy, 2009, *ES&T*)

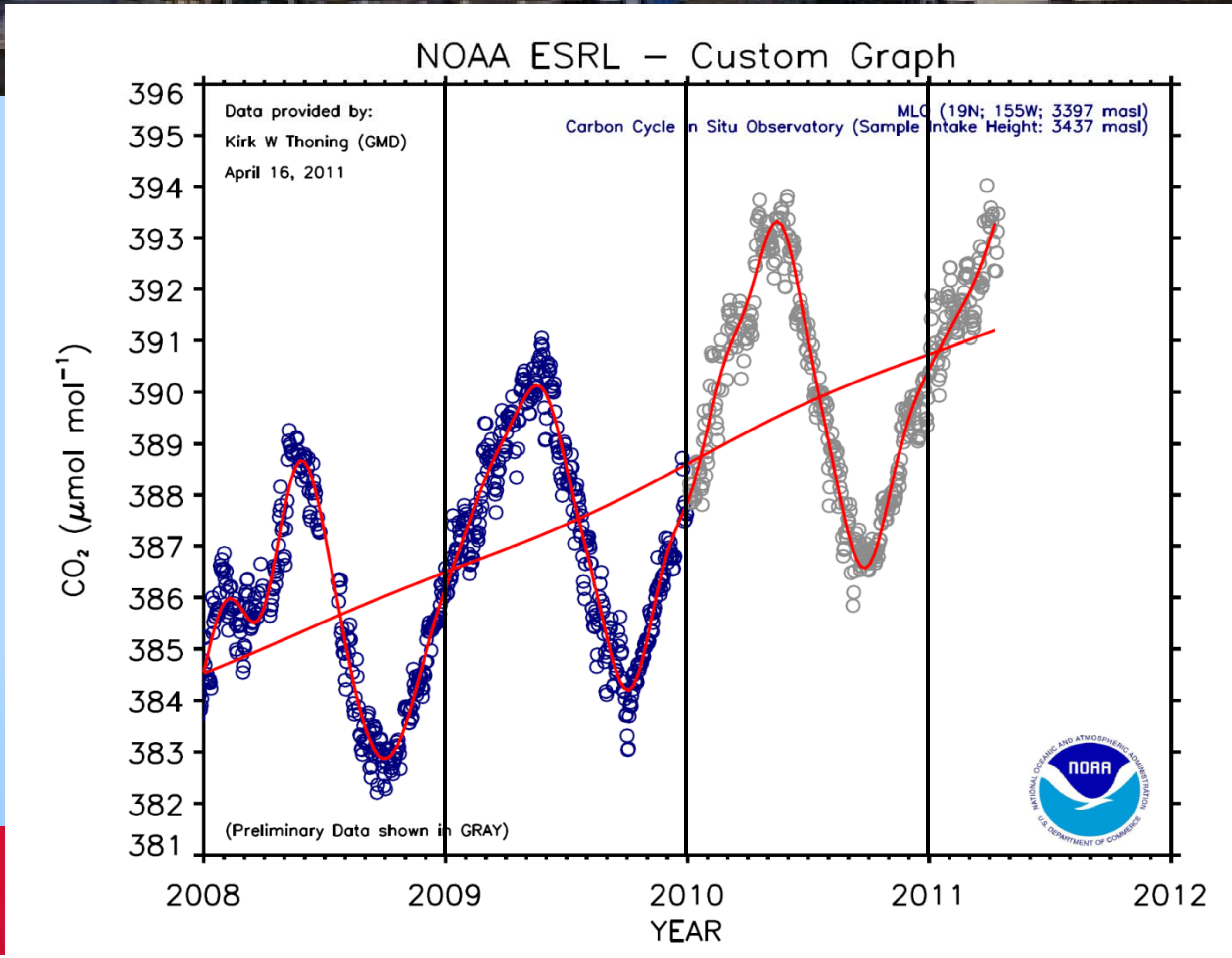

RUTGERS

Alan Robock
ental Sciences

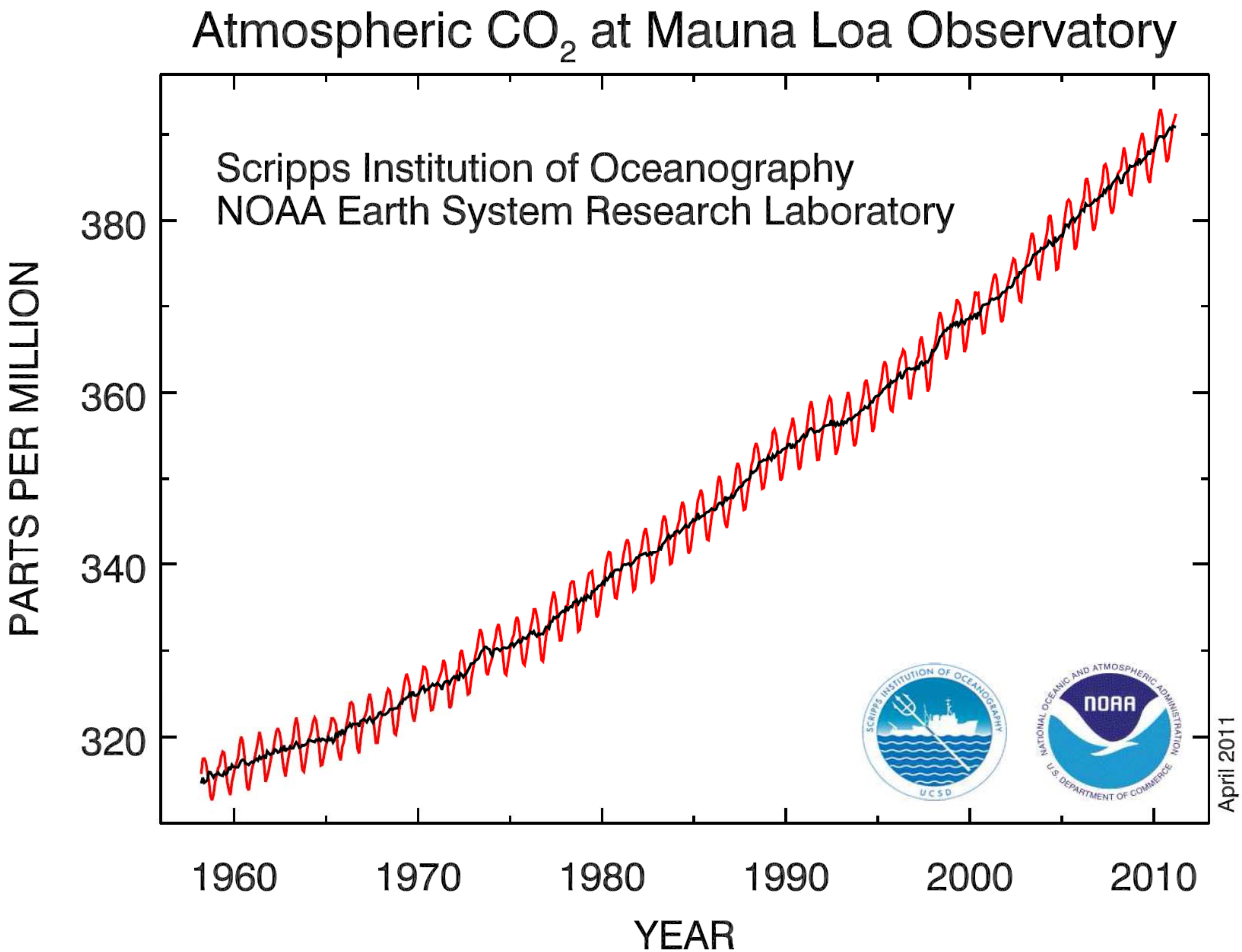
Atmospheric CO_2 at Mauna Loa Observatory
Scripps Institution of Oceanography
NOAA Earth System Research Laboratory
PARTS PER MILLION
380
360
340
320
1960
1970
1980
1990
2000
2010
YEAR
NOAA
April 2011

Global Distribution of Atmospheric Carbon Dioxide

NOAA ESRL Carbon Cycle

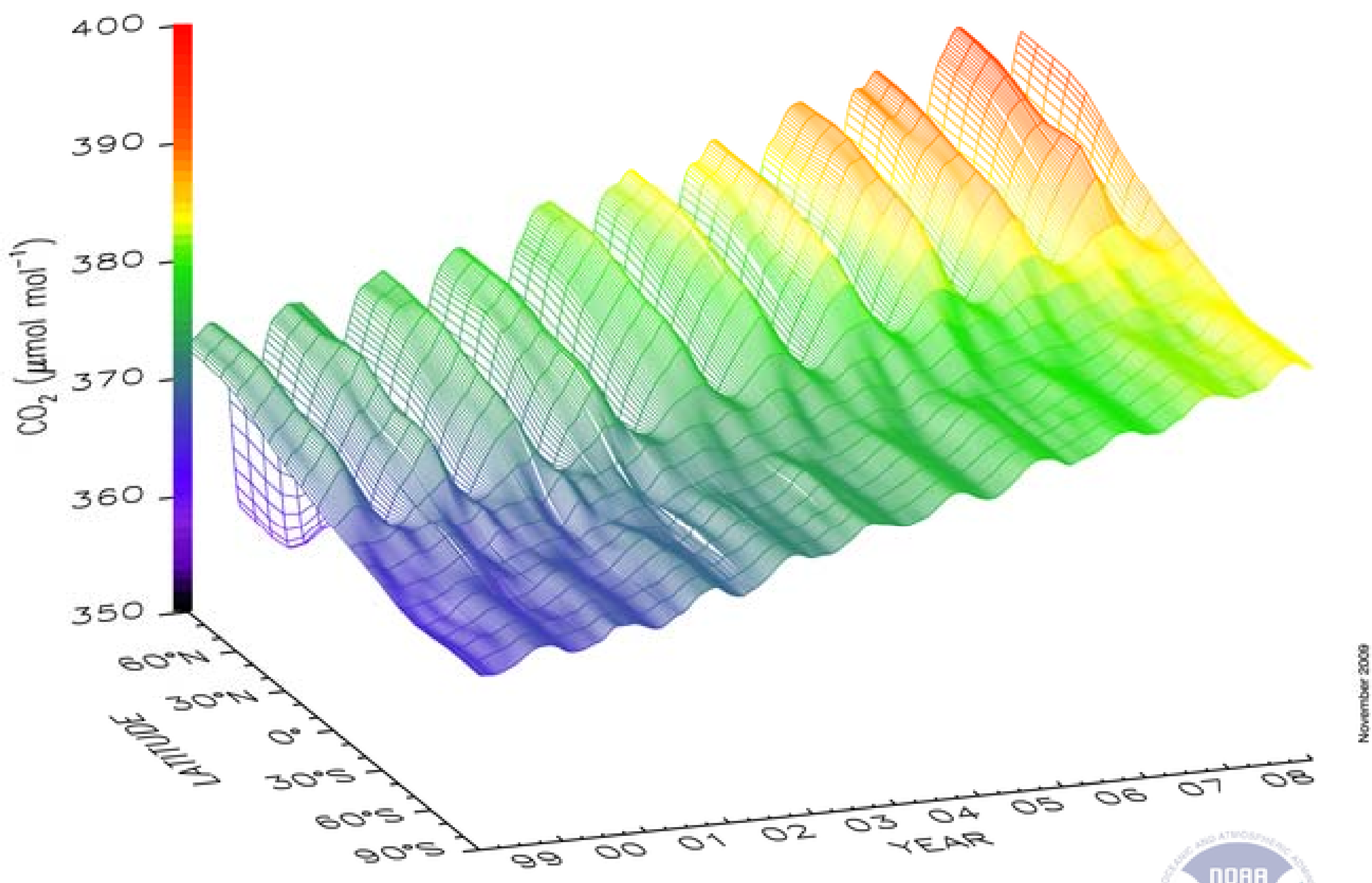

Three-dimensional representation of the latitudinal distribution of atmospheric carbon dioxide in the marine boundary layer. Data from the Carbon Cycle cooperative air sampling network were used. The surface represents data smoothed in time and latitude. Contact: Dr. Pieter Tans and Thomas Conway, NOAA ESRL Carbon Cycle, Boulder, Colorado, (303) 497-6678, pieter.tans@noaa.gov, http://www.esrl.noaa.gov/gmd/ccgg/.

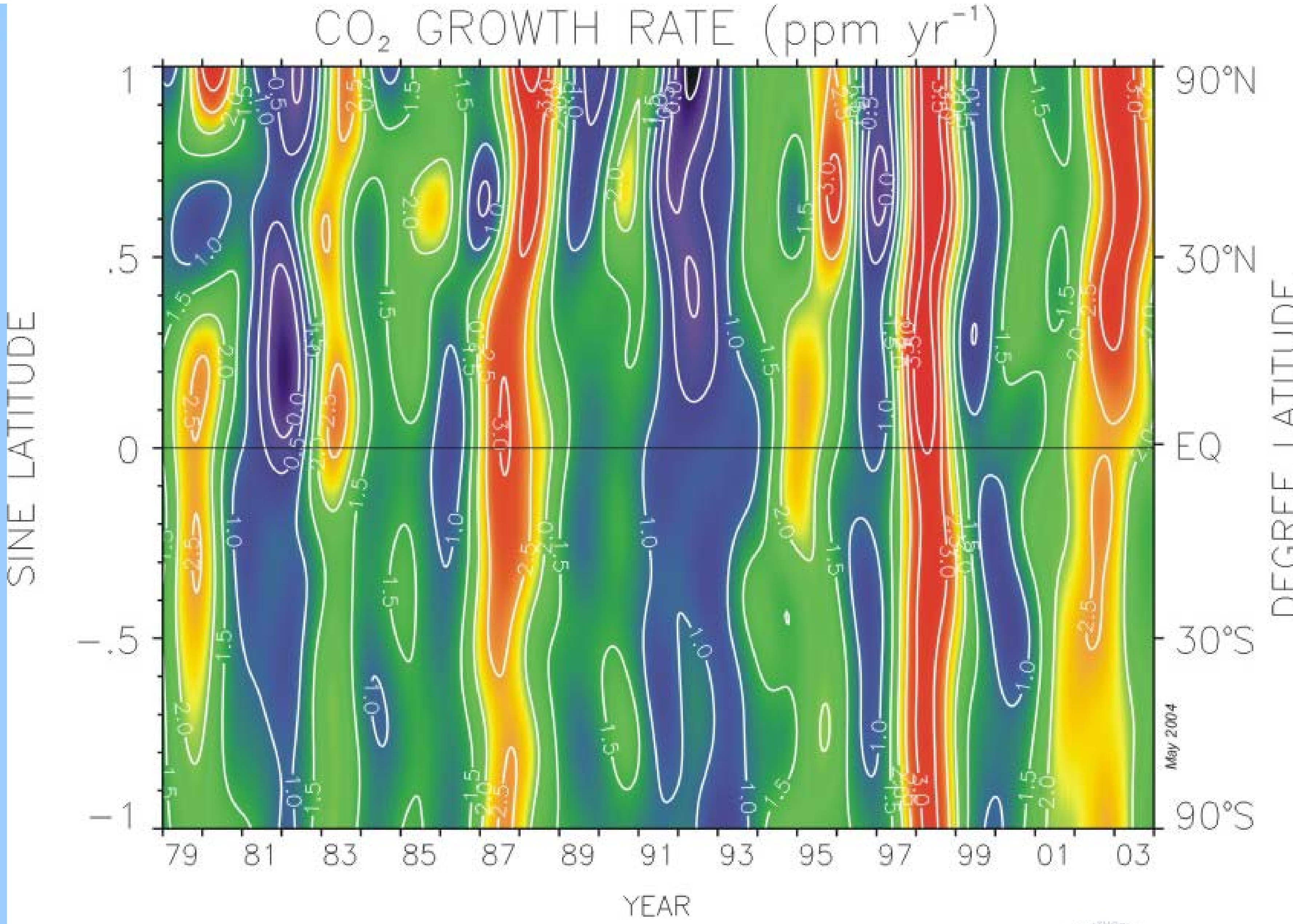

RUTGERS

Principal investigator: Thomas Conway, NOAA CMDL

http://www.cmdl.noaa.gov/ccgg

Alan Robock
Department of Environmental Sciences

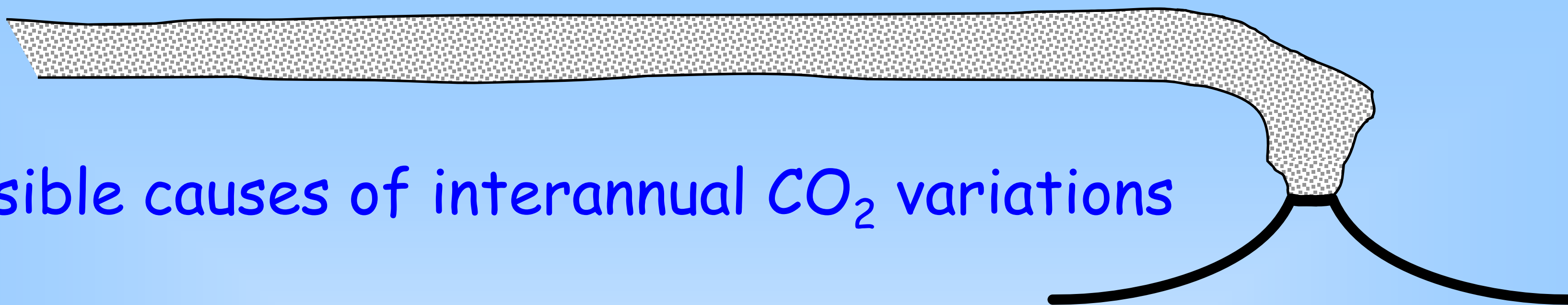

Possible causes of interannual CO_2 variations

- Changes in emissions
- Land use changes
- Unusual atmospheric temperatures or precipitation (e.g., drought)
- El Niño and La Niña episodes
- Volcanic eruptions through effects on diffuse radiation

Alan Robock
Department of Environmental Sciences

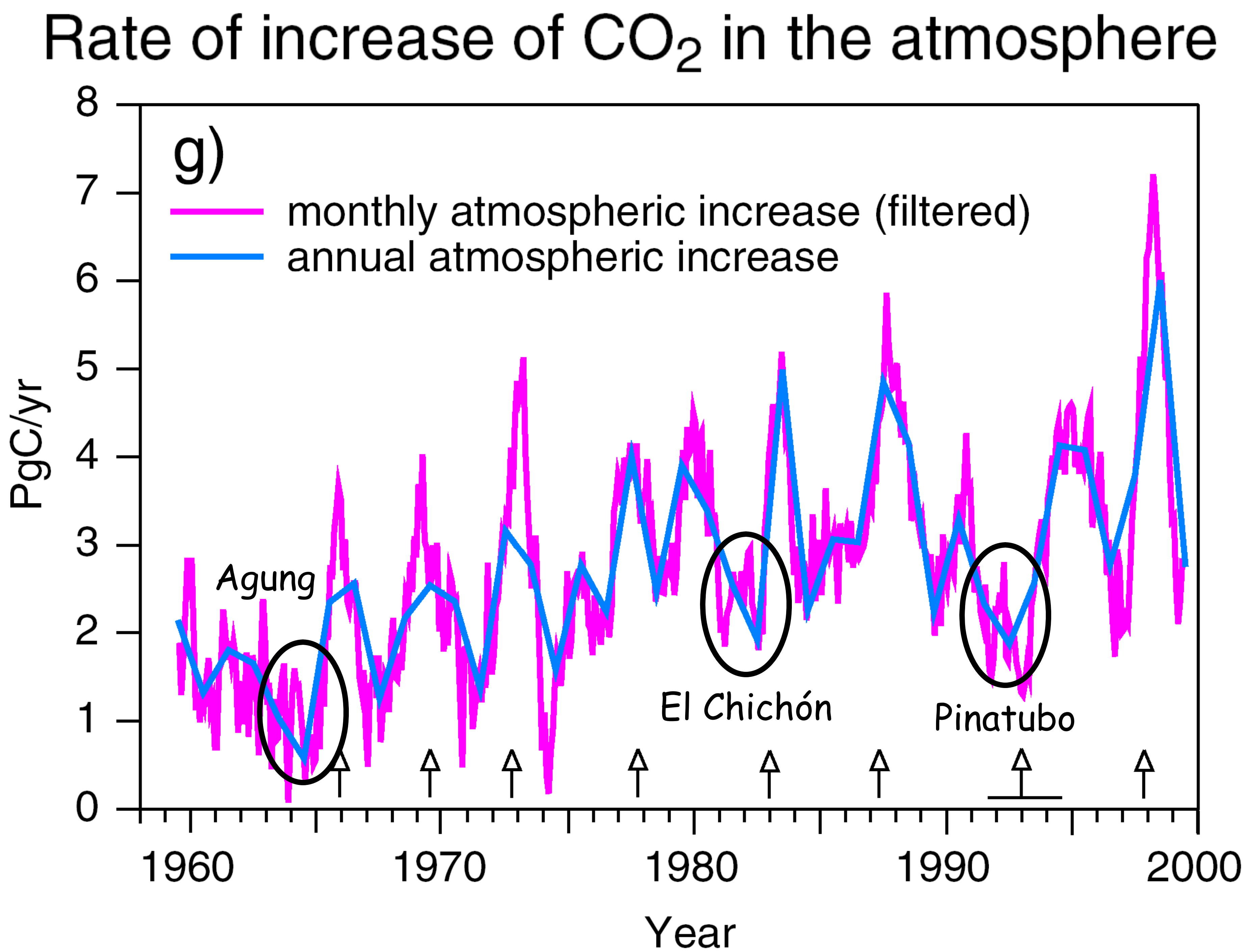

Rate of increase of CO2 in the atmosphere
g)
monthly atmospheric increase (filtered)
annual atmospheric increase
PgC/yr
0
1
2
3
4
5
6
7
8
Agung
El Chichón
Pinatubo
1960
1970
1980
1990
2000
Year

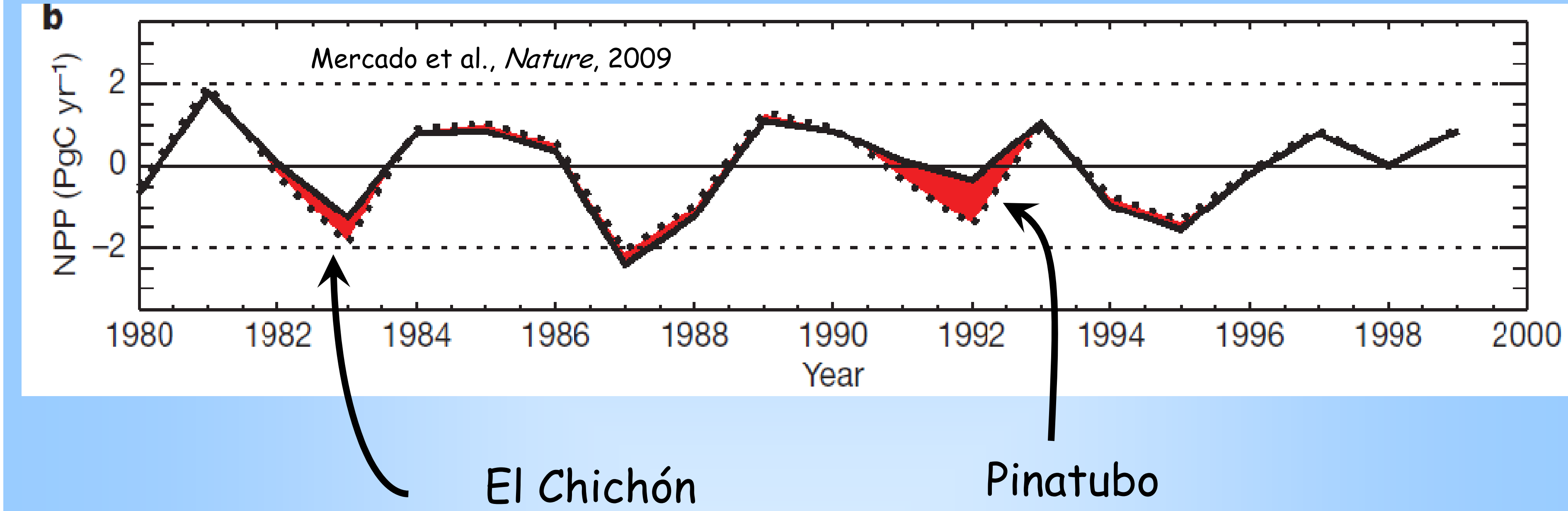

Additional carbon sequestration after volcanic eruptions because of the effects of diffuse radiation, but certainly will impact natural and farmed vegetation.

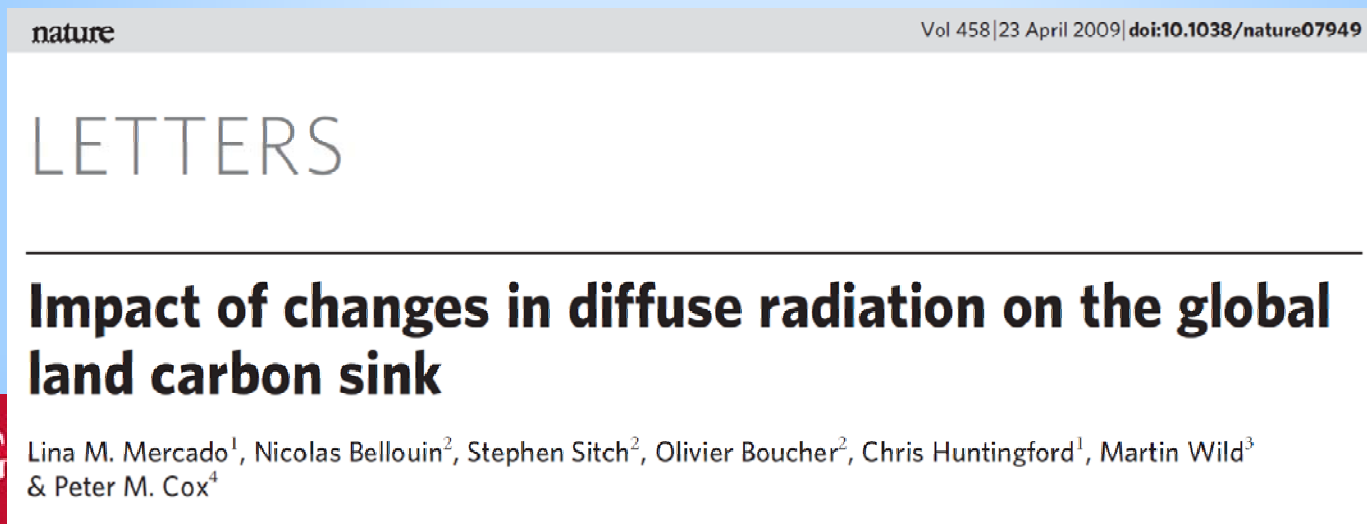

nature Vol 458|23 April 2009|**doi:10.1038/nature07949**

LETTERS

Impact of changes in diffuse radiation on the global land carbon sink

Lina M. Mercado[1], Nicolas Bellouin[2], Stephen Sitch[2], Olivier Boucher[2], Chris Huntingford[1], Martin Wild[3] & Peter M. Cox[4]

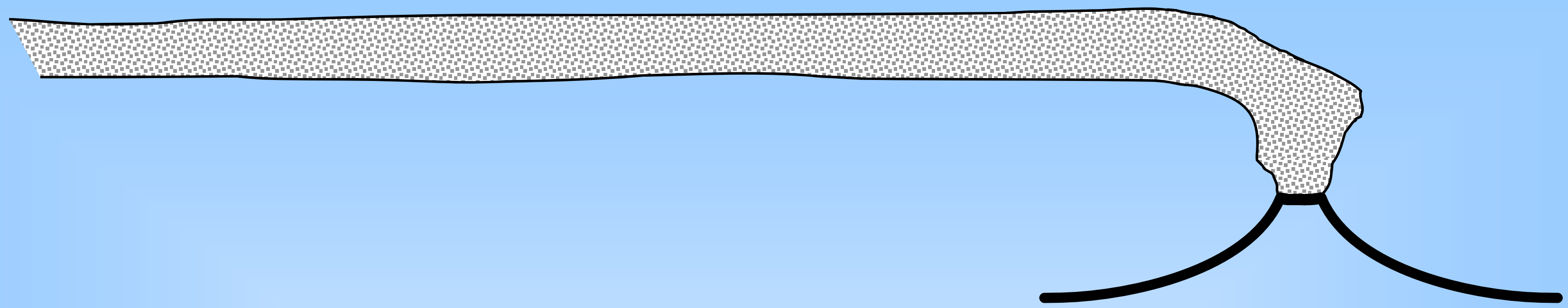

Summer Cooling

Superposed epoch analysis of six largest eruptions of past 120 years

Robock and Mao (1995)

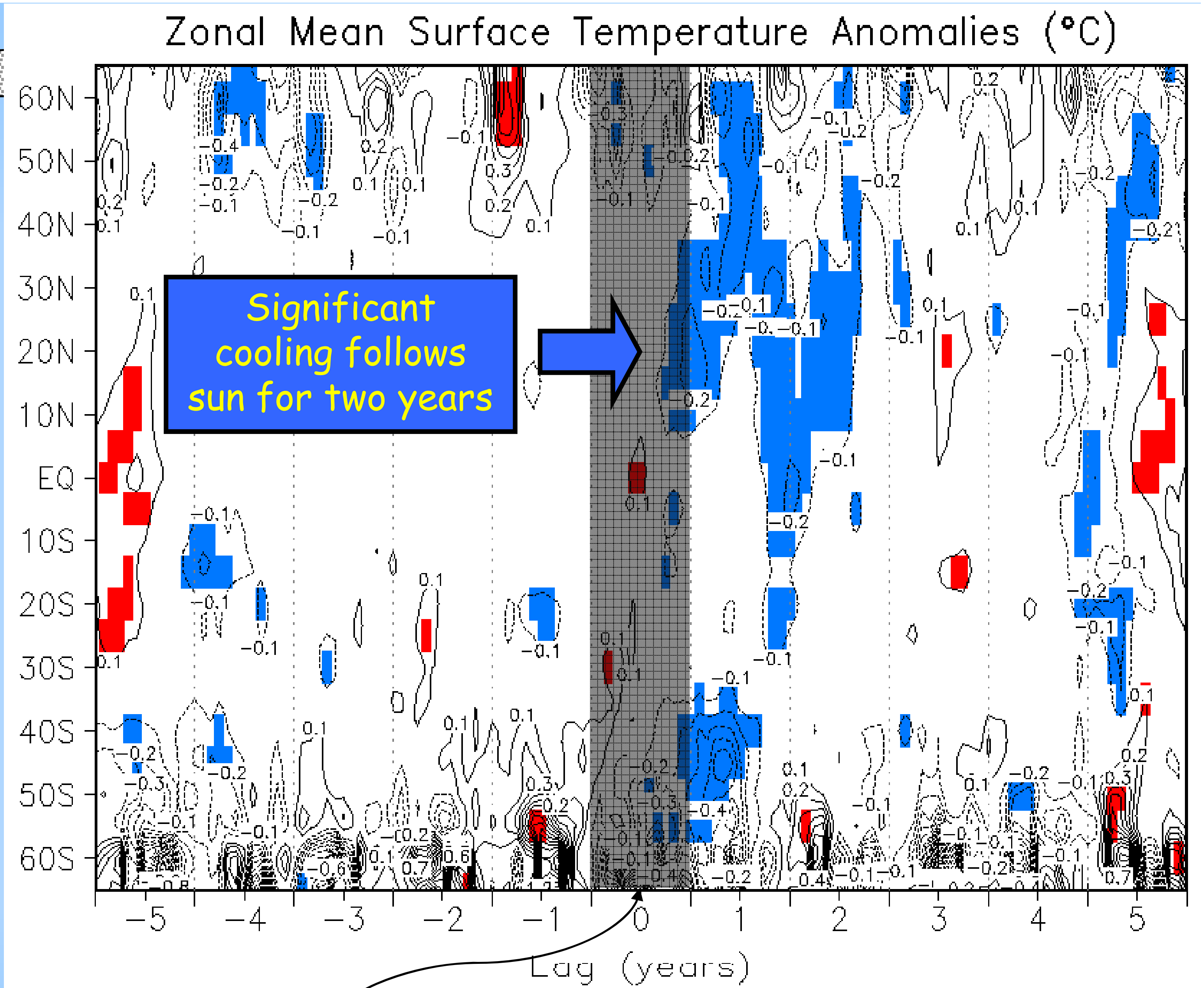

Year of eruption

Alan Robock
Department of Environmental Sciences

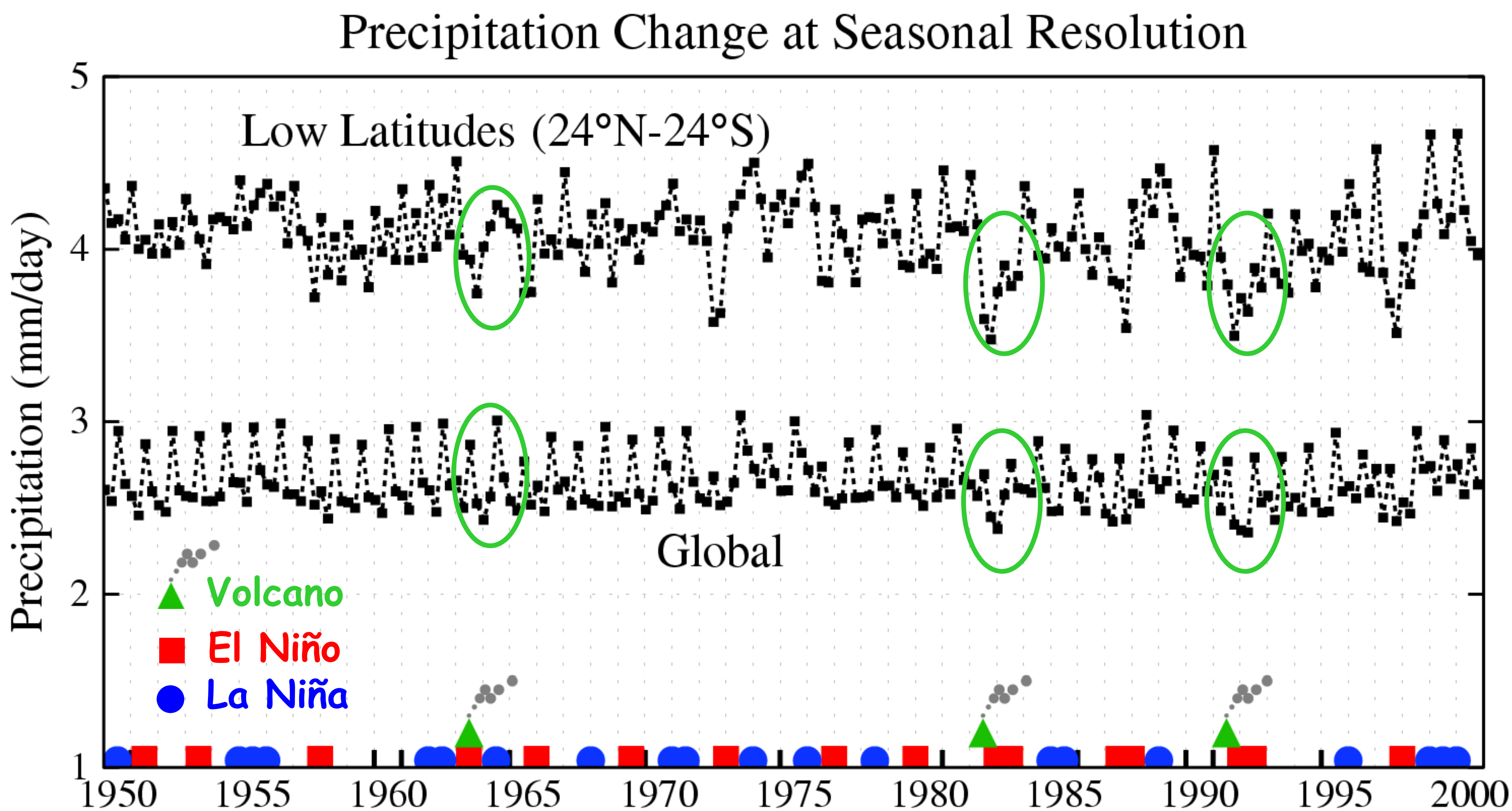

Drawn by Makiko Sato (NASA GISS) using CRU TS 2.0 data

Trenberth and Dai (2007)

Effects of Mount Pinatubo volcanic eruption on the hydrological cycle as an analog of geoengineering

Geophys. Res. Lett.

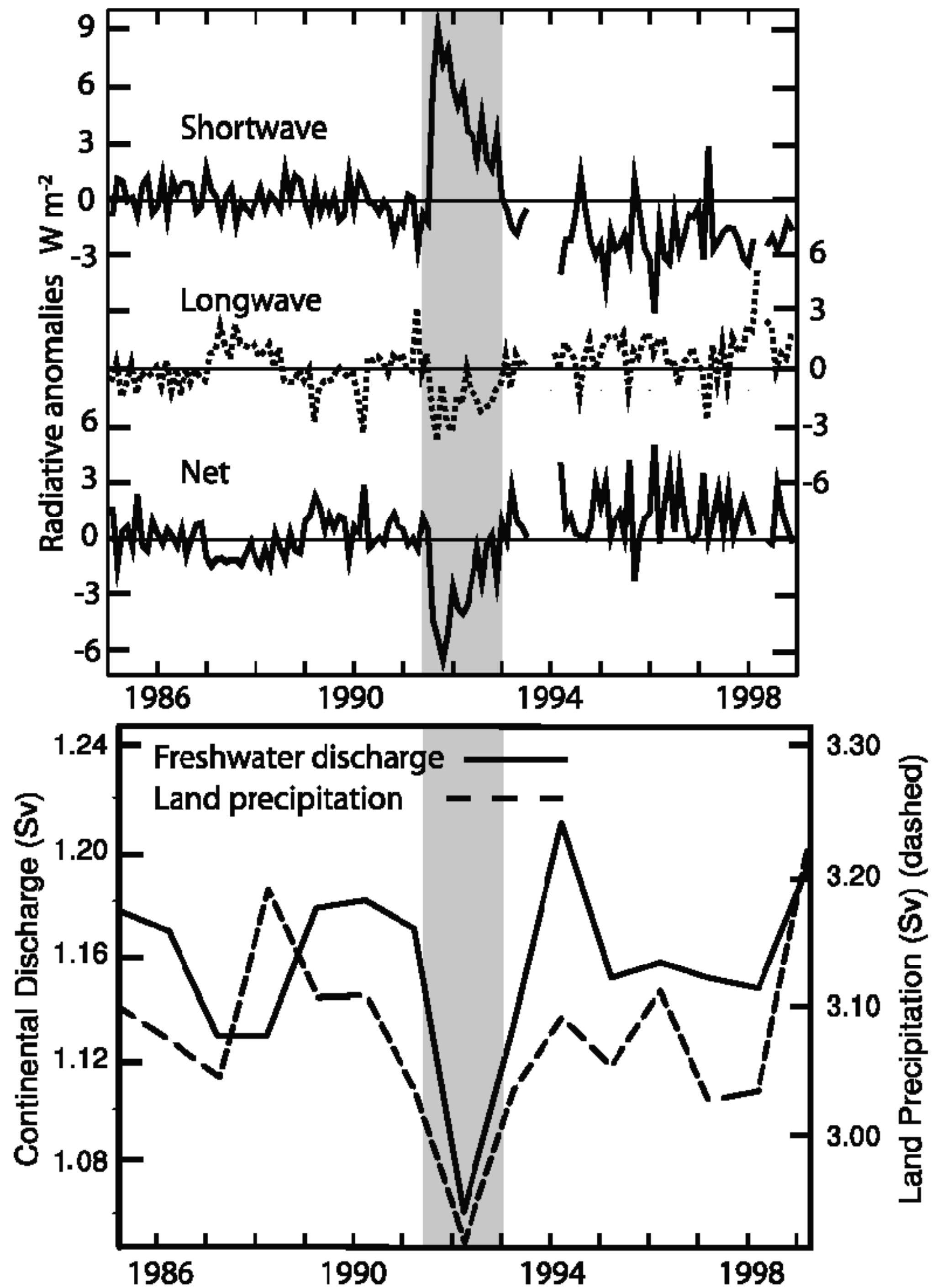

Figure 2. (top) Adapted time series of 20°N to 20°S ERBS non-scanner wide-field-of-view broadband short-wave, longwave, and net radiation anomalies from 1985 to 1999 [*Wielicki et al.*, 2002a, 2002b] where the anomalies are defined with respect to the 1985 to 1989 period with Edition 3_Rev 1 data [*Wong et al.*, 2006]. (bottom) Time series of the annual water year (Oct. to Sep.); note slight offset of points plotted vs. tick marks indicating January continental freshwater discharge and land precipitation (from Figure 1) for the 1985 to 1999 period. The period clearly influenced by the Mount Pinatubo eruption is indicated by grey shading.

RUTGERS

Trenberth and Dai (2007)

Effects of Mount Pinatubo volcanic eruption on the hydrological cycle as an analog of geoengineering

Geophys. Res. Lett.

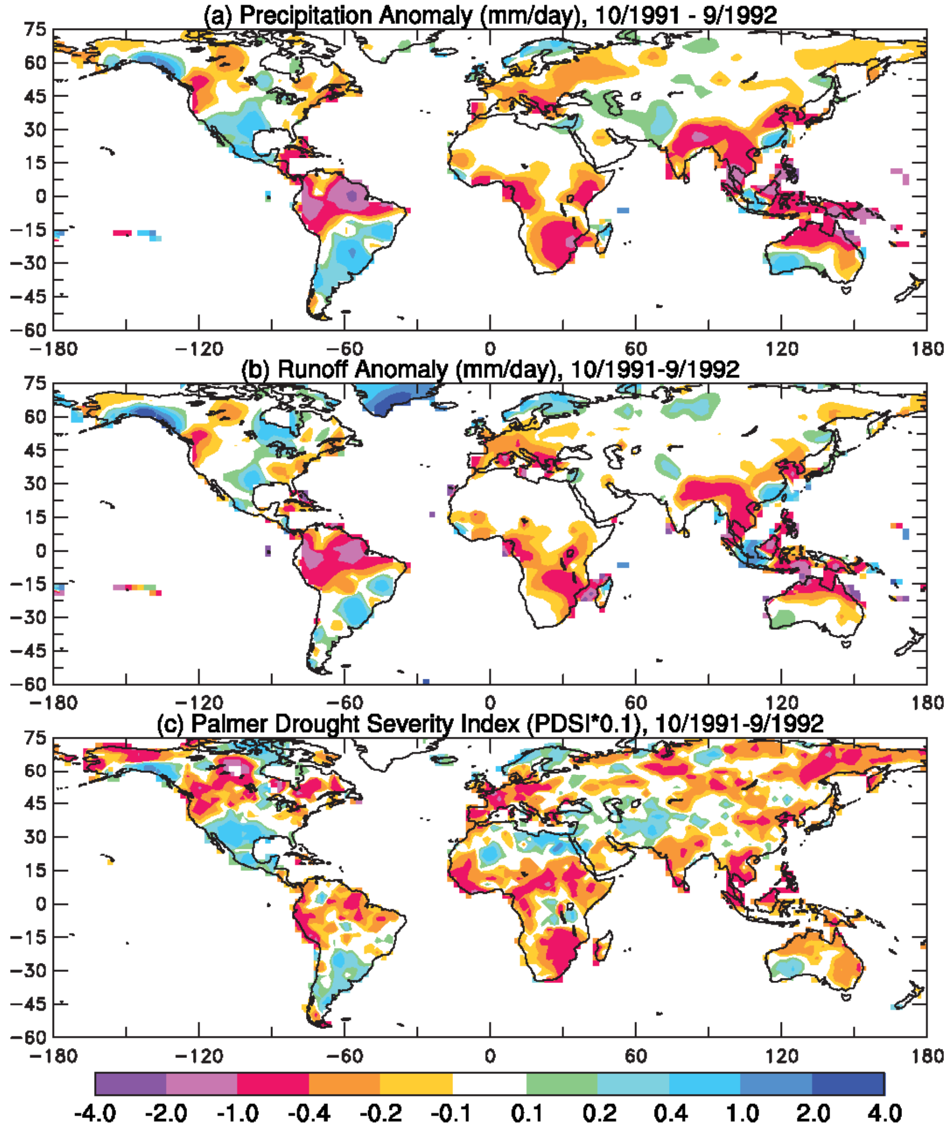

Figure 3. (a) Observed precipitation anomalies (relative to 1950–2004 mean) in mm/day during October 1991–September 1992 over land. Warm colors indicate below normal precipitation. (b) As for Figure 3a but for the simulated runoff [*Qian et al.*, 2006] using a comprehensive land surface model forced with observed precipitation and other atmospheric forcing in mm/day. (c) Palmer Drought Severity Index (PDSI, multiplied by 0.1) for October 1991–September 1992 [*Dai et al.*, 2004]. Warm colors indicate drying. Values less than −2 (0.2 on scale) indicate moderate drought, and those less than −3 indicate severe drought.

RUTGERS

Summer monsoon drought index pattern using tree rings for 750 years

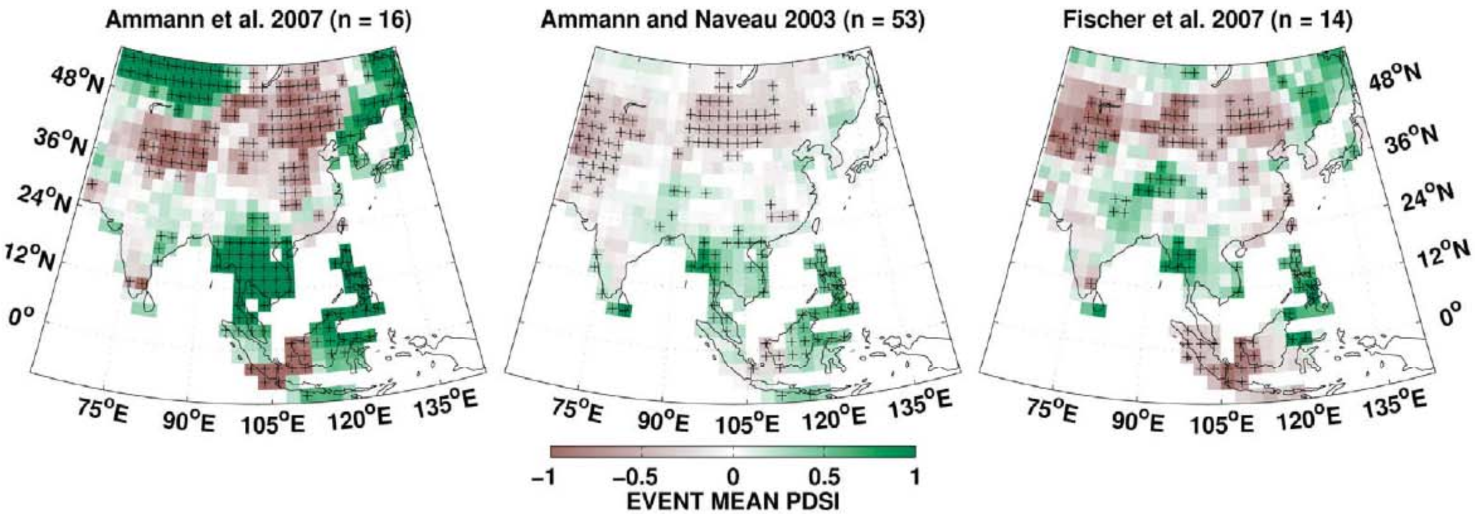

Figure 2. Superposed epoch analysis using the reconstructed PDSI values from the Monsoon Asia Drought Atlas (MADA) [*Cook et al.*, 2010] and the sets of events years shown in Table 1. Statistically significant (90% one-tailed) epochal anomalies based on Monte Carlo resampling (n = 10,000) are indicated by crosses.

Anchukaitis et al. (2010), Influence of volcanic eruptions on the climate of the Asian monsoon region. *Geophys. Res. Lett.*, *37*, L22703, doi:10.1029/2010GL044843

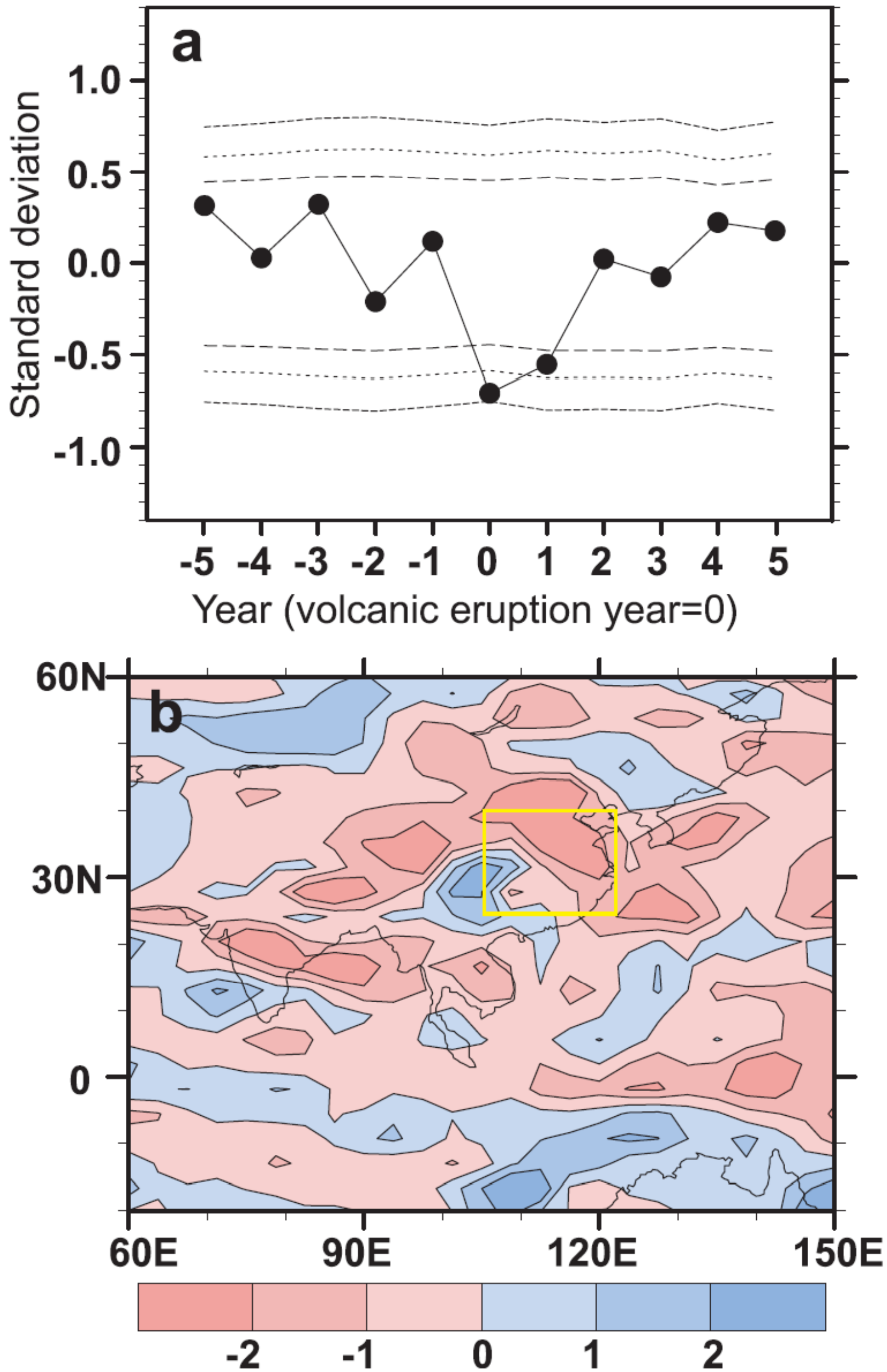

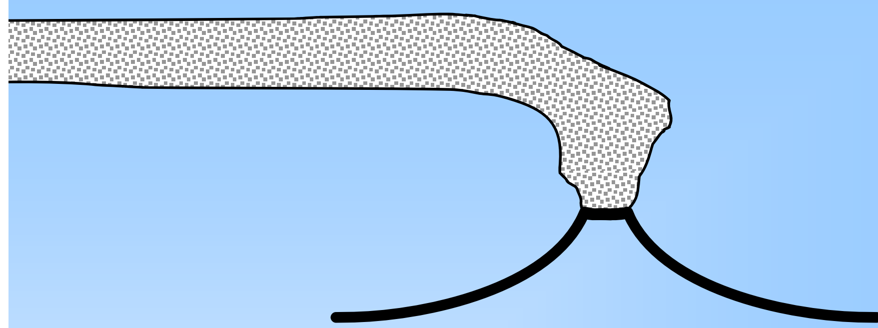

FIG. 1. (a) Results of superposed epoch analysis of modeled summer precipitation for 18 cases of large volcanic eruption showing the response of summer precipitation over eastern China. Bootstrapping procedures are used to assess the statistical significance of summer precipitation above and below the mean. The dashed and dotted lines represent confidence intervals of 90%, 95%, and 99% derived from 1000 Monte Carlo simulations. (b) Spatial pattern of composite anomalies of summer precipitation over East Asia and tropical oceans during the volcanic eruption year for 18 cases of large volcanic eruption; yellow box shows our study area.

NCAR CCSM 2.0.1 simulation for past 1000 years

Peng, Youbing, Caiming Shen, Wei-chyung Wang, and Ying Xu, 2010: Response of summer precipitation over Eastern China to large volcanic eruptions. *J. Climate*, **23**, 818-825.

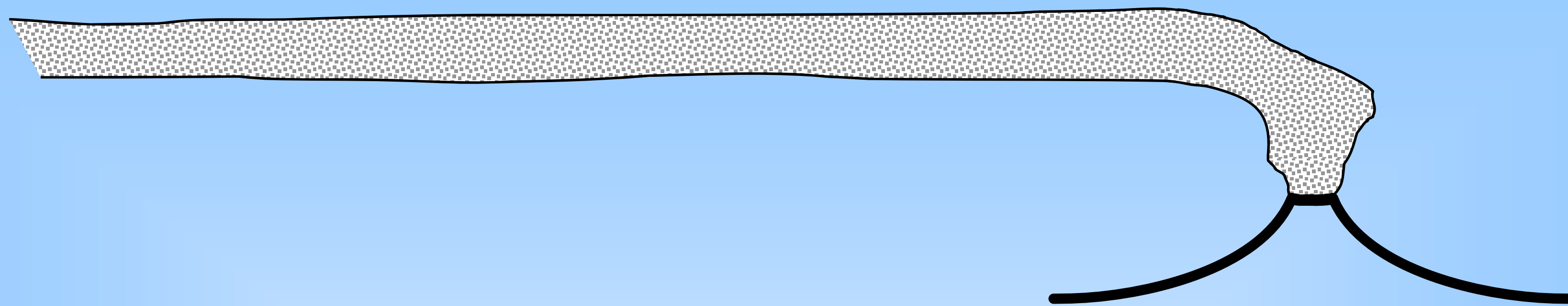

Stratospheric Temperature Response

RUTGERS

Alan Robock
Department of Environmental Sciences

NCEP Observations

Stratospheric temperature anomaly at 50 mb with respect to 1985-1990 mean

Hatching shows 90% significance

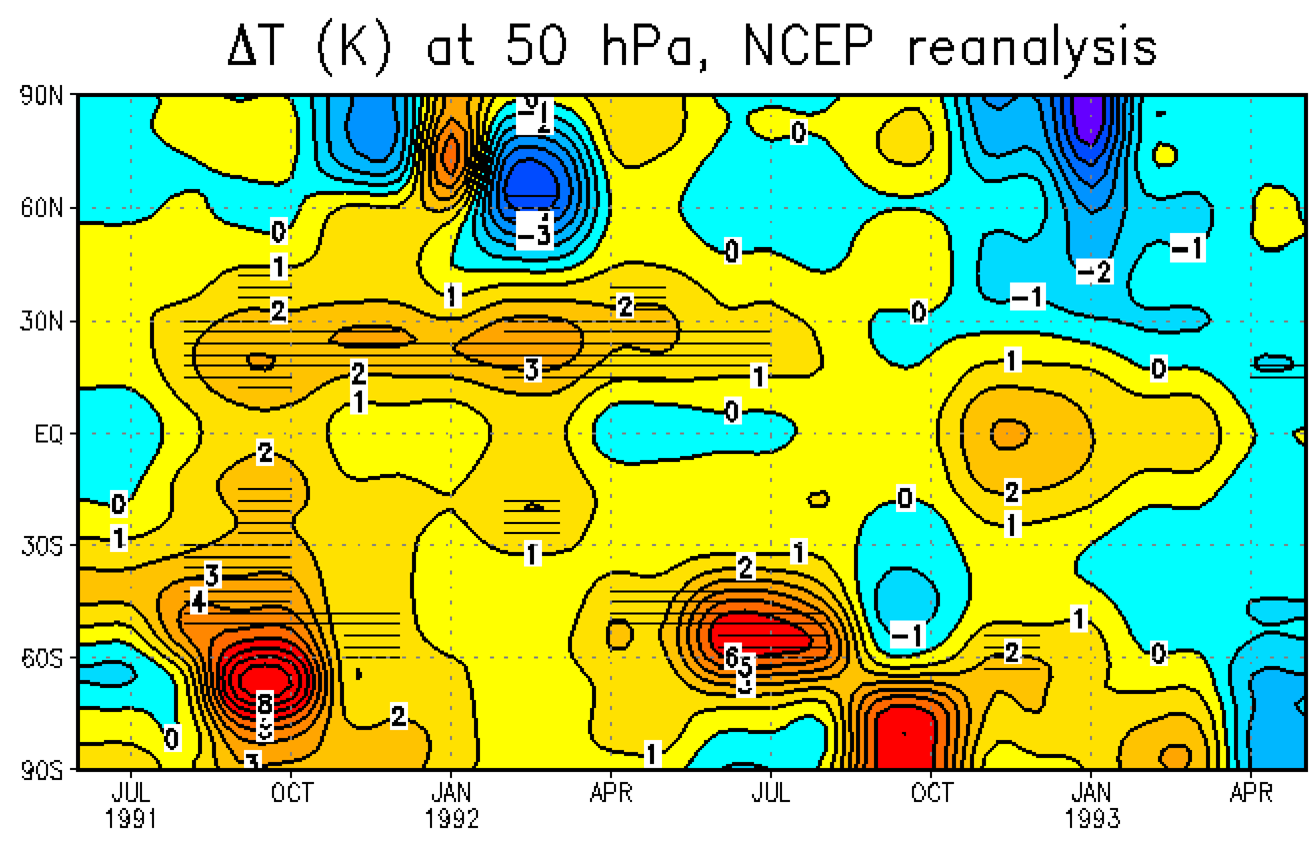

Alan Robock
Department of Environmental Sciences

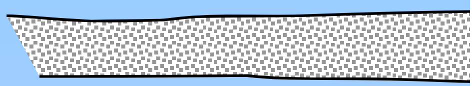

SKYHI simulations

Zonal mean temperature anomaly (K) at 50 mb caused by aerosols only (A)

Hatching shows 90% significance

NCEP observations

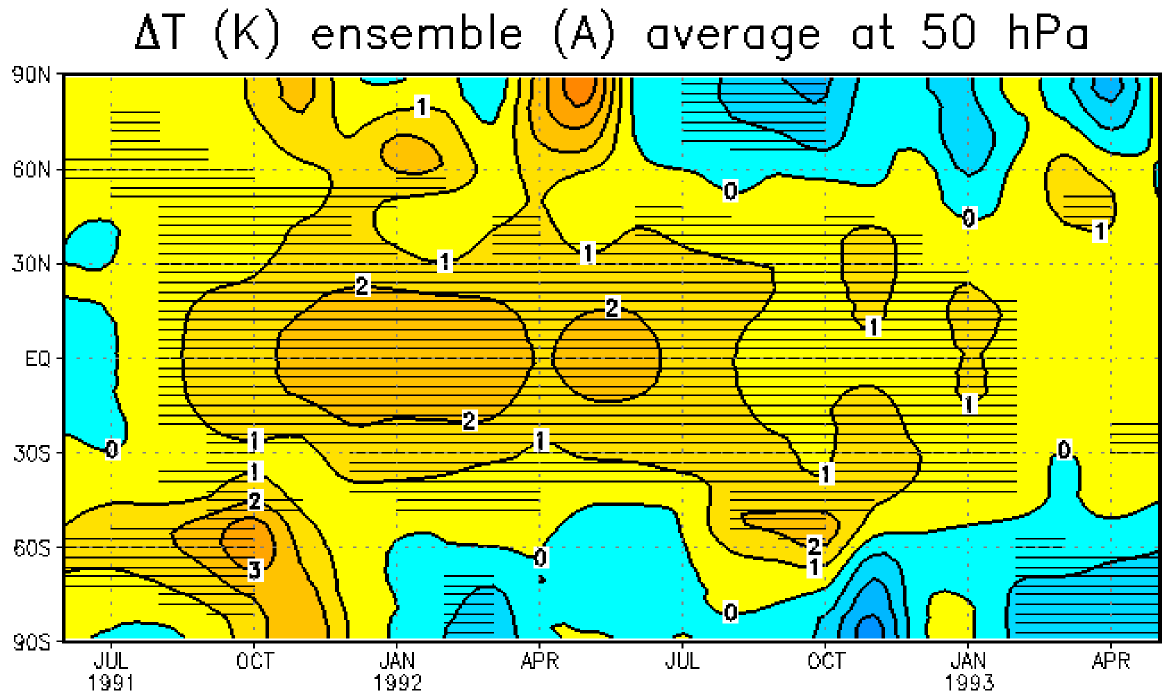

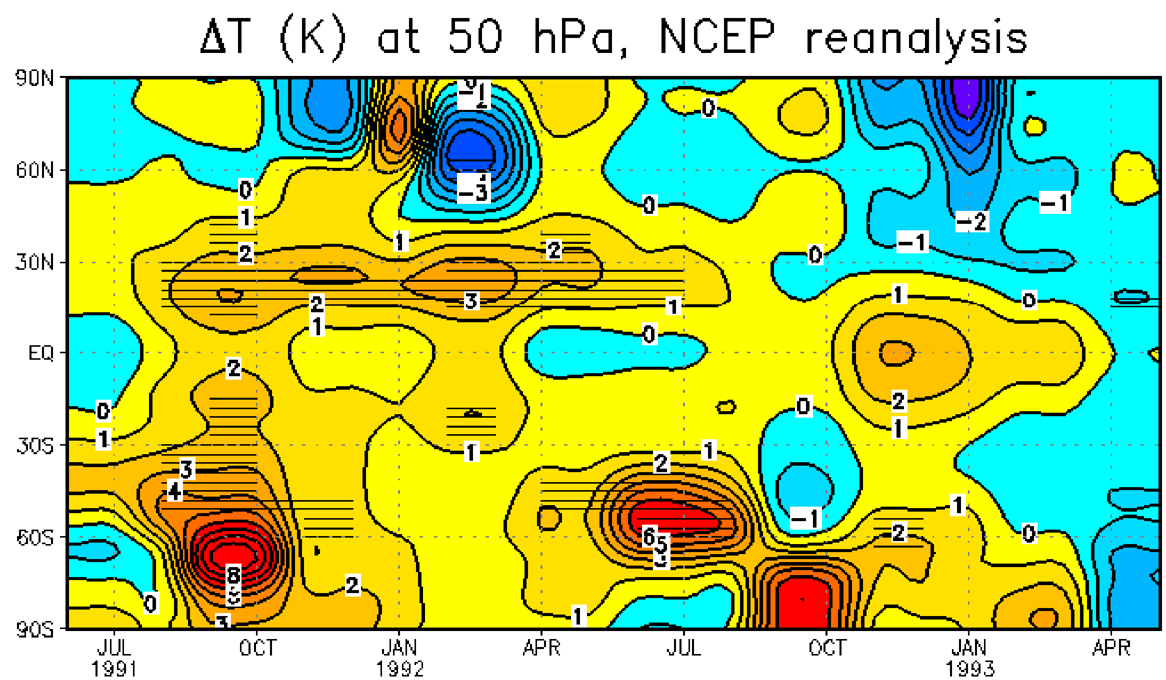

QBO forcing

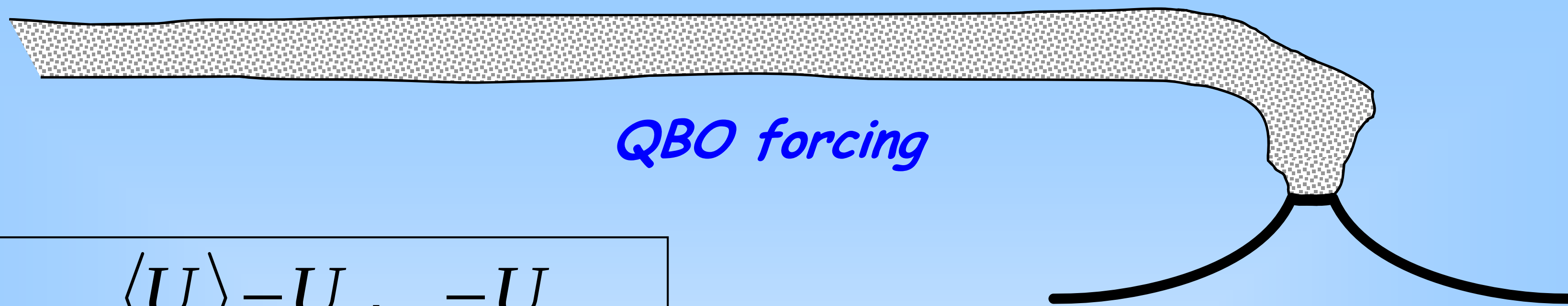

$$\frac{dU}{dt} = -\frac{\langle U \rangle - U_{clim} - U_{QBO}}{\tau(p,\phi)}$$

$$U_{QBO}(p,\phi,t) = U_{Sing} \times e^{-\left(\frac{\phi}{13^\circ}\right)^2}$$

U_{Sing} - *smoothed deseasonalized monthly-mean Singapore zonal wind*

ϕ - *latitude*, p - *pressure*, $\tau(p,\phi)$ - *characteristic time*

$\tau(p,\phi) > 5$ *day for 0.01 hPa* $< p <$ *100 hPa*

$\langle U \rangle$ - *zonal mean zonal wind*

U_{clim} - *climatological mean of zonal mean zonal wind*

RUTGERS

Alan Robock
Department of Environmental Sciences

SKYHI simulation

Zonal mean zonal wind (m/s) from 11-year QBO control run

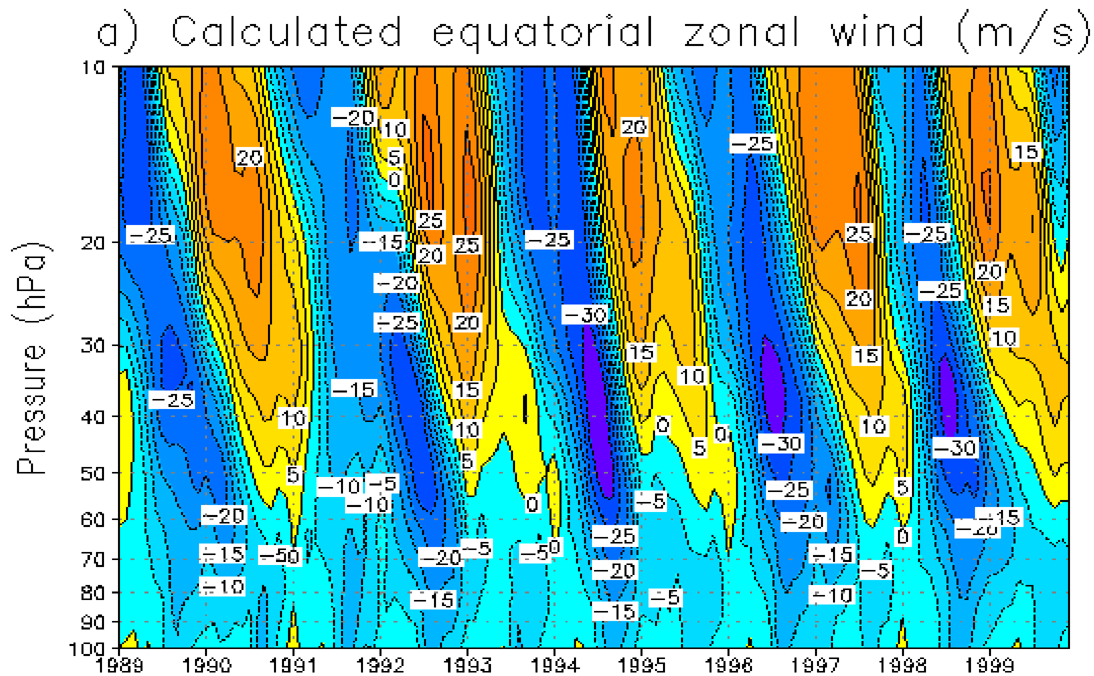

Observed zonal mean zonal wind (m/s) at Singapore

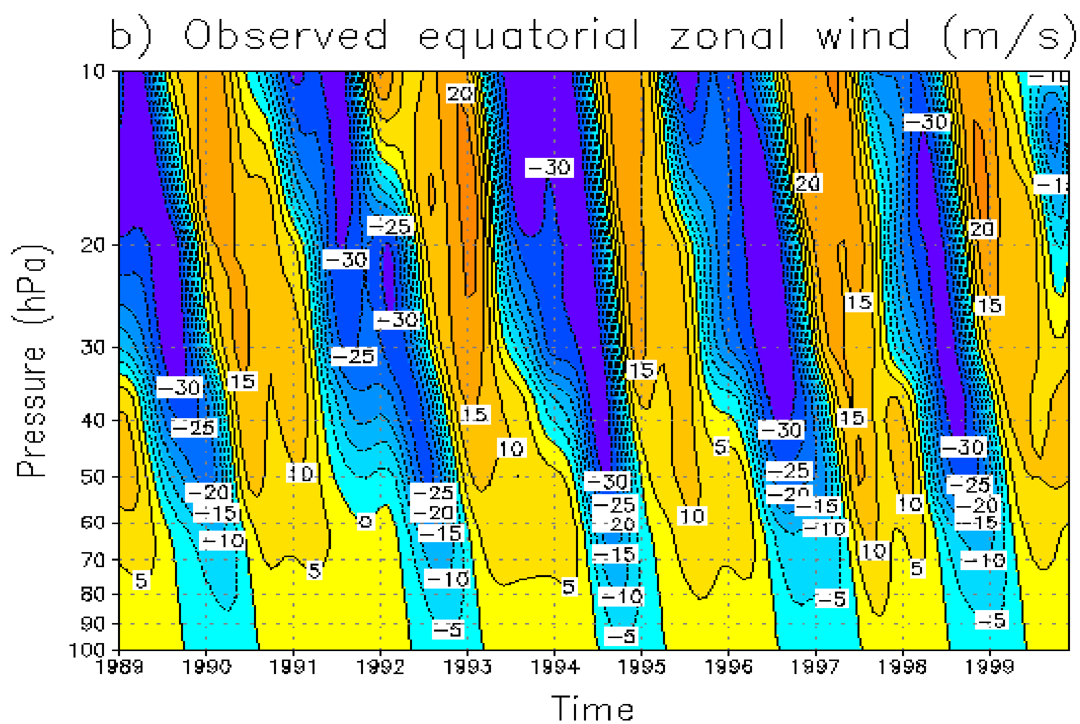

RUTGERS

SKYHI simulations

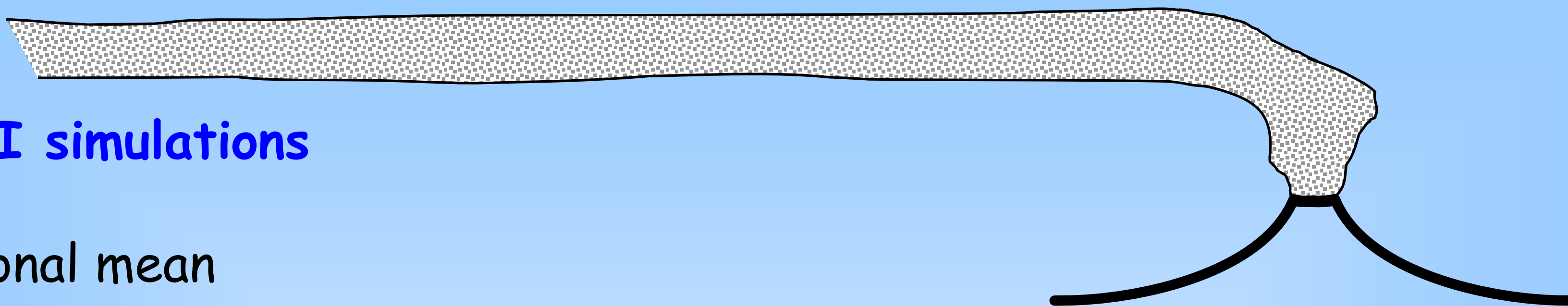

Zonal mean temperature anomaly (K) at 50 mb caused by QBO only (from QBO control run)

Hatching shows 90% significance

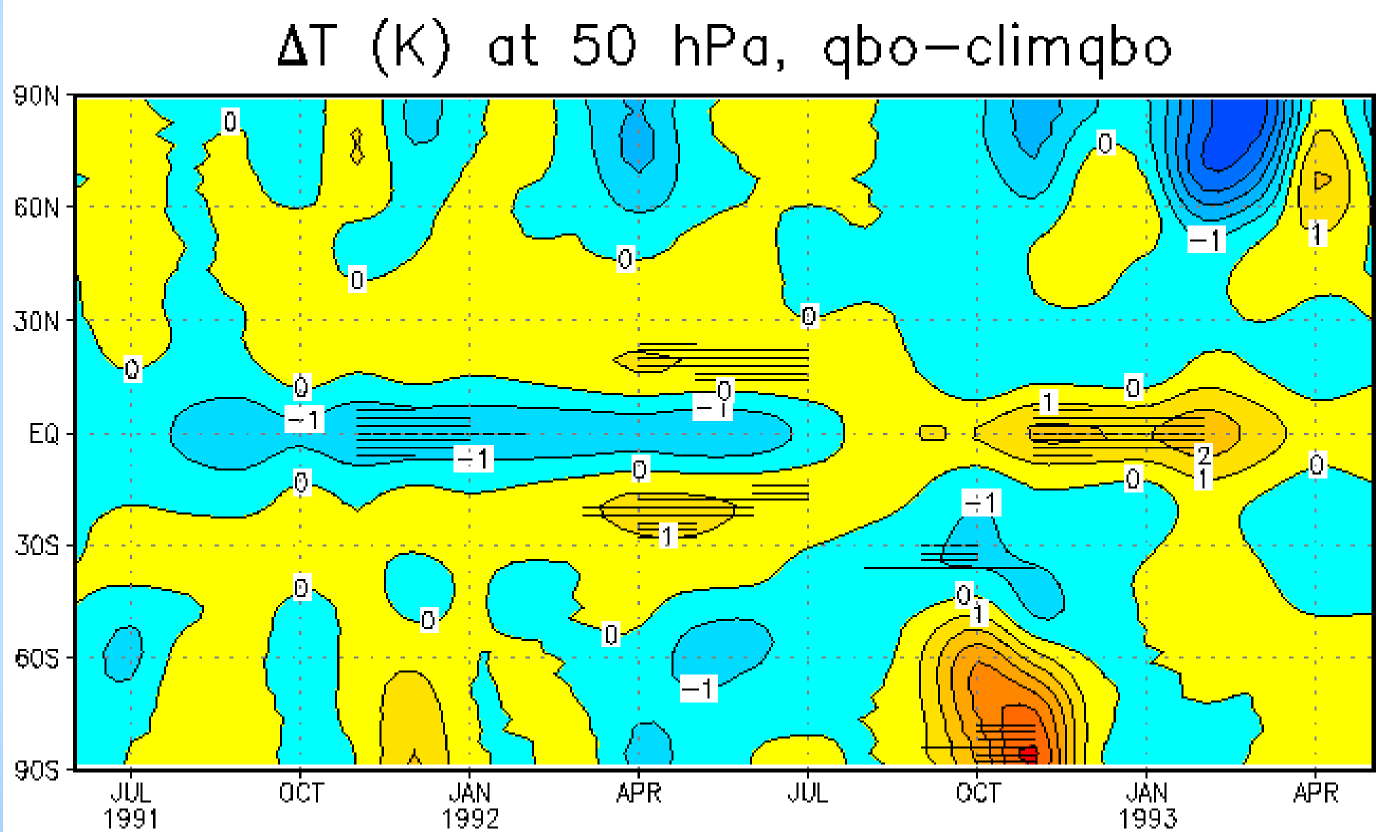

RUTGERS
Alan Robock
Department of Environmental Sciences

SKYHI simulations

Zonal mean temperature anomaly (K) at 50 mb caused by aerosols and QBO (AQ)

Hatching shows 90% significance

NCEP observations

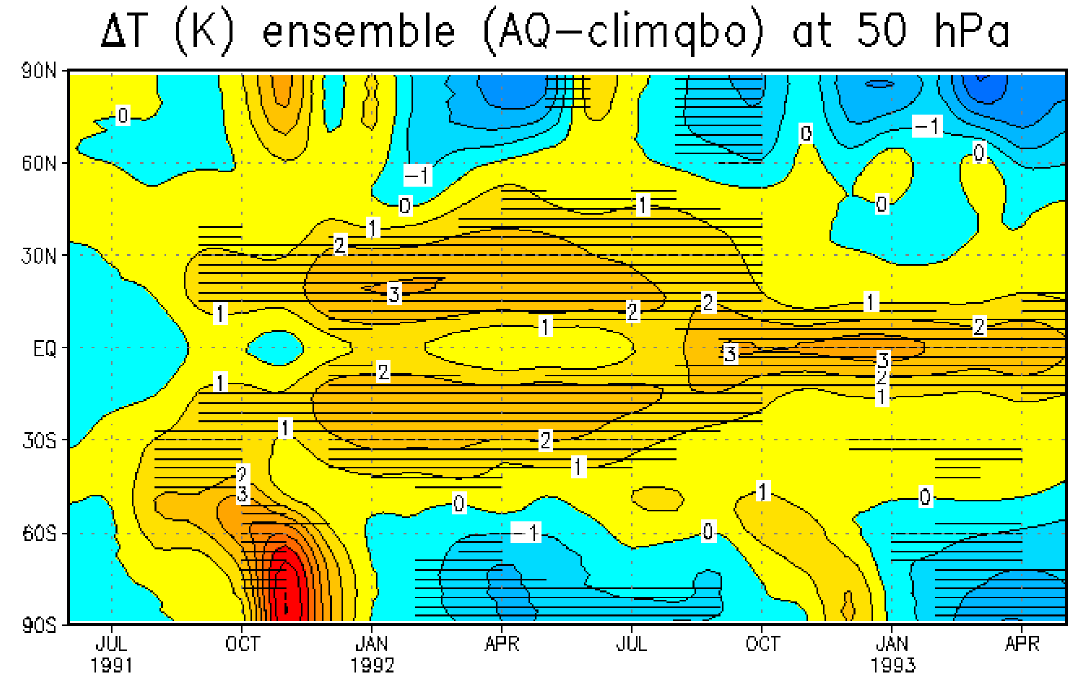

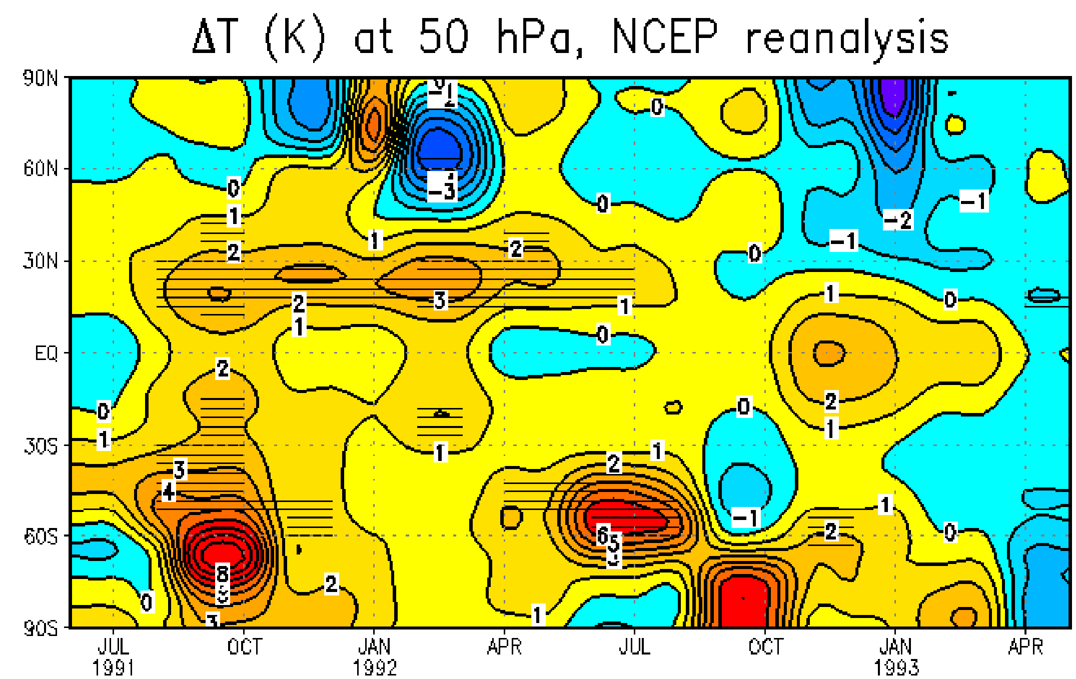

RUTGERS

SKYHI 4-ensemble mean - 50 mb temperature anomaly

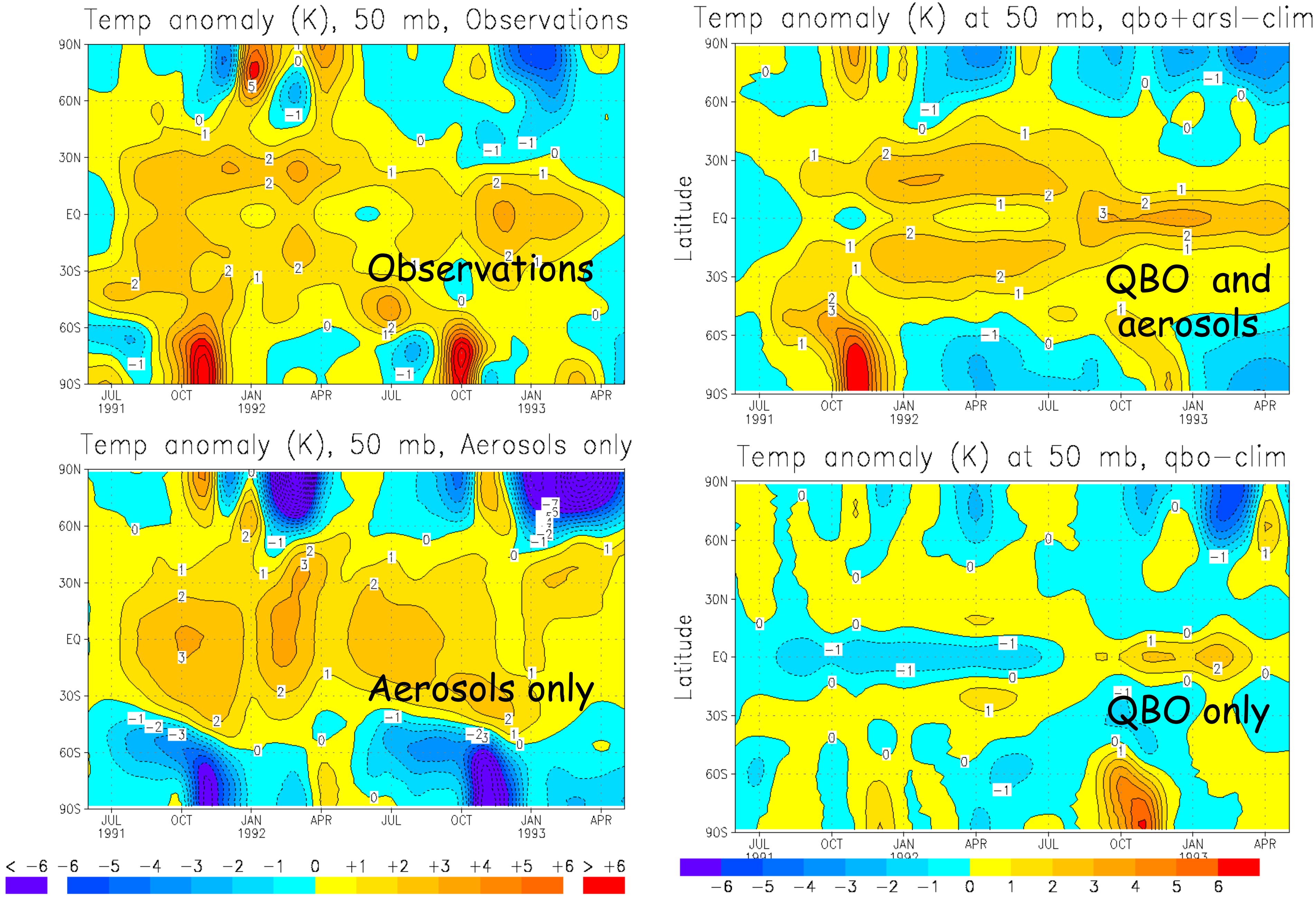

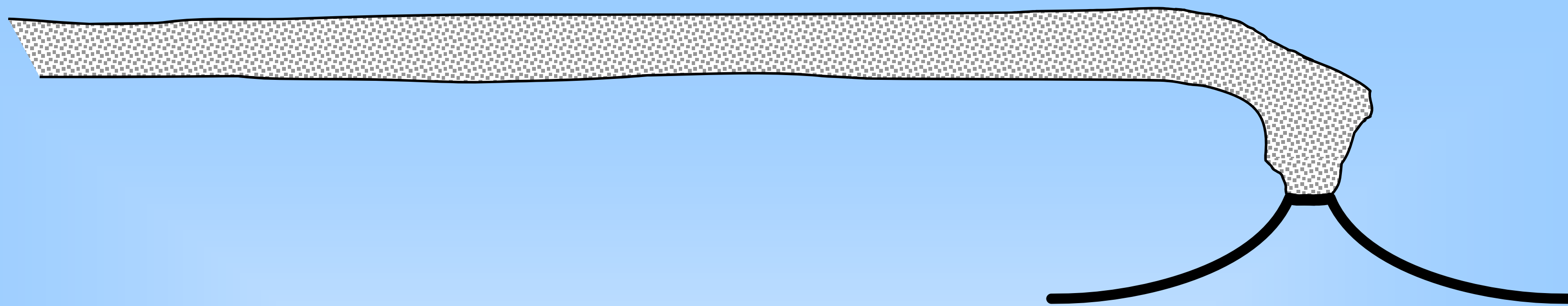

Winter Warming

RUTGERS

Alan Robock
Department of Environmental Sciences

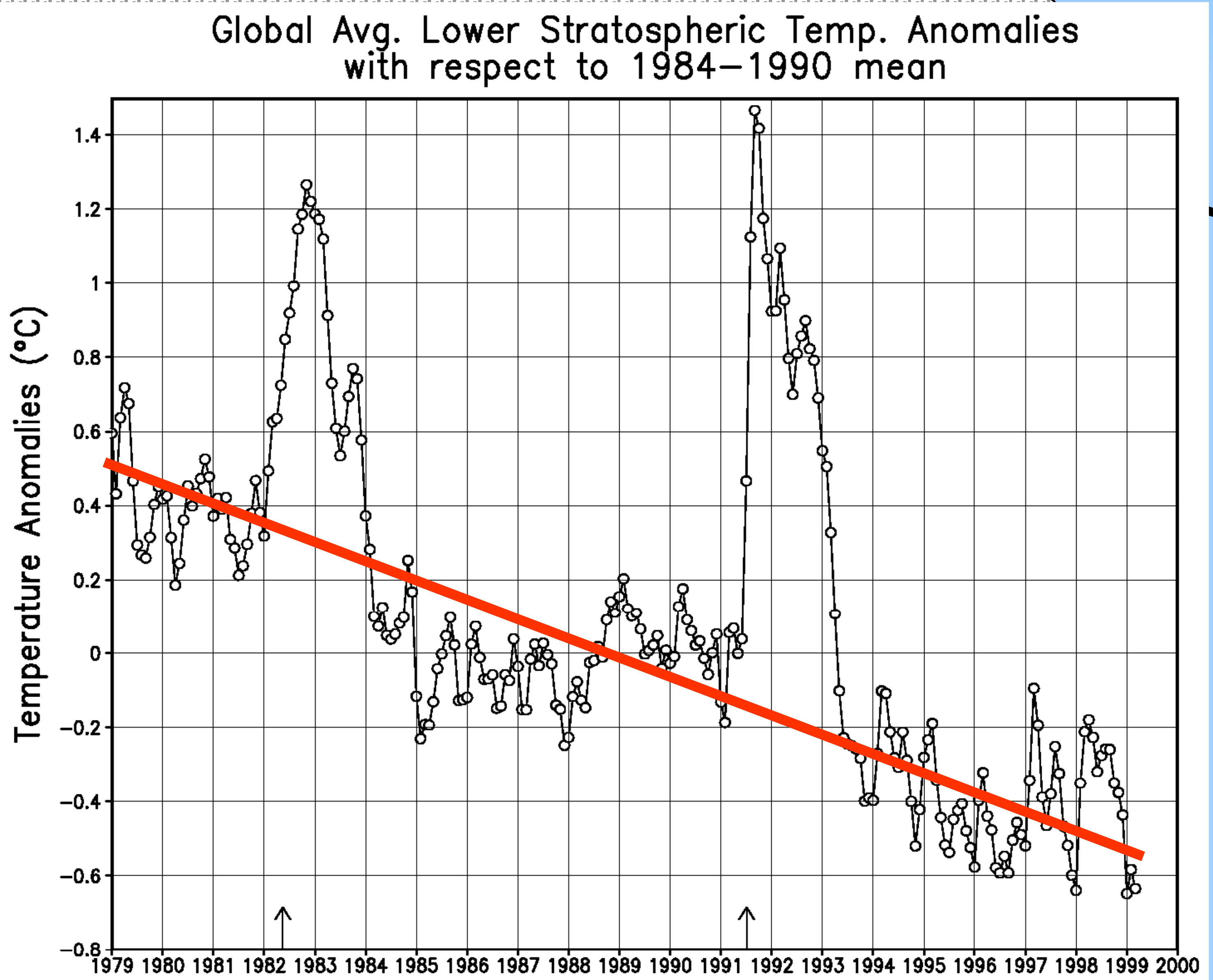

Alan Robock
Department of Environmental Sciences

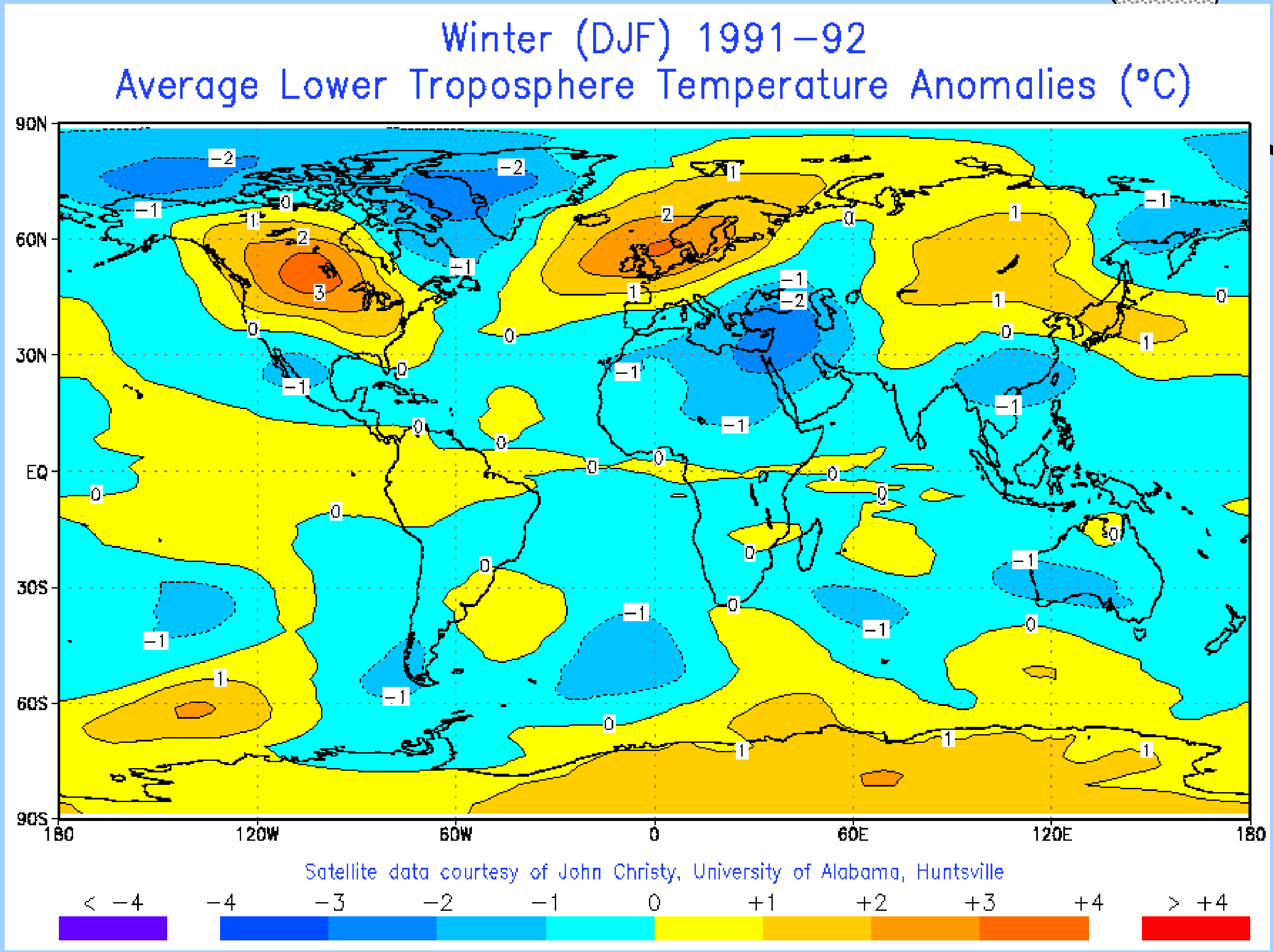

Winter (DJF) 1991–92
Average Lower Troposphere Temperature Anomalies (°C)
90N
60N
30N
EQ
30S
60S
90S
180
120W
60W
0
60E
120E
180
Satellite data courtesy of John Christy, University of Alabama, Huntsville
< −4
−4
−3
−2
−1
0
+1
+2
+3
+4
> +4

Genin et al. (1995) found coral death in the Red Sea in the winter following the Pinatubo eruption.

Cooling induced mixing, bringing nutrients which produced an algae bloom, which smothered the coral.

a. Dec. 15, 1994 (normal)

b. April 6, 1992 (after Pinatubo)

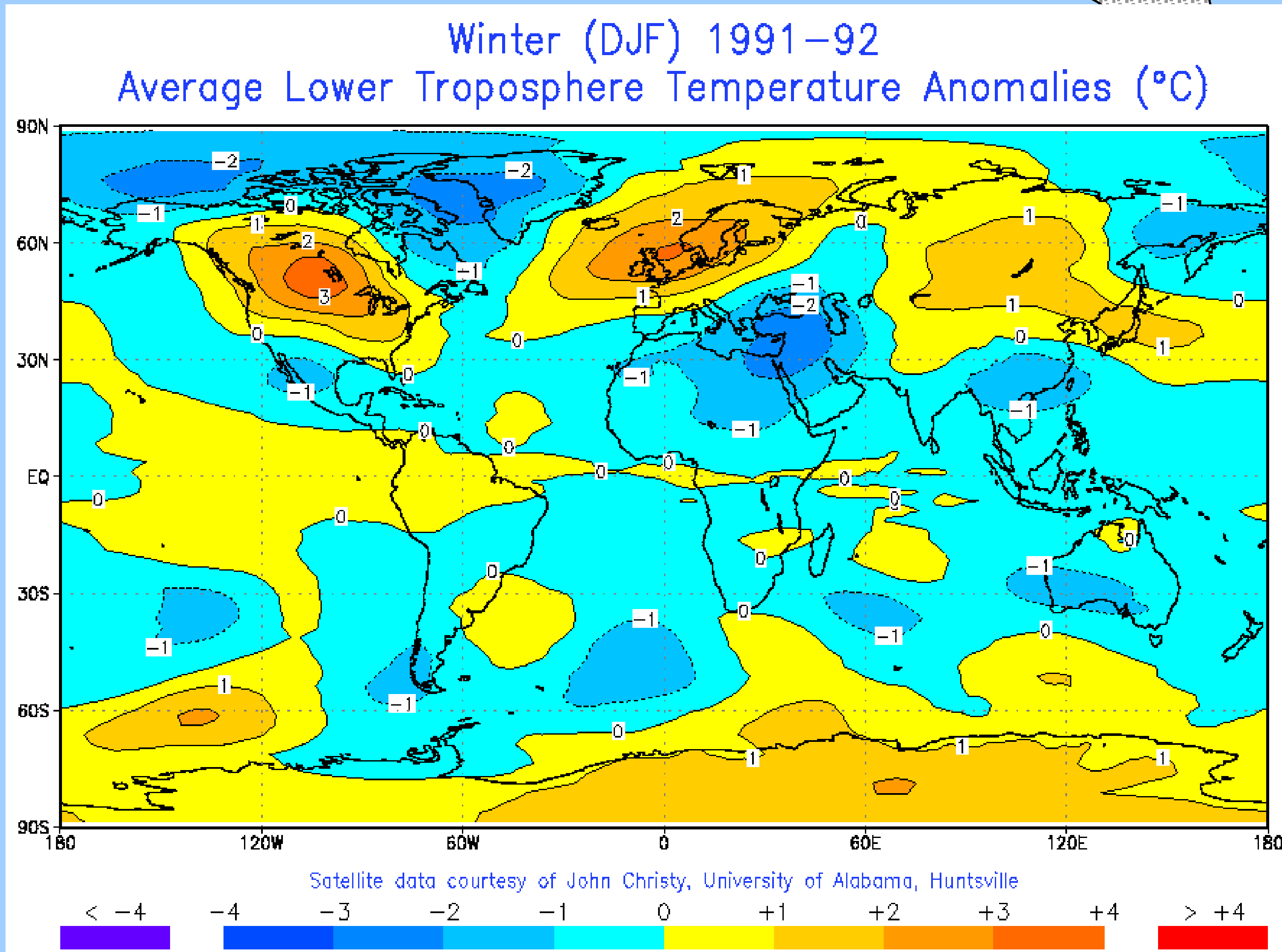
Winter (DJF) 1991–92
Average Lower Troposphere Temperature Anomalies (°C)
90N
60N
30N
EQ
30S
60S
90S
180
120W
60W
0
60E
120E
180
Satellite data courtesy of John Christy, University of Alabama, Huntsville
< −4
−4
−3
−2
−1
0
+1
+2
+3
+4
> +4

Winter (DJF) 1992–93
Average Lower Troposphere Temperature Anomalies (°C)

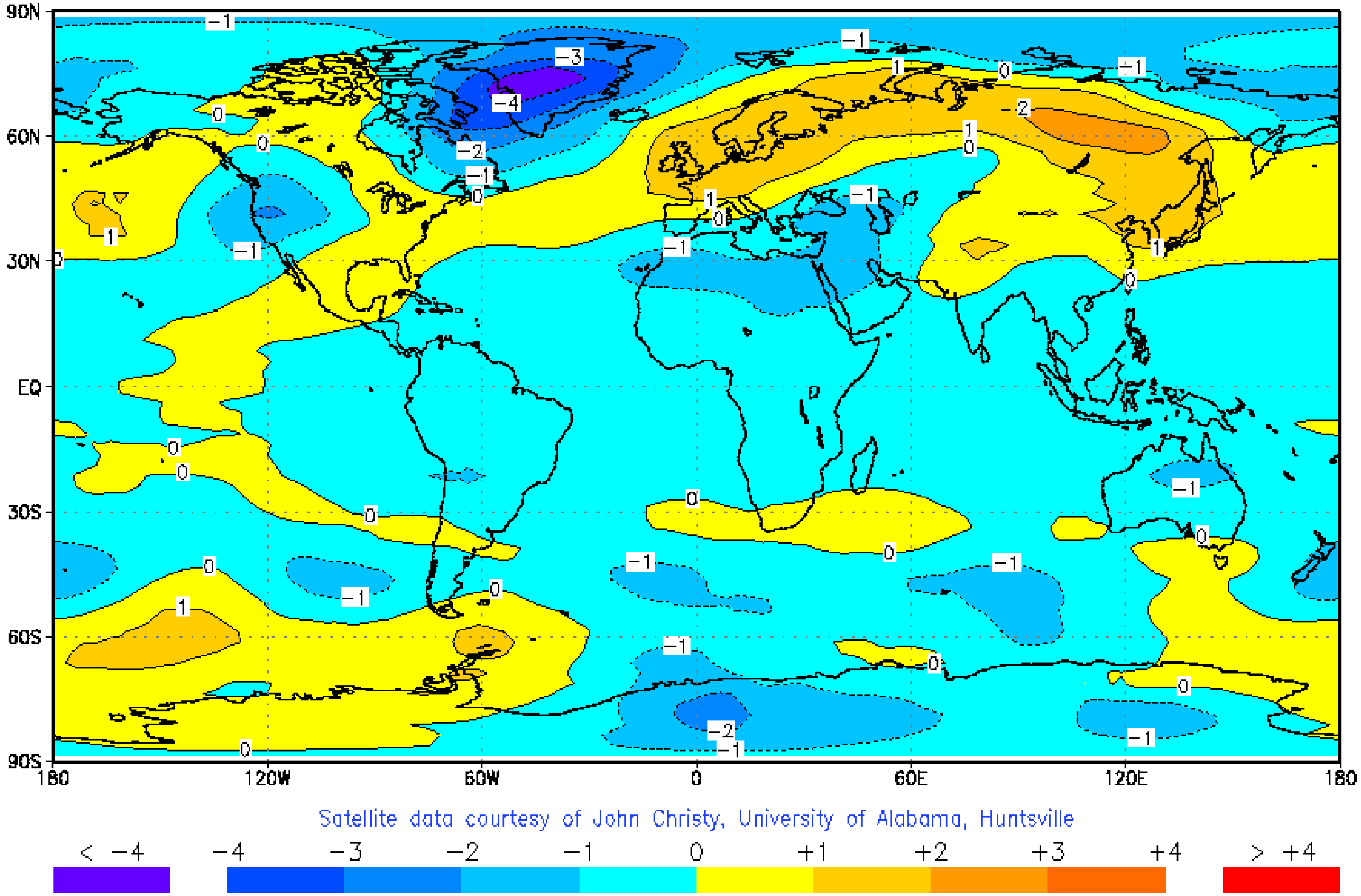

Satellite data courtesy of John Christy, University of Alabama, Huntsville

RUTGERS

Alan Robock
Department of Environmental Sciences

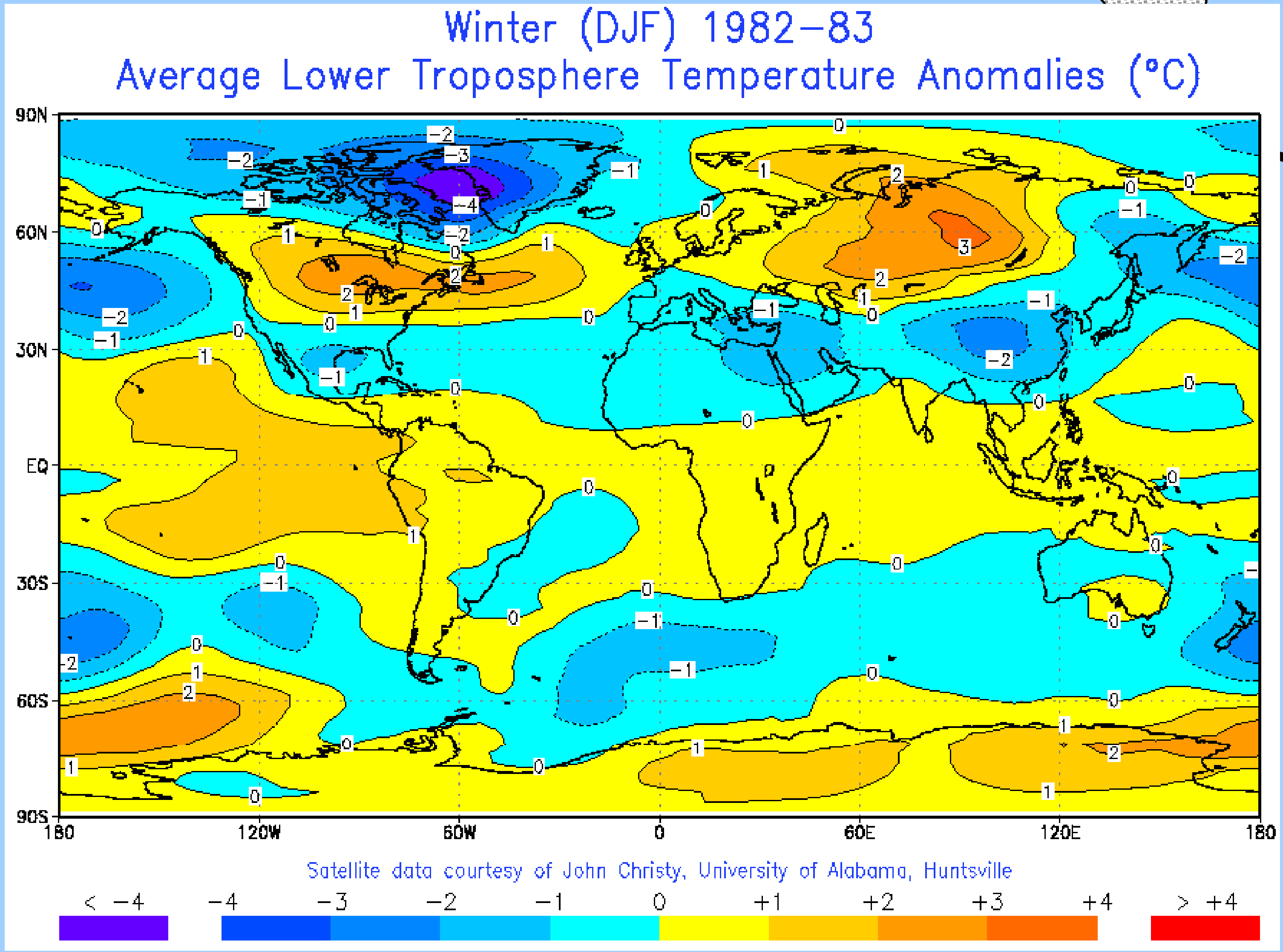
Winter (DJF) 1982–83
Average Lower Troposphere Temperature Anomalies (°C)
90N
60N
30N
EQ
30S
60S
90S
180
120W
60W
0
60E
120E
180
Satellite data courtesy of John Christy, University of Alabama, Huntsville
< −4
−4
−3
−2
−1
0
+1
+2
+3
+4
> +4

Tree ring analysis shows winter warming over most of U.S. after large low latitude eruptions

Average temperature anomaly (K)

Dots are stations with 95% significance

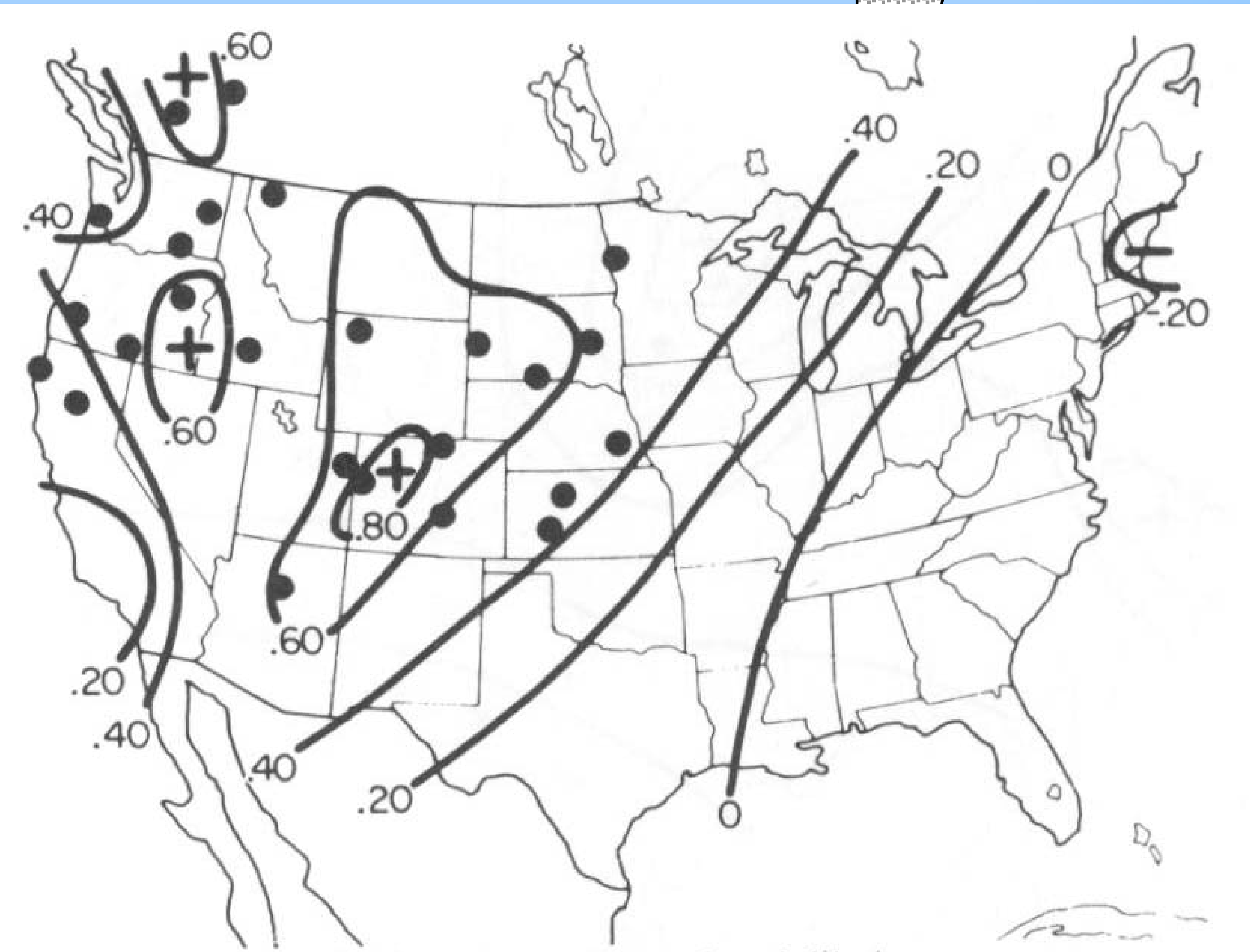

a) Winter temperature: Low latitude

Lough and Fritts (1987)

Winter Warming for largest eruptions of the past 120 years

Observed surface air temperature anomalies

Robock and Mao (1992)

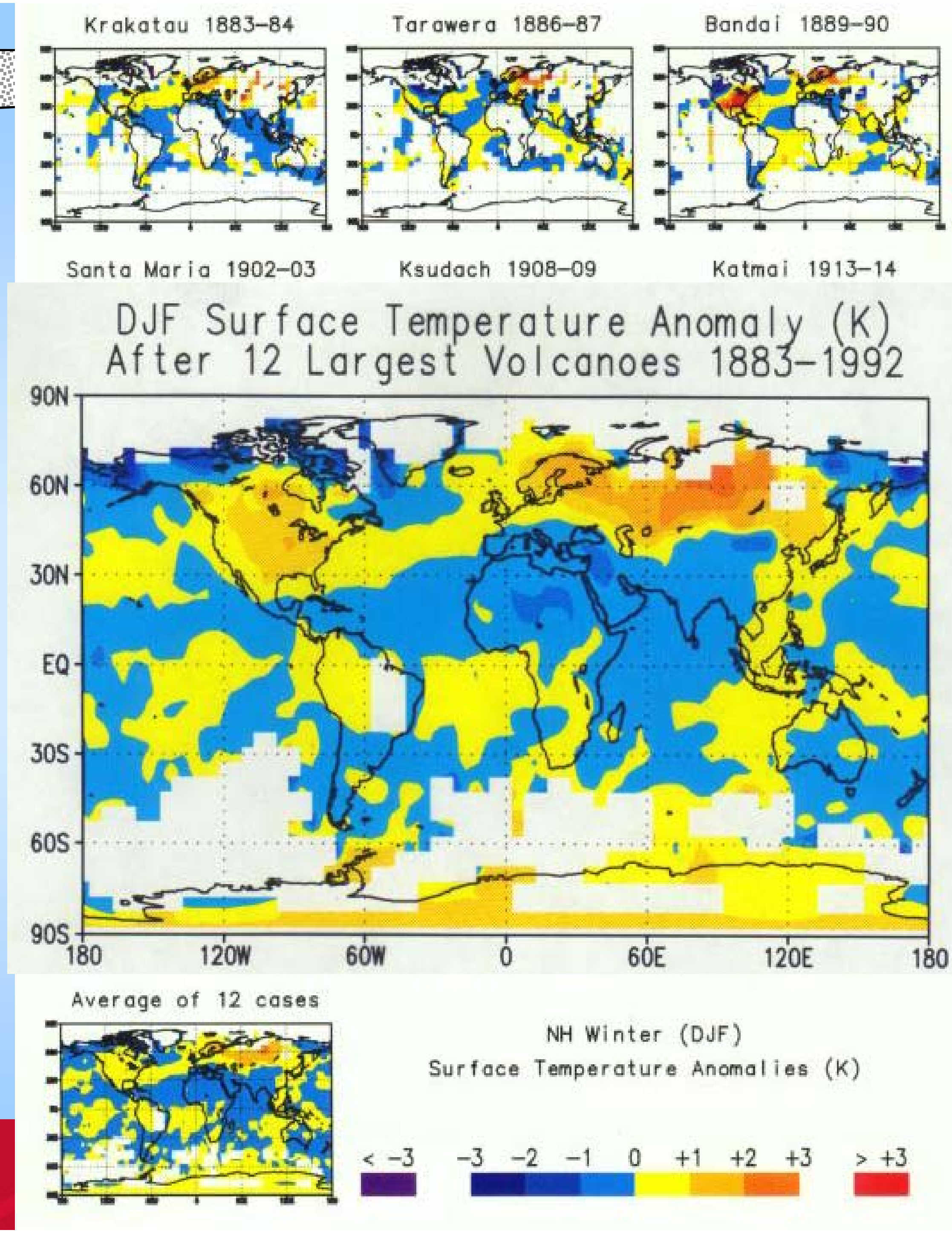

RUTGERS

The Arctic Oscillation

Thompson and Wallace (1998)

Stronger polar vortex

Winter warming

Positive mode is the same as the response to volcanic aerosols.

RUTGERS

The Arctic Oscillation signature in the wintertime geopotential height and temperature fields (Fig. 1 maps)

David W. J. Thompson and John. M. Wallace

Geophysical Research Letters, May 1, 1998

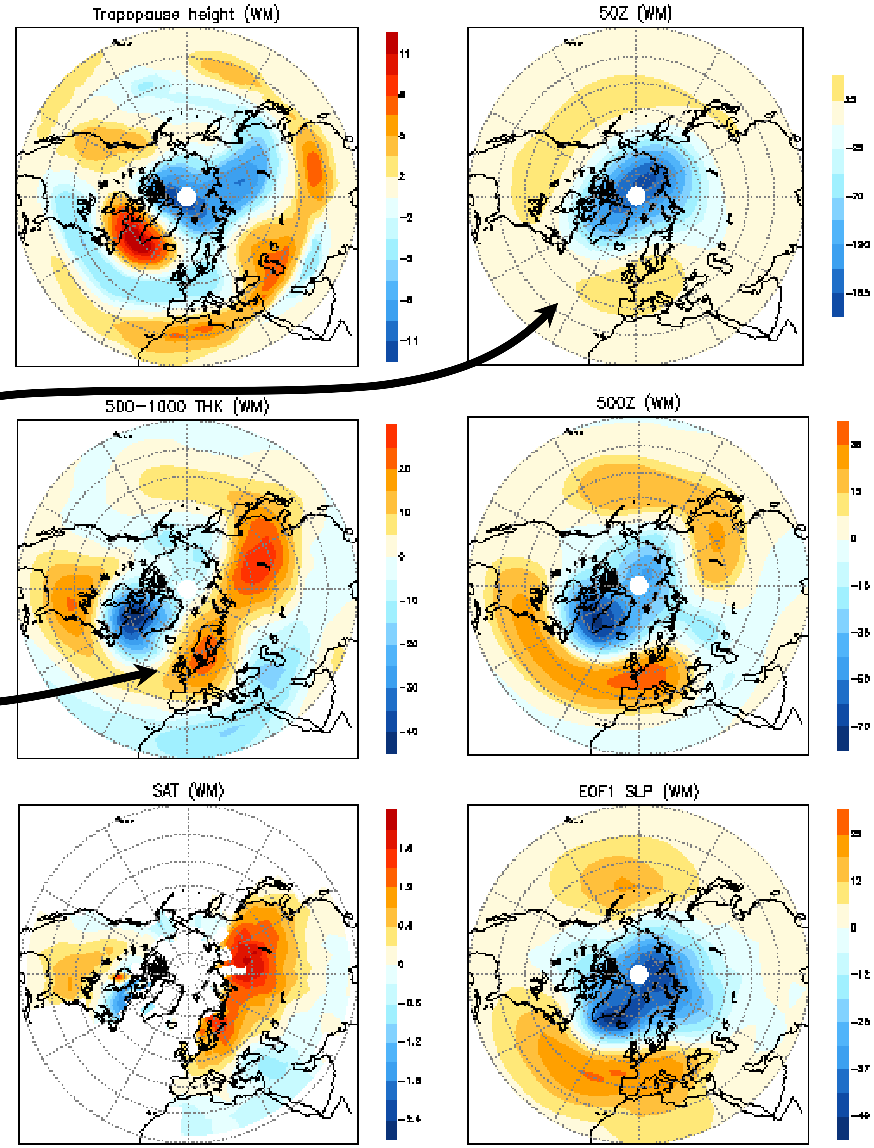

Figure 1. Regression maps for geopotential height (*meters*), tropopause pressure (*Pa*), 1000-500-hPa thickness (*m*), SLP (expressed as Z_{1000}: *m*) and surface air temperature (SAT-*K*) anomalies as indicated, based upon the AO index for 1947-1997. See text for details.

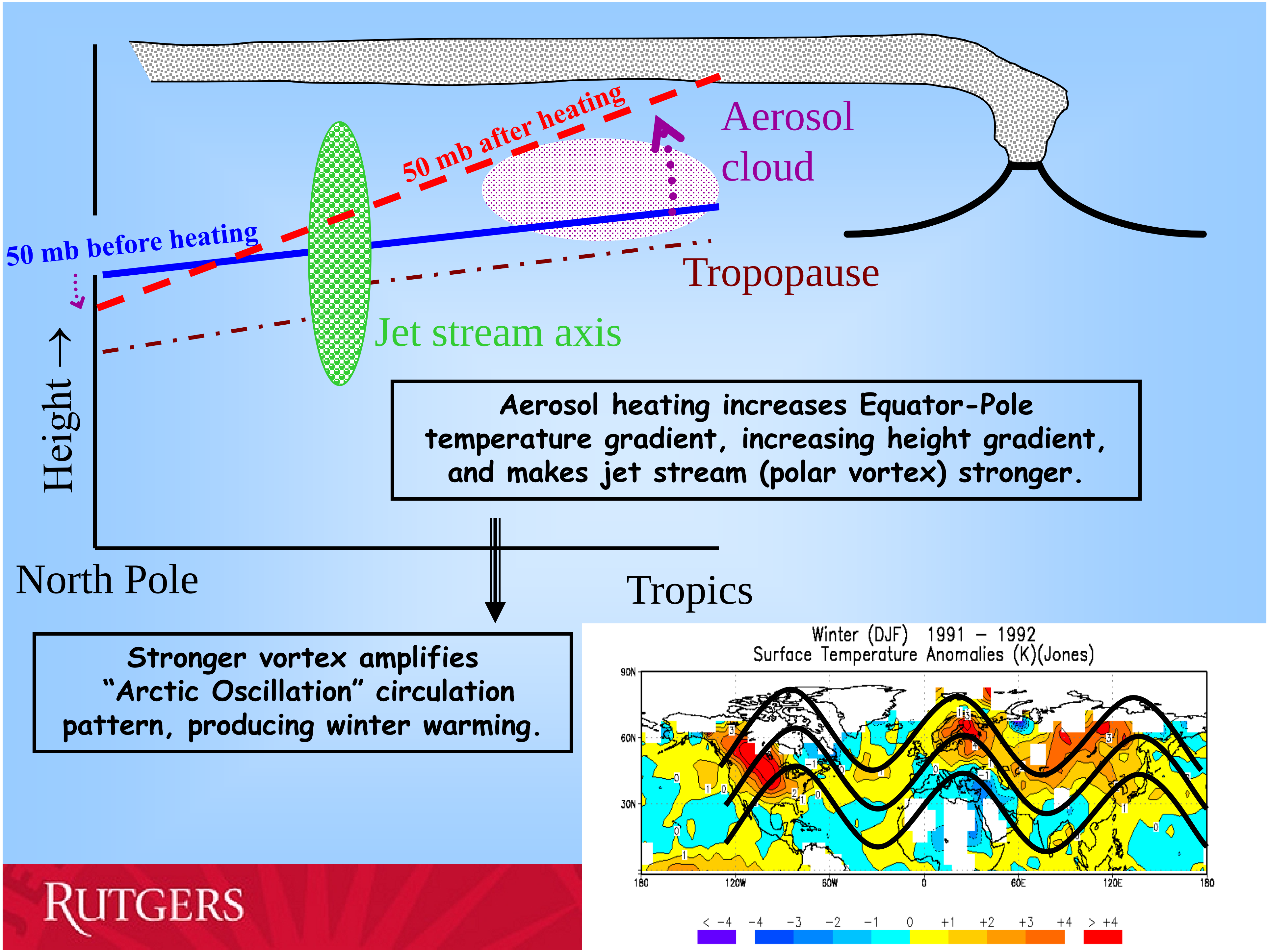
Aerosol
cloud
50 mb after heating
50 mb before heating
Tropopause
Jet stream axis
Height →
Aerosol heating increases Equator-Pole temperature gradient, increasing height gradient, and makes jet stream (polar vortex) stronger.
North Pole
Tropics
Stronger vortex amplifies "Arctic Oscillation" circulation pattern, producing winter warming.
Winter (DJF) 1991 – 1992
Surface Temperature Anomalies (K)(Jones)
90N
60N
30N
180
120W
60W
0
60E
120E
180
< -4
-4
-3
-2
-1
0
+1
+2
+3
+4
> +4
RUTGERS

SKYHI Experiments

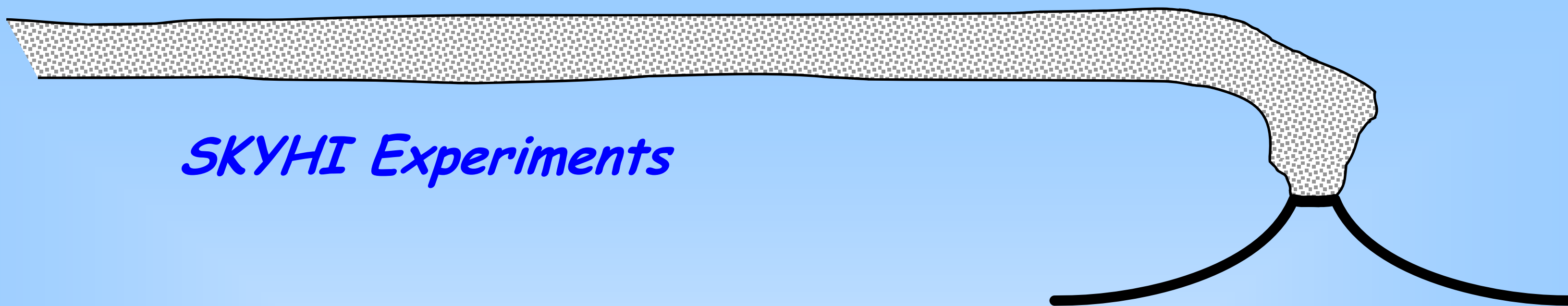

Ensembles of 2-year runs with specified climatological SST:

- **Aerosols with stratospheric and surface forcing (A)**
  - ***8 ensemble members***

- **Aerosols with only surface Cooling (no stratospheric heating) (C)**
  - ***4 ensemble members***

- **Observed Ozone anomalies only (O)**
  - ***6 ensemble members***

- **Aerosols + QBO with stratospheric and surface forcing (AQ)**
  - ***4 ensemble members***

Alan Robock
Department of Environmental Sciences

Volcanic aerosols produce more reactive chlorine

NO_x

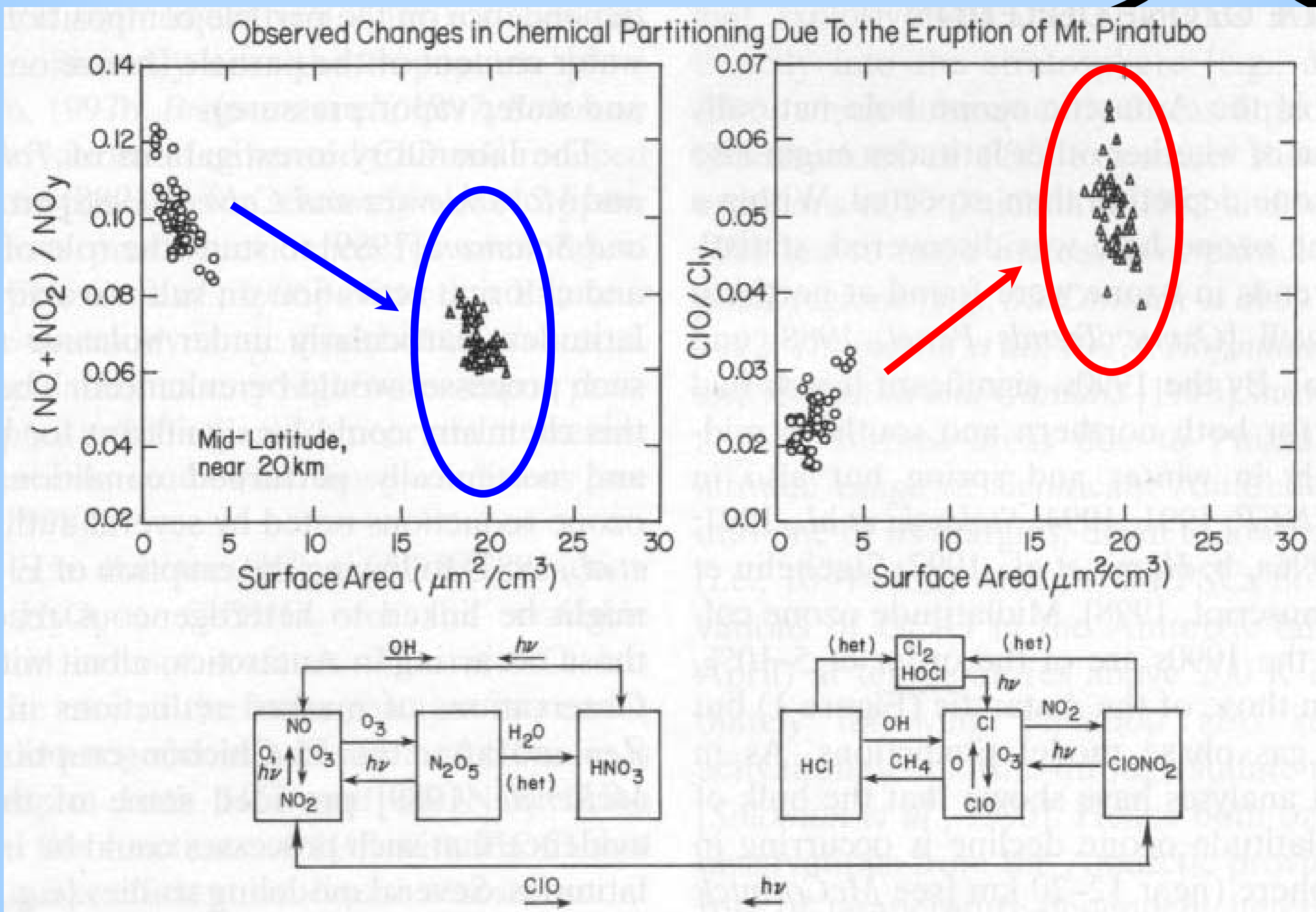

ClO

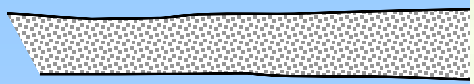

Tropospheric chlorine diffuses to stratosphere.

Volcanic aerosols make chlorine available to destroy ozone.

Solomon (1999)

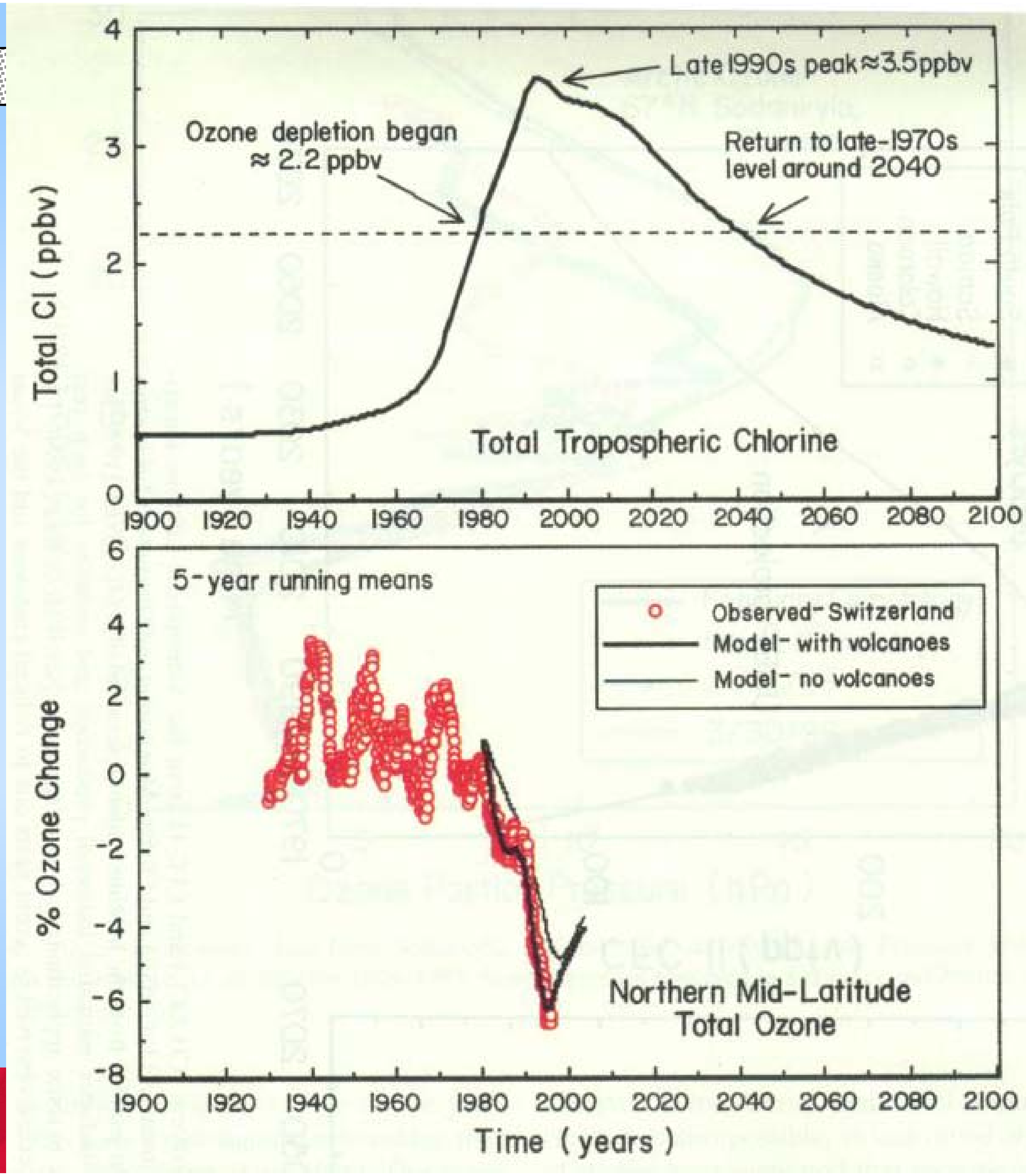

Ways Volcanic Eruptions Force Positive AO Mode in Winter

"stratospheric gradient" mechanism

"tropospheric gradient" mechanism

"wave feedback" mechanism

"QBO phase" effect

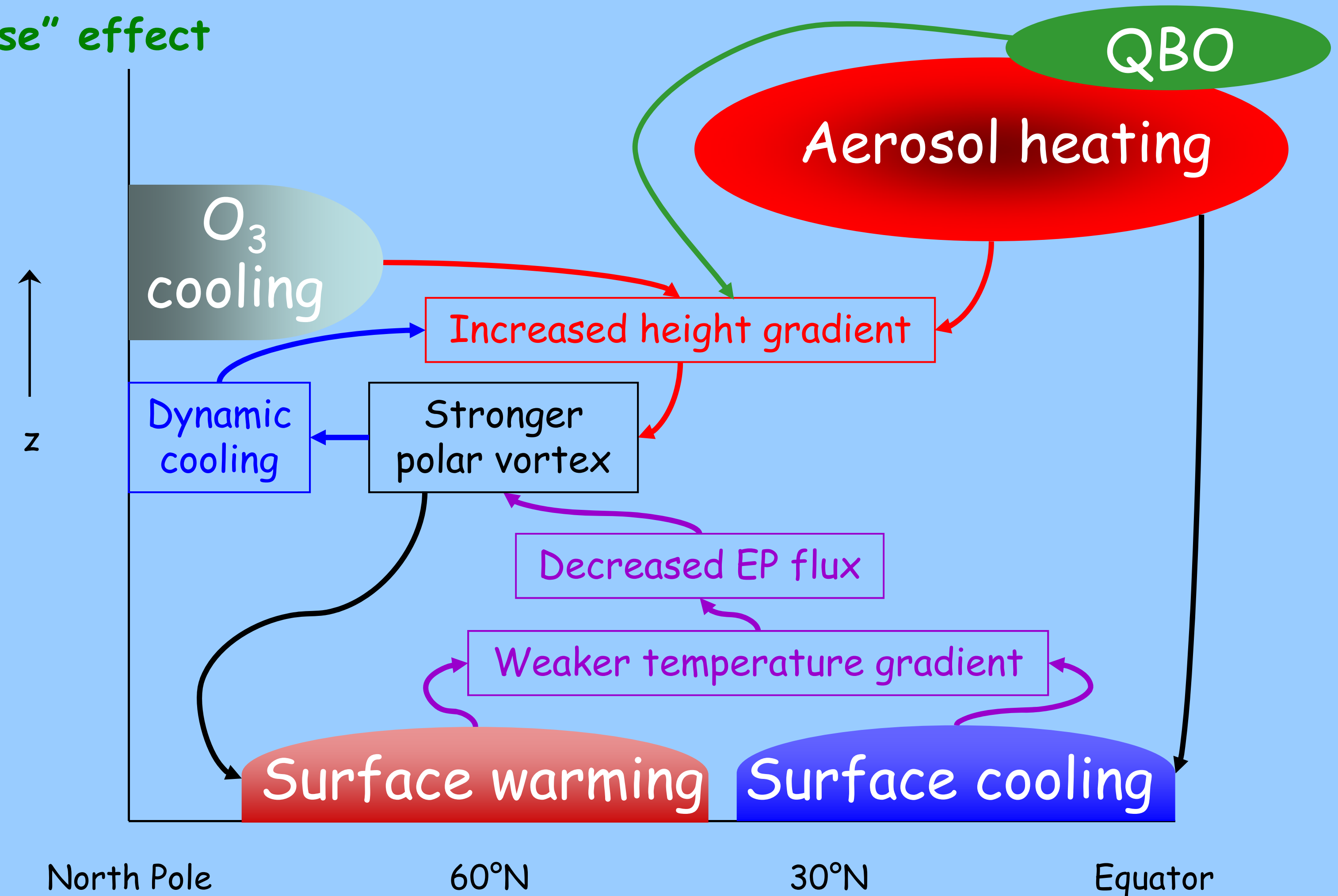

Alan Robock
Department of Environmental Sciences

London Sunset After Krakatau

4:40 p.m., Nov. 26, 1883

Watercolor by William Ascroft

Figure from Symons (1888)